2014

Measurement of Working, Reflected, and Detrimental Active Power in a Three Phase System

Tracy Toups
Louisiana State University and Agricultural and Mechanical College

MEASUREMENT OF WORKING, REFLECTED, AND DETRIMENTAL ACTIVE POWER IN A THREE PHASE SYSTEM

A Dissertation

Submitted to the Graduate Faculty of the
Louisiana State University and
Agricultural and Mechanical College
in partial fulfillment of the
requirements for the degree of
Doctor of Philosophy

in

The Division of Electrical & Computer Engineering

by
Tracy N. Toups
B.S., Louisiana State University, 2007
M.S., Louisiana State University, 2011
May 2015

ACKNOWLEDGMENTS

I would like to thank my family and friends for supporting my academic studies and financially backing me. I feel extremely privilege to work and study under major professor Dr. Leszek Czarnecki. My highest regards go to Dr. Czarnecki for his academic professionalism, guidance, and principles. There are few professors of his caliber left in this world and I am honored to be a student of his. Additionally, I would like to thank Dr. Ernest Mendrela, Dr Shahab Mehraeen, Dr. Hisao-Chun Wu, and Dr. Edgar Berdahl for serving on my graduate committee. Lastly, I want to thank Mr. Michael McAnelly for letting me be a part of his company as a relay engineer and help me garner experience on the industrial side of power engineering.

TABLE OF CONTENTS

LIST OF TABLES

LIST OF FIGURES

ABSTRACT

Study of the decomposition of the active power into composite components with respects to power industry economics namely, working active power, reflected active power, and detrimental active power. The working active energy is considered the permanent flow of useful energy to the load that results in deliberate heat, lighting, or torque on the motor shaft. The reflected active energy is the extra component of active energy originating from the load and dissipates on the supply impedance that does not contribute to useful energy. Lastly, detrimental active energy is the flow of harmonic energy from the supply to the load due to supply asymmetry and distortion that does not contribute to useful energy to the load.

Traditional revenue meters measure active energy as a whole. This means that the reflected active energy component does not get billed to the customer even though the utility must provide energy for the reflected active power and ultimately, not being compensated for energy delivered. Detrimental active energy gets charged by the traditional revenue meter yet does not contribute to useful energy. Instead this detrimental active energy is converted to useless energy, namely heat in an induction motors windings yet the customer still pays for the useless energy harming his own equipment.

As one can see, active power in the sense of economics is not a simple quantity as originally thought. With the introduction of a new working active power concept, energy accounts can be fairer to both the customer and utility. Using revenue meters based on working active power concept can pinpoint economic responsibilities of the customer and utility and accurately compensated.

CHAPTER 1. INTRODUCTION

1.1 Present Day Electrical Power Industry

In today's society, we cannot think of a world without electric energy as it has revolutionized industrial worlds far beyond what was envisioned in the 19th century. Today, most households are connected to the electrical grid to power devices such as dryers, microwaves, and television sets. In addition, there are large scale customers such as chemical plants, oil refineries, and foundries connected to the electric grid. All these customers critically rely on the power grid for a constant source of electric energy.

The United States power grid consists of three major grids with DC interconnects between them. First there is the western interconnection ranging from the Pacific Ocean to the mid-states such as South Dakota, Kansas, Nebraska, and Oklahoma. The eastern interconnect stretches from the Atlantic Ocean to the edge of the western power grid with the exception of the last interconnection, the Texas interconnection supervised by the Electricity Reliability Council of Texas (ERCOT).

The power grid is the largest man made machine on the face of the earth consisting of several millions of transmission lines, power plants, and transformers [1]. This is not to say that it has stopped growing, the demand for energy has risen at an alarming rate in the last few decades. From 1996 to 2006, the world generated 40% more electric energy [1] which will continue to rise in the future. Even today, new technologies are coming out to help improve the reliability and efficiency of the power grid. An entire industry is being formed over the idea of these new "smart grid" systems. It is hard to realize how much effort is put into continuously operating and evolving such a system that was created before the transistor was invented.

1.2 Energy Providers and Customers

In the United States, there are almost seven thousand power plants having a combined four hundred billion kilowatt-hours (kWh) of energy annually [2][3]. These power plants are owned by many energy providers that offer services for delivering reliable and affordable electric energy to the consumers. These energy providers are responsible for the delivery of energy from the power plant all the way down to the customer's meter.

These companies operate electric generators that provide electrical energy to the power grid and then transmit this electric energy via transmission lines. These transmission lines then deliver the electric energy to the local distribution network that provides electric energy to the customers. The consumer is then charged for the energy that flows through the revenue meter. Typical rates for energy billing are roughly 12 cents per kWh.

These billing rates are decided by regulatory committees in each state with the objective of offering affordable electric energy to the everyday customer while still being a lucrative business for the energy provider. Additionally, standards are developed to insure that the electric energy provided has sufficient supply quality for the consumer. Similar rules are in place for the consumer's loading quality such as power factor penalties. With the fast paced technology growth of today's society, these standards may become out of date and inaccurate. Unfortunately, regulatory committees tend to have lengthy processes to re-evaluate standards that could take many years.

1.3 Dissertation Subject and Objective

The dissertation subject is the study and measurement of decomposing the active power into several components, namely "working active power," reflected active power," and "detrimental active power" that can accurately describe the economic impact of distortion and asymmetry in the power system.

The dissertation objective is a study on the decomposition of the active power into working active power, reflected active power, and detrimental active power components within the current's physical components (CPC) theory. Then, physical measurements of the working active power will be accomplished with the aid of digital signal processing (DSP) hardware to synchronously sample real time measurements for single and three phase quantities in the electrical power system to verify the concept. Lastly, a look at the integration of the working active power concept into microgrids via the advanced metering infrastructure (AMI) will be simulated in Matlab.

Several experiments will be demonstrated to verify scenarios pertaining to working, reflected, and detrimental active power for both single phase and three phase systems. The first experiment will be performed on a linear time invariant (LTI) loads for single and three phase systems. Next, four experiments will be demonstrated with single phase harmonic generating loads (HGLs). Then, an additional four experiments will be demonstrated with three phase loads consisting of HGLs, unbalanced loads, and asymmetrical and distorted sources supplying the induction motor.

1.4 Approach of Dissertation Objective

First, the concept of working, reflected, and detrimental active powers will be described in the power system along with its prospective meaning for the economics of the power industry. Then, a mathematical concept will be drawn from the CPC power theory to illustrate the economic impact of harmonic distortion and asymmetry in the power system. This mathematical concept will cover single phase and three phase systems as well as disturbances originating from the load and the supply.

To study the integration of the working active power concept into microgrids via the AMI, several simulations with Matlab will be observed. The first simulation will be a simple straight bus setup with a HGL, an unbalanced resistive load, and an induction motor supplied from a three phase source. The purpose of this simulation is to observe the impact of the working active power with several devices running simultaneously. Then, a microgrid system with the working active power concept integrated into the AMI will be simulated. This will show the overall economic effects of asymmetry and distortion in a microgrid system.

The experimentation equipment will consist of National Instruments DSP hardware and software to develop a metering device that will measure all three active power quantities in real time. The single phase experiments will consist of a microwave oven, compact fluorescent light (CFL) bulbs, Xbox 360 gaming console, and a single phase rectifier. The three phase experiments will consist of an unbalanced three phase resistive load, three phase rectifier with a capacitive filter, and a two experiments consisting of a three phase induction motor supplied by a distorted or asymmetrical power supply. Lastly, experiments on a three phase system with varying supply impedance will be conducted for distorted and unbalanced loads.

CHAPTER 2. ELECTRICAL POWER SYSTEM

2.1 Energy Providers and Supply Quality

Energy providers are charged with generating, transmitting, and distributing energy to the customer while maintaining a sufficient level of supply quality. Some energy providers consist of large private companies spanning several states such as Entergy; operating in Texas, Arkansas Mississippi, and Louisiana and having generation capabilities of 30,000 megawatts [4]. Other energy providers consist of smaller companies who operates at lower distribution levels which span a few parishes such as DEMCO whose coverage spans seven parishes with no generation capabilities [5].

The term generation used in the power industry includes all sources of electric energy produced generators and supporting systems. Typical generator terminal voltages are rated at 25kV and the output capacity ranges from a few megawatts to over twenty gigawatts. Various types of fuel sources used to run generators are found in the United States ranging from fossil fuels such as coal, oil, and natural gas to nuclear and renewable energies such as hydro, wind, and solar power plants. The United States' generation capabilities are listed below in the Table 2.1 [6].

Table 2.1: U.S. Energy Generation by Energy Source

Electricity Generation Sector	Percentage of Net Generation
Fossil Fuels	69%
Renewables	12%
Nuclear	19%

From the generation units, the energy must be transferred over long distances to all of the homes and businesses in the country. This is accomplished by the transmission grid consisting of long distance power lines ranging from 69kV to 500kV and higher. From the generation units, the voltage is stepped up by a step up transformer to transmission voltage levels. With higher voltage levels, lower current is needed to send energy, thus reducing the line losses of the system. Lastly, the voltage is stepped down for the distribution grid and industrial users.

The distribution grid accounts for the majority of the national power grid. Nearly every home in the United States is connected to a distribution grid, making it very wide and dense. The distribution grid receives electric energy from the previously stated transmission grid at substations by a step down transformer to lower the voltage level to distribution levels. Typical distribution voltage levels are rated from 13.8kV to 25kV on the power lines adjacent to the streets and neighborhoods. With lower distribution line voltages, load current increases resulting in greater line losses and inefficiencies.

Supply quality is very important at the distribution level. The customer connects to the distribution grid at their meter and expects a voltage supply with a certain standard of quality. There are several IEEE standards to mandate minimum supply quality levels such as the IEEE standards for harmonics in power systems. Good supply quality is very important, as the customer will suffer from a low supply quality in terms of wasted energy, equipment over heating, and possibly malfunction or damage to their equipment. Thus, it is the responsibility of the energy provider to be within the minimum requirements of IEEE standards or be faced with citations.

2.2 Customers and Loading Quality

Customers are the entities that receive electric energy from energy providers and pay a monthly bill based mainly on energy usage but can include additional fees. Customers range from individual houses in a neighborhood, remote farmland complexes, to some of the largest refineries in the world. Every modern business and family is a customer in one way or another. Some examples of the customers include large industrial plants like ExxonMobil, Shin-tech Chemicals, and Boeing Everett Factory.

A single customer can be made up of many electrical machines in their compound that consumes electric energy from the power grid. From the energy provider's standpoint, a load on the power grid is considered an entity with a metering point. It is worthy to note, even though a customer might have many large or small electrical machines, the compound is considered a single entity for each meter installed. Typical range of household monthly usage was 903 kWh [7]. In contrast, larger entities might need several megawatts of constant energy flow for an entire month. These loads can be categorized by industrial, transportation, residential, and commercial usage. The United States' categories of load distribution are shown in Table 2.2 by sector [8].

Table 2.2: U.S. Energy Consumption by Sectors

Electricity Consumption by Sector	Percentage of Energy Consumption
Transportation	38.6%
Industrial	34.3%
Residential	15.7%
Commercial	11.4%

Loading quality is equally as important for the power grid as supply quality. Customers with good loading quality offer efficient energy billing for the energy provider while disturbing the power system minimally. One example of bad loading quality would be if a significant portion of the load current is shifted with respects to the voltage, thus a reactive power component is present that is not billed under energy usage. Another significant effect is an unbalanced load's current and/or a HGL's non-sinusoidal current that causes disturbances in the power system. Currently, the customer is responsible for the loading quality of his equipment. Thus, the energy providers include a power factor penalty to penalize customers with bad loading quality with respects to reactive power. Unfortunately, for the energy provider, there are no standardized penalties for loads that are asymmetry and/or harmonic generating.

2.3 Billing and Revenue

The energy provider's main source of revenue comes from the energy bill that customers pays for which typically has a cycle of one month. For residential billing, a metering technician goes to each household's energy meter and reads the energy usage every month. For industrial and commercial billing, complicated billing contracts are signed that gives a discount the more electric energy used. Regardless of which method is used, the core structure of energy billing is a set rate of cents to kWh consumed. Additionally, other penalties and fees can be present in the billing cycle such as power factor penalty.

Residential billing usually consists of a flat billing rate per kWh used in a monthly cycle with some additional fees included. Mechanical kilowatt meters have a built in counter that tracks energy usage in kWh. Typical rates include 8.4 cents per kWh for Louisiana and as high as 17.6 cents per kWh for New England states [9]. In addition, there is a peak kW reading that

shows the maximum rate of energy delivery in a given time instant that is used to track the energy needs of the consumer. Lastly, there are fuel surcharges, government taxes, and special circumstantial fees added to the monthly bill. Below is a bill from Entergy in Louisiana [10].

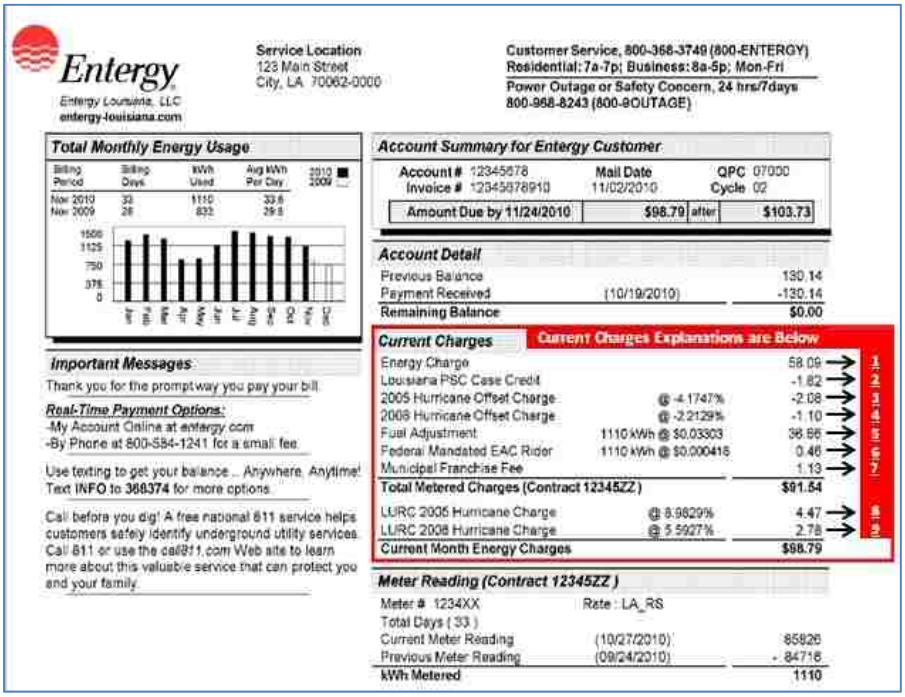

Figure 2.1: Sample Entergy Bill

The energy bill shown in figure 2.1 marks several components of a typical residential bill. The first entry, red label no. 1, is the flat rate charged for energy usage by kWh shown in the "Meter Reading" section. Entry 2, 3, and 4 are offsets charges and credits. Entry 5 charges the customer for fuel usage for generation. Entry 6 and 7 are additional fees and taxes. Next, entry 8 and 9 are circumstantial charges, in this case, additional charges for hurricane damage in the previous years. In total, the monthly billing cycle is $98.79 for 1,110 kWh metered. This rate is quite acceptable for Louisiana during November. In contrast, energy bills can rise as high as $300 dollars or more during the summer months.

Industrial and commercial customers are still billed on a monthly basis, but has a more complicated structure. One main component introduced is the "demand." This demand quantity is simply the total peak energy usage by a consumer at a given instance in time [10] expressed in kW. Customers are usually charged for the highest demand averaged in a small interval, such as 15 minutes. Industrial and commercial loads tend to have higher energy requirements so the energy provider must spend more money on higher rated equipment to send the energy at the needed peak rate. Of course, this charge for demand is in addition to the standard energy usage charge. It is worthy to note that if you compare two bills having the same energy usage; a higher demand can drastically raise the energy bill. Therefore, a low demand is the most optimal solution which can be accomplished by spreading equipment running time across the day instead of running all of them at once or looking into energy efficient improvements [10]. An example below can show the monetary difference where customer B pays less than customer A for the same amount of energy delivered.

Table 2.3: Billing of Industrial Customer [10].

Bills for Customer A and Customer B	Demand rate ($3.50 per kW) Energy rate (₵5.42 per kWh)	Charges for energy bill in US dollars ($)
Bill A: Demand 20kW	20kW x $3.50	$70.00
Bill A: Run time 50 hours	20kW x 50 hours x $0.0542	$54.20
Bill A: Total Charges		$124.20
Bill B: Demand 2kW	2kW x $3.50	$7.00
Bill B: Run time 500 hours	2kW x 500 hours x $0.0542	$54.20
Bill B: Total Charges		$61.20

From the energy provider's perspective, economic operations is a very important aspect for returning a profit from the capital invested to ensure the company's future. Capital investments include generation units, transmission lines, distribution grids, along with the maintenance, and support. All these capital investments and additional yearly costs are factored into a company's profile. Then regulatory bodies decide the billing rates for the area that is both sufficient for the energy provider and competitive for the consumer. With this tight margin, the energy provider is compelled to reach maximum efficiency for energy delivery. Remember, the energy provider is paid at the metering point mainly for energy delivered regardless of energy losses on the system [11].

CHAPTER 3. POWER THEORY

3.1 Current's Physical Components for LTI Load

The development of Current's Physical Components (CPC) power theory started in 1984 by Dr. Leszek Czarnecki and summarized later in the journal papers [12, 13]. The basics of CPC power theory is a derivation from a LTI load supplied by a nonsinusoidal voltage source. This nonsinusoidal voltage source can be described using complex rms (crms) notation in the form of $\boldsymbol{U}_n$ that describes both the magnitude and phase angle of the voltage per harmonic order n.

$$u(t) = U_0 + \sqrt{2}\,\mathrm{Re}\sum_{n\in N}\boldsymbol{U}_n e^{jn\omega_1 t}\ ,\ \boldsymbol{U}_n = Ue^{j\alpha} \tag{1}$$

Additionally, any LTI load can be described in a form of its admittance,

$$\boldsymbol{Y}_n = G_n + jB_n \tag{2}$$

Thus, the current is the product of the voltage (1) and admittance (2) in the form,

$$i(t) = Y_0U_0 + \sqrt{2}\,\mathrm{Re}\sum_{n\in N}\boldsymbol{Y}_n\boldsymbol{U}_n e^{jn\omega_1 t} \tag{3}$$

The key component of the CPC theory is to decompose the current into several fictitious currents to represent physical phenomenon that are observed such as active power and reactive power. First, the load current can be described by separating the current in (3) into an active current, $i_a(t)$ component responsible for permanent energy flow P with the equivalent conductance G_e of the load, i.e.,

$$i_\mathrm{a}(t) = G_\mathrm{e}U_0 + \sqrt{2}\,\mathrm{Re}\sum_{n\in N}G_\mathrm{e}\boldsymbol{U}_n e^{jn\omega_1 t}\ ,\ G_\mathrm{e} = \frac{P}{\|u\|^2} \tag{4}$$

Then the active current is subtracted from the load current leaving the remaining components,

$$i(t) - i_{\mathrm{a}}(t) = (Y_0 - G_{\mathrm{e}})U_0 + \sqrt{2}\,\mathrm{Re}\sum_{n\in N}(\boldsymbol{Y}_n - G_{\mathrm{e}})\boldsymbol{U}_n e^{jn\omega_1 t} \tag{5}$$

$$i(t) - i_{\mathrm{a}}(t) = (Y_0 - G_{\mathrm{e}})U_0 + \sqrt{2}\,\mathrm{Re}\sum_{n\in N}(jB_n + G_n - G_{\mathrm{e}})\boldsymbol{U}_n e^{jn\omega_1 t} \tag{6}$$

It is clear in (6) that the remaining current is composed of two components. The first component has a 90° phase shift which is known as reactive current written in the form,

$$i_{\mathrm{r}}(t) = \sqrt{2}\,\mathrm{Re}\sum_{n\in N} jB_n\boldsymbol{U}_n e^{jn\omega_1 t} \tag{7}$$

The other remaining component of (6) is coined as the ***scattered current***. This scattered current component is present in circuits that have conductance that changes per harmonic order written in the form,

$$i_{\mathrm{s}}(t) = (G_0 - G_{\mathrm{e}})U_0 + \sqrt{2}\,\mathrm{Re}\sum_{n\in N}(G_n - G_{\mathrm{e}})\boldsymbol{U}_n e^{jn\omega_1 t} \tag{8}$$

So with all the components defined, one can decompose the load current into three components, active current, reactive current, and scattered current in the form,

$$i(t) = i_{\mathrm{a}}(t) + i_{\mathrm{r}}(t) + i_{\mathrm{s}}(t) \tag{9}$$

With the proof of orthogonally of all three components [12], one can simply calculate the rms value of the load current from the current components, i.e.,

$$\|i\|^2 = \|i_{\mathrm{a}}\|^2 + \|i_{\mathrm{r}}\|^2 + \|i_{\mathrm{s}}\|^2 \tag{10}$$

With this knowledge, observation, analysis, and compensation goals can be achieved.

3.2 Current's Physical Components for HGL

Harmonic generating loads on the power system act like current sources of higher order harmonics that inject distortion back into the power system. Such examples of HGLs are AC/DC converters, fluorescent lamps, and some devices with switching elements. It is also possible to have a harmonic source on the supply side that in turn will cause harmonic current to flow to the load. These supply side harmonic sources can be represented as voltage source of higher order harmonics caused by the voltage drop across the system impedances due to the distorted current flow from the HGL. These current and voltage sources can be expressed as a sum of voltage harmonics at the load terminals, i.e.,

$$u(t) = \sum_{n \in N} u_n(t), \quad i(t) = \sum_{n \in N} i_n(t) \tag{11}$$

Then from the load voltage and currents, active power can be defined per harmonic in the form,

$$P_n = \frac{1}{T} \int_0^T u_n(t) i_n(t) dt \tag{12}$$

Samples of the voltages u_k and currents i_k can be acquired from the load terminals with the discrete Fourier Transform (DFT). The crms quantities and the phase angle between the voltage and current can be calculated as such,

$$\boldsymbol{U}_n = U e^{j\alpha_n}, \quad \boldsymbol{I}_n = I e^{j\beta_n}, \quad \varphi_n = \alpha_n - \beta_n \tag{13}$$

Thus, with the crms quantities and the phase angles, the active power can be described per harmonic in the form,

$$P_n = \mathrm{Re}\{\boldsymbol{U}_n \boldsymbol{I}_n^*\} = U_n I_n \cos\varphi_n \tag{14}$$

If one observes the phase angle φ_n, the phase angle corresponds to a positive or negative energy flow where,

$$|\varphi_n| \le \frac{\pi}{2}, \quad \textit{positive power} \tag{15}$$

$$|\varphi_n| > \frac{\pi}{2}, \quad \textit{negative power} \tag{16}$$

Therefore, a subset of N can be formed with notation N_C that represents the positive energy flow orientation (source to load) and N_L that represents the negative energy flow orientation (load to source). With (15) and (16), the subsets can be written in the form,

$$\textit{if } |\varphi_n| \le \frac{\pi}{2}, \quad \textit{then } n \in N_C \tag{17}$$

$$\textit{if } |\varphi_n| > \frac{\pi}{2}, \quad \textit{then } n \in N_L \tag{18}$$

With subsets (17) and (18), the voltages and currents can be decomposed into specific components based on energy flow orientation, i.e.,

$$i(t) = \sum_{n \in N} i_n(t) = \sum_{n \in N_L} i_n(t) + \sum_{n \in N_C} i_n(t) = i_C(t) + i_L(t) \tag{19}$$

$$u(t) = \sum_{n \in N} u_n(t) = \sum_{n \in N_L} u_n(t) + \sum_{n \in N_C} u_n(t) = u_C(t) - u_L(t) \tag{20}$$

Note that the sign of voltage $u_L(t)$ in (20) is negative which means that this voltage corresponds to the voltage drop across the supply source impedances. This voltage drop is caused by the harmonic load current flowing through the source impedance.

Because of the orthogonality principle, the system can then be separated into two group. One group is composed of voltage harmonics located on the supply side resulting in energy flowing from the supply to the load for that harmonic order. The second group is composed of

current harmonics that originated from the HGL resulting in energy flowing from the load back to the supply. This decomposition results in two separate systems show in figures 3.1 and 3.2.

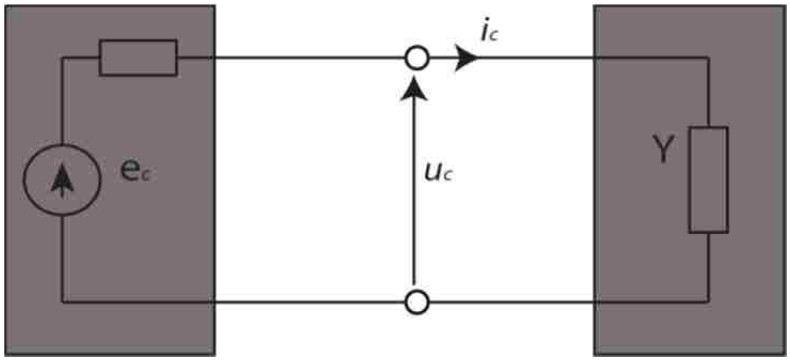

Figure 3.1: Circuit for $n \in N_C$ Subset

The voltage $u_C(t)$ in figure 3.1 is composed of voltage sources of harmonic orders n from the subset N_C. Next, the load is represented with admittance $\boldsymbol{Y}_n$ corresponding to each harmonic order.

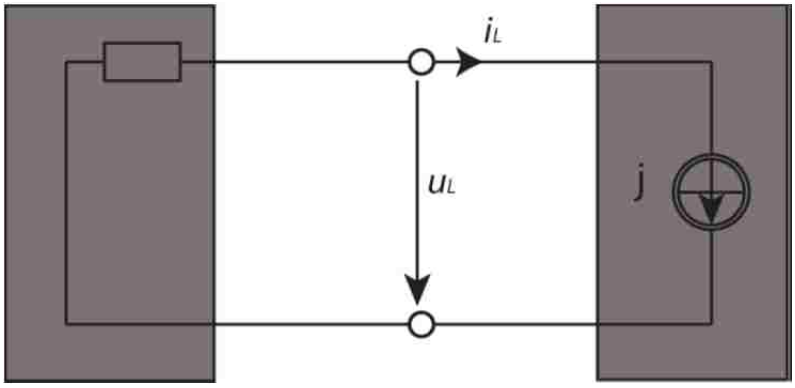

Figure 3.2: Circuit for $n \in N_L$ Subset

Additionally, the voltage $u_L(t)$ in figure 3.2 is composed of voltage drops across the source impedance represented by voltage harmonics of the order n from the subset N_L. This voltage drop is caused by the current harmonic source originating from the HGL.

It is important to note a potential problem in the separation of harmonic sources to a load generating subset, N_L and supply generating subset, N_C. There is an assumption that at each harmonic order, all source of harmonic generation are one sided (load or supply sided). In the real world, it is possible to have a harmonic generating source from both the load and supply side. Such an example is a HGL being supplied by a distorted supply. Since components of the same harmonic order are not orthogonal, two distorted sources from different sides cannot be categorized in the subsets N_L or N_C for the same harmonic order. Thus, an approximation is chosen by recognizing the greater source and neglecting the lesser source.

The load in figure 3.1 is a LTI load in which CPC theory can be used to decompose current $i_C(t)$ into active, reactive, and scattered current as such,

$$i_C(t) = i_{aC}(t) + i_r(t) + i_s(t) \tag{21}$$

where $i_{aC}(t)$ is defined as,

$$i_{aC}(t) = G_e U_0 + \sqrt{2}\,\mathrm{Re}\sum_{n\in N} G_{eC}\mathbf{U}_n e^{jn\omega_1 t}\ ,\ G_{eC} = \frac{P}{\|u_C\|^2} \tag{22}$$

Thus, the load current can be transposed into the form,

$$i(t) = i_C(t) + i_L(t) = i_{aC}(t) + i_r(t) + i_s(t) + i_L(t) \tag{23}$$

Finally, since $i_C(t)$ and $i_L(t)$ are orthogonal, the rms values for the current components can fulfill the relationship,

$$\|i\|^2 = \|i_{aC}\|^2 + \|i_r\|^2 + \|i_s\|^2 + \|i_L\|^2 \tag{24}$$

which gives us a final rms form that can be used to decompose the load current easily.

3.3 Effects of Distortion and Asymmetry on the Power System

Distortion and asymmetry are a component of the current and the voltage caused by loading characteristics. Some examples include arc furnaces, AC/DC converters, and switches that lead to nonsinusoidal current waveforms while asymmetry is caused by unbalanced loading in a three phase system. Additionally, distortion and asymmetry can be present on the supply side as well caused by switching converters of renewable sources, voltage drops across the system impedances, and uneven power line lengths and/or unbalanced loading of single phase lines in a distribution grid.

Distortion in the power system causes many problems for the customer and the energy provider. Current distortion caused by the customer causes higher current rms which requires higher rated equipment. Also, capacitor banks and other harmonic sensitive equipment suffer from degraded lifespan as well as interference in the normal operation of such devices. Additionally, this current distortion causes a voltage drop across the system impedance and thus adds a harmonic component in the supply voltage.

Voltage harmonics in the supply causes many problems for customers as well. Sensitive electronic equipment can be disturbed by voltage harmonics in the supply and possibly shorten the life span of such devices. Motors are also affected by voltage harmonics by reducing torque and increasing heat. It is clear that distortion in the power system is not a good thing, and should be reduced to a minimum when possible.

Asymmetry in the power system also causes problems for the customer, but it is more of a concern to the energy provider. Unbalance in the current mainly stems from loading three phases unequally. This is usually not done intentionally as the loading topology can be inflexible at times. This is inevitable as some distribution lines will be more loaded than others because of

residential growth in certain areas or having a single phase load in a remote location. Other culprits could be in industrial sites where the design, upgrade, or decommission of equipment in the plant caused loads to be concentrated on one a single phase.

The unbalanced current cause problems for the energy provider as line losses are higher in an unbalanced line as compared to an equivalent balanced line. This is due to the fact that line losses grow exponentially as load current increases. Additionally, equipment will have to be rated higher to accommodate the line with higher current. Moreover, as with the previous distortion problem, unbalanced load current will create a voltage drop across the supply impedance causing asymmetry to appear in the supply voltage. Three phase loads such as converters and motors will have issues with operation and could possibly affect the lifespan and output.

3.4 Useful vs Useless Active Energy

The main component of billing for the energy provider is the energy delivered to the customer over billing interval (typically monthly), meaning the integral of active power P, i.e.,

$$W_{\mathrm{a}} = \int_{month} P dt \tag{25}$$

This energy is referred to as *active energy* in the dissertation. Active power and active energy has a clear physical meaning and is the fundamental quantity used for billing, equipment design, and performance evaluation.

Active energy can be classified as useful energy if it is deliberately converted to heat, light, or work such as resistive heaters, incandescent light bulbs, and rotating electrical machinery. Conversely, it is known in the engineering community that energy conveyed by current harmonics and negative sequence components could possibly disturb and overheat

electronic equipment with the exception of purely resistive loads. Another classic example is a three phase induction motor since energy conveyed by harmonics and negative sequence currents do not convert into useful torque. Therefore, active power P in a power system composed of nonsinusoidal and/or asymmetrical voltages and currents contain a component that does not convey useful energy. In this regard, active power is not synonymous to "useful power" and should be considered a power composed of useful and useless powers.

3.5 Working Active Power Concept

In the eyes of the general electrical engineering community, active power is regarded as useful power, but as stated in the previous section, this might not always be true. Asymmetry and distortion are responsible for the active power component that cannot be considered useful power. Thus, a separation between useful active power and useless active power needs to be considered.

For the majority of the loads in the 22nd century power system, distortion and asymmetry in the voltage should be considered a detrimental effect. One of the more popular loads on the power system are electric motors that suffer from the detrimental effects of distortion. The motor's rotor produces torque by a rotating magnetic field created by the positive sequence voltage of the fundamental harmonic. Asymmetry and 2nd and 5th ordered harmonics introduces negative sequence components in the voltage that creates a magnetic field in the opposite direction of the main rotating field resulting in a negative torque component. Additionally, the 4th and 7th order harmonics in the supply voltage produces a magnetic field that rotates much faster than the main rotating field. This high speed rotating magnetic field does not produce useful torque, but instead acts similar to a locked rotor situation producing heat.

The component of active power that conveys useful energy to the operation of the load is defined as *working active power*, P_w. This useful energy is delivered by the working active power component to the load at normal operations for output, efficiency losses, and energy used for harmonic generation. It would be natural that the customer should be charged for the working active power since that is the true rate of energy he draws from the power system.

The task to differentiate active power and working active power is not possible with traditional analog energy meters and traditional active power standards. A new meter based on digital signal processing (DSP) capabilities would be needed to differentiate useful and useless active power. Fortunately, with smart grid technology being so popular and emerging, advanced metering infrastructure (AMI) has the required capabilities already integrated which has several references to supply and loading quality supporting the AMI's capabilities [14-15].

CHAPTER 4. SINGLE PHASE ACITVE POWER

4.1 Working Active Power for Single Phase Systems

Working active power is defined as the component of active power that is needed for normal operation of loads. The basic circuit in figure 4.1 shows can differentiate active power P from working active power P_w. The system is assumed to have sinusoidal supply voltage with supply resistance R_s loaded with a HGL with current source j composed of harmonic order n = 2,3,4....,N, i.e.

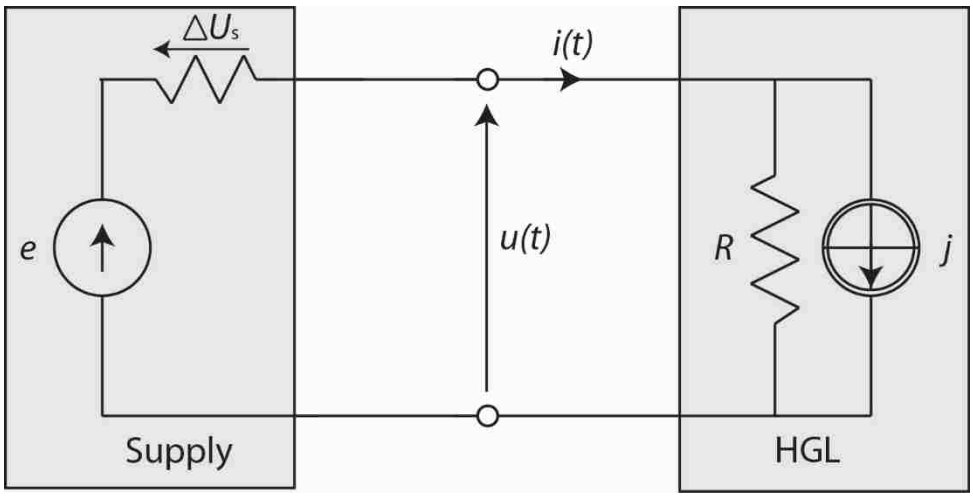

Fig. 4.1: Single Phase Sinusoidal Supply with Resistive HGL

Assuming that the load generated current j is composed of higher order harmonics; the load current of the HGL has the form of,

$$i(t) = \sum_{n \in N} i_n = i_1 + i_h = i_{1aC} + i_h \tag{26}$$

where i_{1aC} corresponds to the active current of the first harmonic order. This current is in phase with the fundamental voltage and shall be termed *working current*,

$$i_w = i_{1aC} \tag{27}$$

Therefore, the load current can be expressed in the form,

$$i = i_{\mathrm{w}} + i_{\mathrm{h}} \tag{28}$$

Next, the load voltage $u(t)$ contains distortion created by the distorted load current I,

$$u(t) = \sum_{n \in N} u_n = u_1 + u_{\mathrm{h}} \tag{29}$$

Like previously, the fundamental harmonic of the load voltage u_1 is termed as the *working voltage*, i.e.,

$$u_{\mathrm{w}} = u_1 \tag{30}$$

The active power of the load can be defined as,

$$P = \frac{1}{T}\int_0^T u(t)i(t)dt = \sum_{n \in N} P_n = P_1 + P_2 + P_3 + \ldots + P_n \tag{31}$$

The working active power is the product of the fundamental harmonic components of the working voltage and working current, i.e.,

$$P_{\mathrm{w}} = U_1 I_1 \tag{32}$$

Figure 4.2 shows the direction of energy flow for P_{w}.

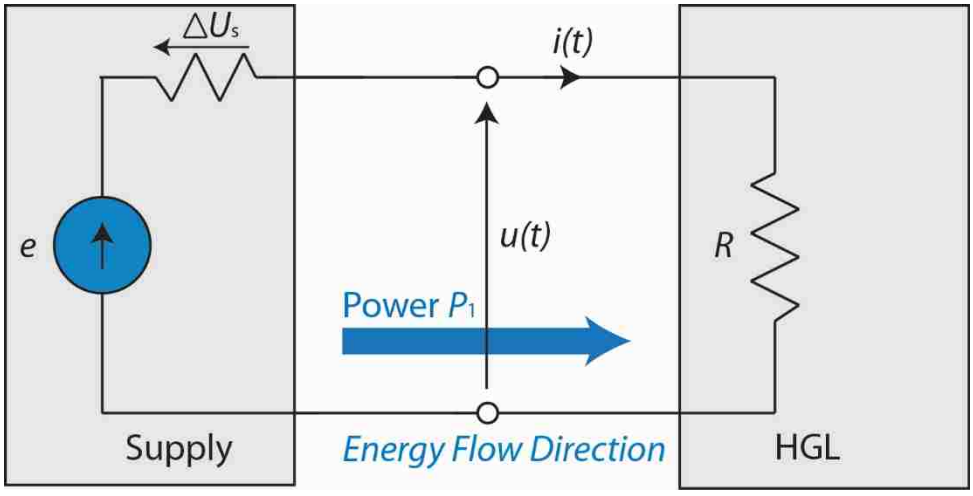

Figure 4.2: Direction of Energy Flow for P_{w} in Single Phase HGL

The rest of the higher order harmonic powers associated with load generated current *j* makes up the remaining active power, i.e.,

$$\sum_{n=2}^{N} P_n = U_n I_n = (-R_s I_n) I_n = -R_s {I_n}^2 \tag{33}$$

The part of active power that originates from the load side is dissipated in the supply resistance, being represented as,

$$P_h = (P_2 + P_3 + \ldots + P_n) < 0 \tag{34}$$

Figure 4.3 shows the direction of energy flow for P_h.

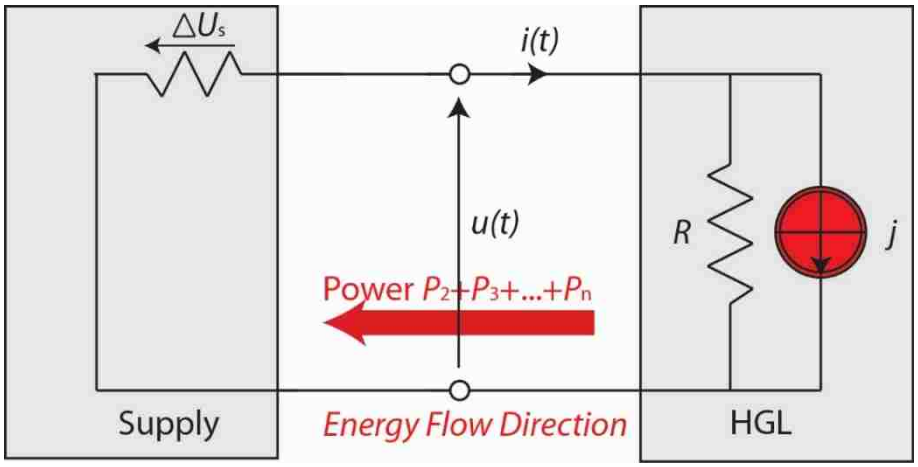

Figure 4.3: Direction of Harmonic Energy Flow for Single Phase HGL

Therefore, the active power has the form of,

$$P = P_w + P_h \tag{35}$$

4.2 Reflected Active Power for Single Phase Systems

Active power of higher order harmonics P_h is the average rate of energy flow at higher order harmonics from the load back to the source over a period *T*. This harmonic active energy is dissipated in the supply resistance and therefore referred to as *reflected active power*, P_r, which has a negative value as compared to P_h, i.e.,

$$P_{\mathrm{r}} = -P_{\mathrm{h}} \tag{36}$$

The reflected active power can be described in terms of energy dissipation off the supply resistance, i.e.,

$$P_{\mathrm{r}} = R_{\mathrm{s}} \left\| i_{\mathrm{h}} \right\|^2 = -P_{\mathrm{h}} \tag{37}$$

The harmonic active power is negative to denote that the energy flows from the load back to the source for harmonics of $n > 1$. This energy is delivered to the load via the fundamental harmonic components of the supply source. Thus, the rms current of the fundamental harmonic of a resistive load is,

$$I_1 = \frac{P_1}{U_1} = I_{\mathrm{w}} = \frac{P_{\mathrm{w}}}{U_{\mathrm{w}}} = \frac{P + P_{\mathrm{r}}}{U_{\mathrm{w}}} > \frac{P}{U_{\mathrm{w}}} = I_{10} \tag{38}$$

where I_{10} denotes the rms current of a non-HGL. The derivation shows that the generating current harmonics in the load increases the fundamental current, I_1, or the rms value of the working current, I_{w}.

The active power of the supply resistance contains two components. First there is the reflected active power associated with harmonic current, i.e.,

$$\Delta P_{\mathrm{sh}} = R_{\mathrm{s}} \left\| i_{\mathrm{h}} \right\|^2 = P_{\mathrm{r}} \tag{39}$$

The second component consists of the power loss on the supply source impedance associated with the fundamental current harmonic, i.e.,

$$\Delta P_{\mathrm{s1}} = R_{\mathrm{s}} I_1^{\,2} \tag{40}$$

These two components increase the overall active power loss on the supply impedance,

$$\Delta P_{\mathrm{s}} = \Delta P_{\mathrm{s1}} + \Delta P_{\mathrm{s}} = R_{\mathrm{s}} I_1^{\,2} + P_{\mathrm{r}} = R_{\mathrm{s}} I_1^{\,2} + P_{\mathrm{w}} - P \tag{41}$$

Notice that it is possible to calculate the supply resistance R_s from the measurements of the voltage and currents from the load terminals, i.e.,

$$R_s = \frac{P}{\|i_h\|^2} = \frac{P_w - P}{\|i\|^2 - I_1^2} \tag{42}$$

Thus, the active power loss on the supply source impedance can be expressed in terms of known parameters, i.e. ,

$$\Delta P_s = R_s I_1^2 + (P_w - P) = (P_w - P)\frac{\|i\|^2}{\|i\|^2 - I_1^2} = P_r \frac{\|i\|^2}{\|i\|^2 - I_1^2} \tag{43}$$

Therefore if it is possible to measure the working and active powers along with the rms values of the load current and the fundamental current, then it is possible to calculate the active power loss of the supply system from the load's point of view.

Illustration 1. Calculate the working and reflected active powers of a load with a rectifier supplying a DC motor from an AC source. This AC source has sinusoidal voltage *e* with purely resistive supply source impedance. Assume that the rectifier is lossless and neglecting the inductance of the motor armature (only purely resistive losses) See Appendix A for detailed calculations.

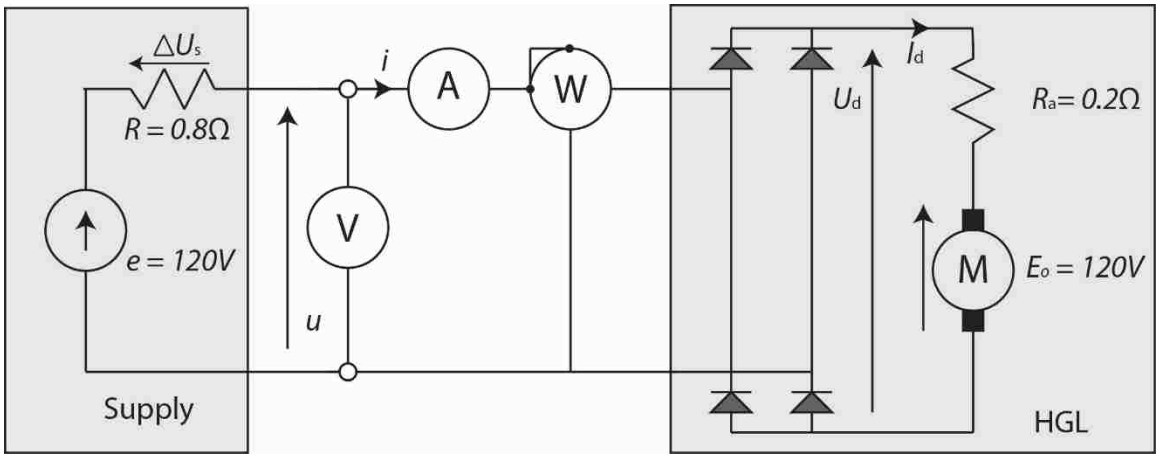

Figure 4.4: Rectifier for DC Motor from AC Voltage Source

The load voltage *u* and the supply current *i* has the waveform of,

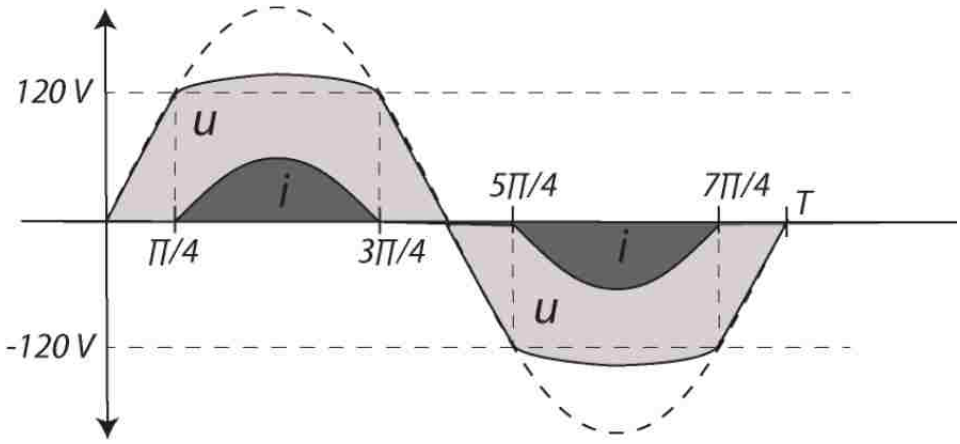

Figure 4.5: Voltage and Current Waveforms for Illustration 1

First, the fundamental current i_1 must be calculated from the supply voltage *e* and supply current *i*, i.e.,

$$e = \sqrt{2}E\cos\omega_1 t = 120\sqrt{2}\cos\omega_1 t \tag{44}$$

$$i(t) = \frac{\sqrt{2}E\cos\omega_1 t - E_0}{R_s + R_a} = \frac{120\sqrt{2}\cos\omega_1 t - 120}{0.8 + 0.2} \tag{45}$$

The crms $\boldsymbol{I}_1$ can be calculated by,

$$\boldsymbol{I}_1 = \frac{\sqrt{2}}{T}\int_0^T i(t)e^{-j\omega_1 t}dt = 21.8e^{-j\frac{\pi}{2}}[A] \tag{46}$$

and the fundamental voltage u_1 should be calculated from the current wave form *i* in Figure 4.4 that has the form,

$$\boldsymbol{U}_1 = \frac{\sqrt{2}}{T}\int_0^T u(t)e^{-j\omega_1 t}dt = 102.56e^{-j\frac{\pi}{2}}[V] \tag{47}$$

Next, the rms load current is calculated from the load current waveform in figure 4.5, i.e.,

$$\|i_{\mathrm{d}}\| = \sqrt{\frac{1}{T}\int_0^T i^2(t)dt} = 25.48[A] \tag{48}$$

Afterwards, the DC current, $\overline{i_{\mathrm{d}}}$ is calculated from the same load current waveform in figure 4.5, i.e.,

$$\overline{i_{\mathrm{d}}} = \frac{1}{T}\int_0^T i(t)dt = 16.39[A] \tag{49}$$

Finally, the working active power can be calculated as a product of the voltage and current magnitudes, i.e.,

$$P_{\mathrm{1}} = U_{\mathrm{1}} I_{\mathrm{1}} \cos\varphi_{\mathrm{1}} = 102.56 \times 21.8 = 2235.8[W] \tag{50}$$

and the active power on the load,

$$P = \overline{i_{\mathrm{d}}} E_0 + R_{\mathrm{a}} \|i_{\mathrm{d}}\|^2 = 16.38(120) + 25.48^2(0.2) = 2097[W] \tag{51}$$

Therefore, the reflected active power can be calculated from (35) and (36), i.e.,

$$P_r = P_{\mathrm{w}} - P = 2235.8 - 2097 = 138.8[W] \tag{52}$$

The main conclusion from illustration 1 is that the working active power P_{w} is higher than active power P by the difference of the reflected active power P_{r}. Since the working active power P_{w} is the power needed to run equipment that generates harmonics, the customer should be charged for the energy needed to run the device, referred to as *working energy*, i.e.,

$$W_{\mathrm{w}} = \int_{month} P_{\mathrm{w}} dt \tag{53}$$

The diagram in figure 4.6 depicts the different energy flow directions for active power, working active power, and reflected active power.

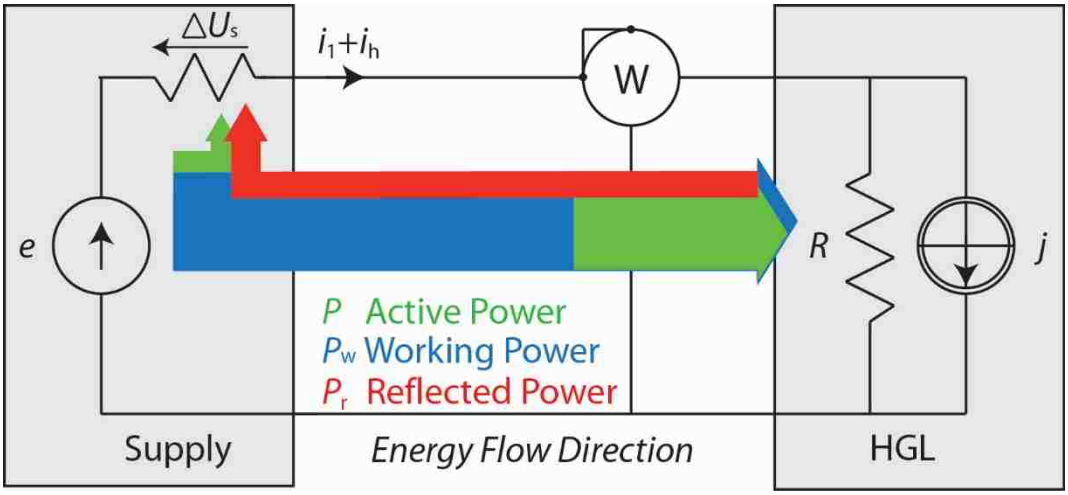

Figure 4.6: Energy Flow Diagram for Single Phase HGL

4.3 Detrimental Active Power for Single Phase Systems

For instances when supply side harmonic distortion occurs, there is a possibility that the harmonic power can also prove harmful to the customer. Normal LTI loads can be affected by this harmonic power originating from the supply, but it is unsure at this point if it is truly harmful or beneficial in terms of active power. One can inquire on a case by case scenario to determine the detrimental effects of supply side distortion, but progress to generalize to a power concept has not been researched. It is worthy to note that there is a possibility for advancement in this area and requires further research at a later point in time.

CHAPTER 5. THREE PHASE ACITVE POWER

5.1 Working Active Power for Three Phase Systems

Similarly to the single phase system, working active power can be defined for three phase systems with HGLs. First consider the model below consisting of a three wire circuit supplied from a three phase symmetrical sinusoidal voltage supply with a balanced HGL.

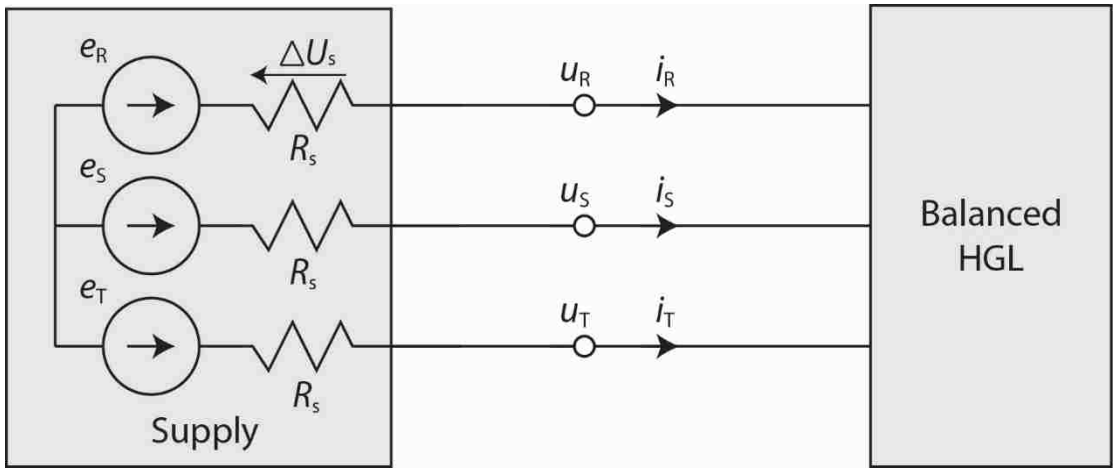

Figure 5.1: Three Phase Three Wire System with Balanced HGL

Because the system is completely balanced, we can treat the three phase system as separate single phase systems. Using vector notation, the three load voltages and currents can be descried as such,

$$\boldsymbol{u} = \begin{bmatrix} u_R \\ u_S \\ u_T \end{bmatrix} \qquad \boldsymbol{i} = \begin{bmatrix} i_R \\ i_S \\ i_T \end{bmatrix} \tag{54}$$

Similarly to the single phase system's (26), the load current can be decomposed,

$$\boldsymbol{i} = \sum_{n \in N} \boldsymbol{i}_n = \boldsymbol{i}_1 + \boldsymbol{i}_h = \boldsymbol{i}_{1aC} + \boldsymbol{i}_h \tag{55}$$

The current of each phase that is in phase with the voltage fundamental harmonic is considered the working current, i.e.,

$$\boldsymbol{i}_{\mathrm{w}} = \boldsymbol{i}_{1\mathrm{aC}} \tag{56}$$

Therefore, the load current can be expressed in the form,

$$\boldsymbol{i} = \boldsymbol{i}_{\mathrm{w}} + \boldsymbol{i}_{\mathrm{h}} \tag{57}$$

In a response to the HGL, the load voltage becomes distorted by the distorted load current having the form,

$$\boldsymbol{u} = \sum_{n \in N} \boldsymbol{u}_n = \boldsymbol{u}_1 + \boldsymbol{u}_{\mathrm{h}} \tag{58}$$

The fundamental harmonic of the load voltage is considered the working voltage, i.e.,

$$\boldsymbol{u}_{\mathrm{w}} = \boldsymbol{u}_1 \tag{59}$$

So that the active power of the load is defined as,

$$P = (\boldsymbol{u}, \boldsymbol{i}) = \sum_{n \in N} P_n = P_1 + P_2 + P_3 + \ldots + P_n \tag{60}$$

The working active power is the scalar product of the fundamental harmonic components of the working current and working voltage, i.e.,

$$P_{\mathrm{w}} = (\boldsymbol{u}_1, \boldsymbol{i}_{1\mathrm{aC}}) \tag{61}$$

The rest of the higher order harmonic powers ($n < 1$) associated with the load generated current are dissipated off the supply resistance in the form,

$$P_n = (\boldsymbol{u}_n, \boldsymbol{i}_n) = -(R_{\mathrm{s}} \|\boldsymbol{i}_n\|) \|\boldsymbol{i}_n\| = -R_{\mathrm{s}} \|\boldsymbol{i}_n\|^2 \tag{62}$$

Similarly to the single phase system,

$$P_{\mathrm{h}} = (P_2 + P_3 + \ldots + P_n) < 0 \tag{63}$$

Therefore the active power will have the form,

$$P = P_{\mathrm{w}} + P_{\mathrm{h}} \tag{64}$$

Three phase systems become more complicated when there is an imbalance in the load, thus a new approach is needed to define the three phase components. Now consider the same three wire, three phase system supplied by a symmetrical sinusoidal supply but with an unbalanced resistive LTI load shown in figure 5.2.

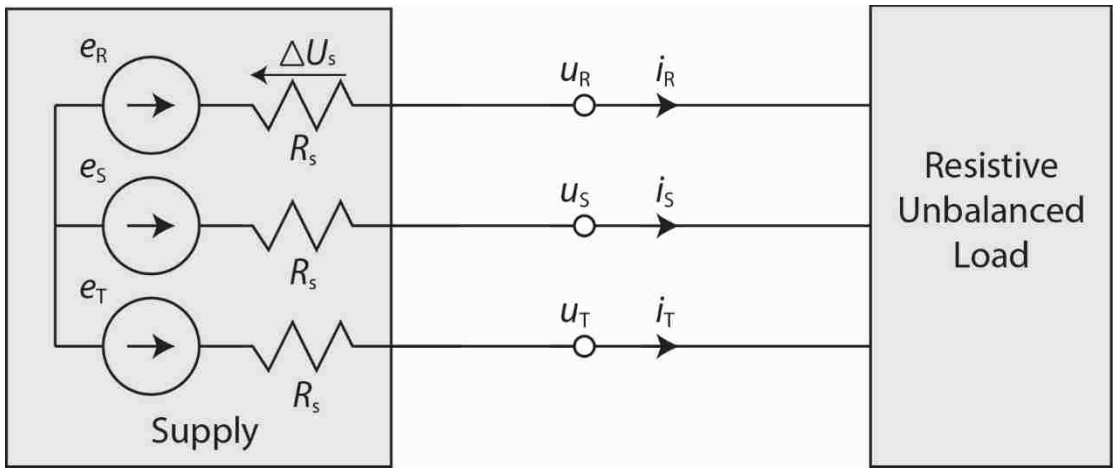

Figure 5.2: Three Phase Three Wire System with Unbalanced LTI Load

This system can be represented with positive and negative symmetrical components,

$$\begin{bmatrix} \boldsymbol{u}^{\mathrm{p}} \\ \boldsymbol{u}^{\mathrm{n}} \end{bmatrix} = \frac{1}{3}\begin{bmatrix} 1 & \alpha & \alpha^* \\ 1 & \alpha^* & \alpha \end{bmatrix}\begin{bmatrix} u_{\mathrm{R}} \\ u_{\mathrm{S}} \\ u_{\mathrm{T}} \end{bmatrix} \qquad \alpha = 1e^{j120^\circ} \tag{65}$$

$$\begin{bmatrix} \boldsymbol{i}^{\mathrm{p}} \\ \boldsymbol{i}^{\mathrm{n}} \end{bmatrix} = \frac{1}{3}\begin{bmatrix} 1 & \alpha & \alpha^* \\ 1 & \alpha^* & \alpha \end{bmatrix}\begin{bmatrix} i_{\mathrm{R}} \\ i_{\mathrm{S}} \\ i_{\mathrm{T}} \end{bmatrix} \qquad \alpha = 1e^{j120^\circ} \tag{66}$$

Such that the load voltage and currents have the form,

$$\boldsymbol{u} = \boldsymbol{u}^{\mathrm{p}} + \boldsymbol{u}^{\mathrm{n}} \tag{67}$$

$$\boldsymbol{i} = \boldsymbol{i}^{\mathrm{p}} + \boldsymbol{i}^{\mathrm{n}} \tag{68}$$

The working current and voltage is the positive sequence components of the current and voltage, i.e.,

$$\boldsymbol{u}_{\mathrm{w}} = \boldsymbol{u}^{\mathrm{p}} \tag{69}$$

$$\boldsymbol{i}_{\mathrm{w}} = \boldsymbol{i}^{\mathrm{p}} \tag{70}$$

Active power is calculated as the scalar product of the positive sequence and negative sequence components of the voltage and currents. The scalar product of components of different sequences is orthogonal, thus having a zero scalar product. (see Appendix B for details) Therefore, the active power at the load terminal can be written as,

$$P = (\boldsymbol{u}, \boldsymbol{i}) = (\boldsymbol{u}^{\mathrm{p}} + \boldsymbol{u}^{\mathrm{n}}, \boldsymbol{i}^{\mathrm{p}} + \boldsymbol{i}^{\mathrm{n}}) = (\boldsymbol{u}^{\mathrm{p}}, \boldsymbol{i}^{\mathrm{p}}) + (\boldsymbol{u}^{\mathrm{n}}, \boldsymbol{i}^{\mathrm{n}}) = P^{\mathrm{p}} + P^{\mathrm{n}} \tag{71}$$

The positive sequence components will contribute to active power P^{p}. Assuming sinusoidal symmetrical voltage source, the negative sequence voltage occurs due to the current passing through the supply resistance R_{s}, i.e.,

$$P^{\mathrm{n}} = (\boldsymbol{u}^{\mathrm{n}}, \boldsymbol{i}^{\mathrm{n}}) = (-R_{\mathrm{s}}\boldsymbol{i}^{\mathrm{n}}, \boldsymbol{i}^{\mathrm{n}}) = -R_{\mathrm{s}} \left\| \boldsymbol{i}^{\mathrm{n}} \right\|^2 < 0 \tag{72}$$

The positive sequence active power is higher than the active power by the difference of the negative sequence active power, i.e.,

$$P^{\mathrm{p}} = P - P^{\mathrm{n}} > P \tag{73}$$

The working active power is then defined as the active power of the positive sequence,

$$P_w = P^p \tag{74}$$

In a three phase three wire system with sinusoidal symmetrical voltage supplies, the two cases of a balanced HGL and a unbalanced resistive LTI load has striking similarities with regards to the orientation of power flow. First there is a positive active power component that sends energy from the supply to the load shown in figure 5.3.

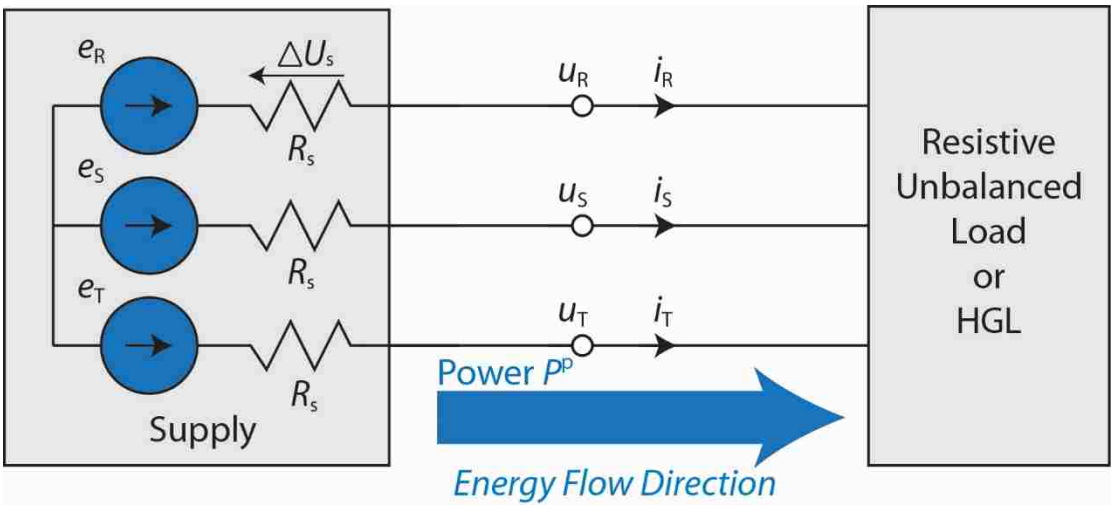

Figure 5.3: Three Phase Three Wire System Positive Energy Flow

The negative active power component sends energy from the load back to the source. This was shown in two scenarios. First, the HGL acts like a current source that has a decomposed current component that sends energy back to the source. Second, an unbalanced load will have unequal current in each phase causing additional losses which can be described as a current source sending energy back to the supply.

It is quiet counter intuitive to think this way so the reader must remember that current decomposition decomposes currents into fictitious currents that represent physical phenomenon. In these cases, HGL's distorted current waveform can be represented as current sources injecting

harmonic current into the system causing additional losses on the supply impedance. Similarly, the unbalanced loading causes unbalanced current flow, represented as current sources, resulting in additional losses on the supply impedance.

5.2 Reflected Active Power for Three Phase Systems

Similar to the single phase system, active power of higher order harmonics contribute to reflected active power in a three phase system. This harmonic active energy is dissipated on the supply impedance. Additionally, shown prior, active power of the negative sequence component also reflects energy back to the supply impedance. Illustrations are shown to further explain and support the reflected active power concept for three phase systems.

First, recall the three phase system in the previous section composed of a balanced HGL supplied with a symmetrical and sinusoidal voltage supply. Equation (62) shows that the higher order harmonic power (n < 1) dissipates off the supply impedance. Following, equation (63) shows that all of the higher order harmonic powers are negative. This means that the higher order harmonic power originates from the HGL and sends energy back to the source. Thus, the same single phase reflected active power equation, (36), can be applied to balanced three phase systems, i.e.,

$$P_{\mathrm{r}} = -P_{\mathrm{h}} = -(\boldsymbol{u}_{\mathrm{n}}, \boldsymbol{i}_{\mathrm{n}}) \qquad n = 2,3,4,...N \tag{75}$$

Thus, the supply resistance can be calculated by the difference of working active power and the load active power divided by the rms of the harmonic current, i.e.,

$$R_{\mathrm{s}} = \frac{P_{\mathrm{w}} - P}{\left\| \boldsymbol{i}_{\mathrm{n}} \right\|^2} \qquad n = 2,3,4,...N \tag{76}$$

As with the single phase system, the rms value of the working active current must be higher than the rms of the active load current. $\|\boldsymbol{i}_{10}\|$ denotes a rms current of a non-HGL of equal active power, i.e.,

$$\|\boldsymbol{i}_1\| = \|\boldsymbol{i}_w\| = \frac{P_w}{\|\boldsymbol{u}_w\|} > \frac{P}{\|\boldsymbol{u}_w\|} = \|\boldsymbol{i}_{10}\| \tag{77}$$

Thus, with a higher rms current, additional losses in the supply impedance will be present along with the energy dissipation from the reflected active power component, i.e.,

$$\Delta P_s = R_s \|\boldsymbol{i}_1\|^2 - P^n = -R_s \|\boldsymbol{i}_1\|^2 + R_s \|\boldsymbol{i}_n\|^2 = R_s \|\boldsymbol{i}\|^2 \tag{78}$$

The second scenario to consider is a bit more complicated as dealing with unbalanced systems; one cannot simply extrapolate concepts from a single phase system. Recall that the previous section's scenario involved a symmetrical sinusoidal supply with an unbalanced resistive LTI load. Active power of this system composed of positive sequence and negative sequence powers were shown in equation (71). Voltages and currents of negative sequence components were shown to cause a negative sequence active power in equation (72). Similar to the previous reflected active power of HGLs, one can also conclude that this negative sequence component also contributes to reflected active power, i.e.,

$$P_r = -P_h = -(\boldsymbol{u}^n, \boldsymbol{i}^n) \tag{79}$$

With the reflected active power, the supply resistance can be calculated by the difference of working active power and the load active power divided by the rms of the negative sequence current component, i.e.,

$$R_{\mathrm{s}} = \frac{P_{\mathrm{w}} - P}{\left\| \boldsymbol{i}^{\mathrm{n}} \right\|^2} \tag{80}$$

As with the single phase system, the rms value of the working active current must be higher than the rms of the active load current, i.e.,

$$\left\| \boldsymbol{i}^{\mathrm{p}} \right\| = \left\| \boldsymbol{i}_{\mathrm{w}} \right\| = \frac{P}{\left\| \boldsymbol{u}_{\mathrm{w}} \right\|} > \frac{P}{\left\| \boldsymbol{u}^{\mathrm{p}} \right\|} \tag{81}$$

Thus, with a higher rms current, additional losses in the supply impedance will be present along with the energy dissipation from the reflected active power component, i.e.,

$$\Delta P_{\mathrm{s}} = R_{\mathrm{s}} \left\| \boldsymbol{i}^{\mathrm{p}} \right\|^2 - P^{\mathrm{n}} = -R_{\mathrm{s}} \left\| \boldsymbol{i}^{\mathrm{p}} \right\|^2 + R_{\mathrm{s}} \left\| \boldsymbol{i}^{\mathrm{n}} \right\|^2 = R_{\mathrm{s}} \left\| \boldsymbol{i} \right\|^2 \tag{82}$$

Illustration 2. A three phase purely resistive system with a balanced load is present in figure 5.4. The supply is symmetrical sinusoidal voltage supply with a line to ground voltage rms of E = 240V. The load parameters are selected to require an active power of P = 100kW to operate. The power loss in the supply resistance is ΔP = 5kW.

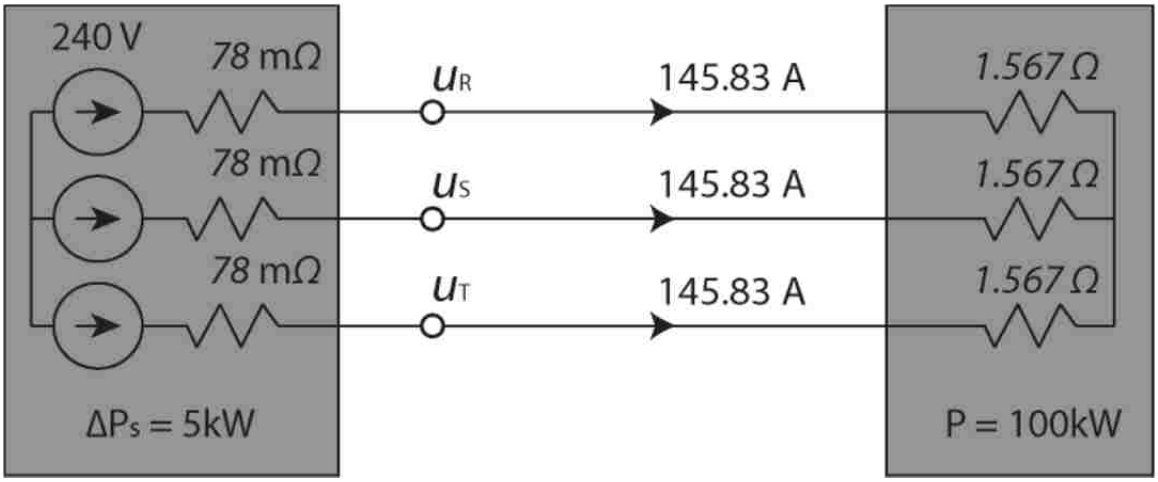

Figure 5.4: Balanced Load for Illustration 2

Keeping the same active power on the load, the load circuit can be reconfigured as an unbalanced load with the same supply shown in figure 5.5.

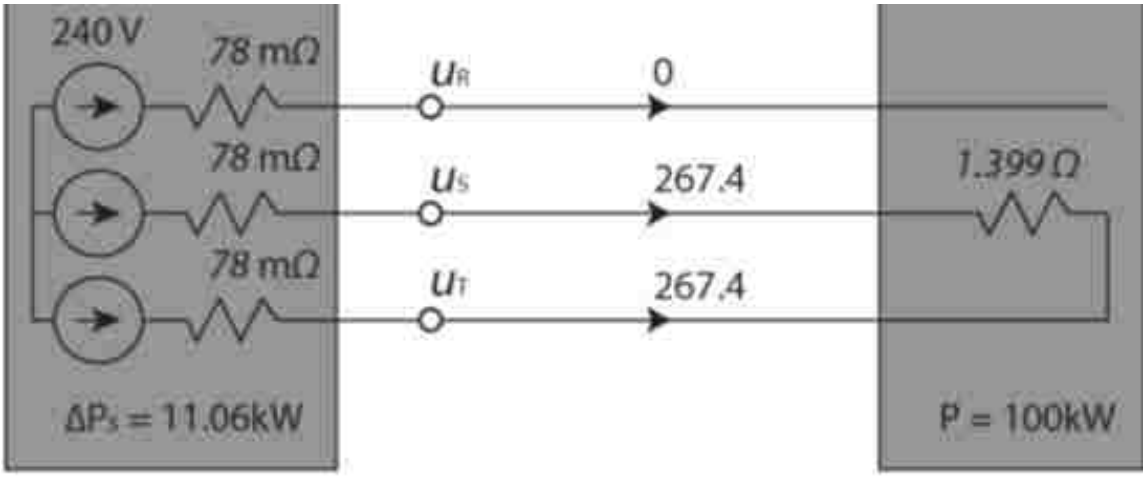

Figure 5.5: Unbalanced Load for Illustration 2

The line voltage for phase R can be expressed as $\boldsymbol{E}_{\mathrm{R}} = 120e^{j0}[\mathrm{V}]$, the line currents crms value of the circuit are then,

$$\boldsymbol{I}_{\mathrm{S}} = \frac{\boldsymbol{E}_{\mathrm{S}} - \boldsymbol{E}_{\mathrm{T}}}{2R_{\mathrm{S}} + R} = \frac{240e^{-j120} - 240e^{j120}}{2(0.078) + 1.399} = 267.4e^{-j90}[\mathrm{A}] \tag{83}$$

$$\boldsymbol{I}_{\mathrm{T}} = -\boldsymbol{I}_{\mathrm{S}} = 267.4e^{j90}[\mathrm{A}] \tag{84}$$

Thus, the crms load voltage can be calculated as such,

$$\boldsymbol{U}_{\mathrm{S}} = \boldsymbol{E}_{\mathrm{S}} - R_{\mathrm{S}}\boldsymbol{I}_{\mathrm{S}} = 240e^{-j120} - 0.078 \times 267.4e^{-j90} = 222.2e^{-j122.6}[\mathrm{V}] \tag{85}$$

$$\boldsymbol{U}_{\mathrm{T}} = \boldsymbol{E}_{\mathrm{T}} - R_{\mathrm{S}}\boldsymbol{I}_{\mathrm{T}} = 240e^{j120} - 0.078 \times 267.4e^{j90} = 222.2e^{j122.6}[\mathrm{V}] \tag{86}$$

The load current for the whole system can be decomposed into symmetrical components, i.e.,

$$\begin{bmatrix} \boldsymbol{I}^{\mathrm{p}} \\ \boldsymbol{I}^{\mathrm{n}} \end{bmatrix} = \frac{1}{3}\begin{bmatrix} 1 & \alpha & \alpha^* \\ 1 & \alpha^* & \alpha \end{bmatrix}\begin{bmatrix} \boldsymbol{I}_{\mathrm{R}} \\ \boldsymbol{I}_{\mathrm{S}} \\ \boldsymbol{I}_{\mathrm{T}} \end{bmatrix} = \frac{1}{3}\begin{bmatrix} 1 & \alpha & \alpha^* \\ 1 & \alpha^* & \alpha \end{bmatrix}\begin{bmatrix} 0 \\ 267.4e^{-j90} \\ 267.4e^{j90} \end{bmatrix} = \begin{bmatrix} 154.4e^{j0} \\ -154.4e^{j0} \end{bmatrix}[\mathrm{A}] \tag{87}$$

Similar to the load current, the load voltage can also be decomposed into symmetrical components, i.e.,

$$\begin{bmatrix} \boldsymbol{U}^{\mathrm{p}} \\ \boldsymbol{U}^{\mathrm{n}} \end{bmatrix} = \frac{1}{3}\begin{bmatrix} 1 & \alpha & \alpha^* \\ 1 & \alpha^* & \alpha \end{bmatrix}\begin{bmatrix} \boldsymbol{U}_{\mathrm{R}} \\ \boldsymbol{U}_{\mathrm{S}} \\ \boldsymbol{U}_{\mathrm{T}} \end{bmatrix} = \frac{1}{3}\begin{bmatrix} 1 & \alpha & \alpha^* \\ 1 & \alpha^* & \alpha \end{bmatrix}\begin{bmatrix} 240e^{j0} \\ 222.2e^{-j122.6} \\ 222.2e^{j122.6} \end{bmatrix} = \begin{bmatrix} 228e^{j0} \\ 11.83e^{j0} \end{bmatrix}[\mathrm{V}] \tag{88}$$

Therefore, the working active power of the load can be calculated as,

$$P_{\mathrm{w}} = P^{\mathrm{p}} = (\boldsymbol{u}^{\mathrm{p}}, \boldsymbol{i}^{\mathrm{p}}) = 3U^{\mathrm{p}}I^{\mathrm{p}} = 3\times 228\times 154.4 = 3(35.2\mathrm{k}) = 105.6\mathrm{k}[\mathrm{W}] \tag{89}$$

and the reflected power can be calculated as,

$$P_{\mathrm{r}} = P^{\mathrm{n}} = (\boldsymbol{u}^{\mathrm{n}}, \boldsymbol{i}^{\mathrm{n}}) = 3U^{\mathrm{n}}I^{\mathrm{n}} = 3\times 11.83\times 154.4 = 3(1.83\mathrm{k}) = 5.48\mathrm{k}[\mathrm{W}] \tag{90}$$

The working active current rms value can then be calculated as,

$$\|\boldsymbol{i}_{\mathrm{w}}\| = \frac{P_{\mathrm{w}}}{\|\boldsymbol{u}_{\mathrm{w}}\|} = \frac{105.6\mathrm{k}}{\sqrt{3}\times 228} = 267.4[\mathrm{A}] \tag{91}$$

Finally, the active power loss on the supply resistance is elevated to,

$$\Delta P_{\mathrm{S}} = R_{\mathrm{S}}\|\boldsymbol{i}_{\mathrm{w}}\|^2 + P_{\mathrm{r}} = 0.078\times 267.4^2 + 5.48\mathrm{k}{=}11.06\mathrm{k}[\mathrm{W}] \tag{92}$$

As one can see, the power loss on the supply nearly doubled in size. Thus, instead of a standard 5% power loss, now the utility suffers from a 10% power loss.

5.3 Detrimental Active Power for Three Phase Systems

Detrimental active power is the active power component delivered to the load that is provided by distorted and/or asymmetrical supplies. This harmonic active energy is then dissipated into the load rather than being converted to useful work. To some loads, such as induction motors, this dissipation of energy can even be harmful to the components. Both, asymmetrical supply and distorted supply will be analyzed.

Assume that the supply voltage at the load terminals of an induction motor is asymmetrical. The equivalent circuit of a supply is shown in figure 5.6. Since the load voltage and currents are asymmetrical, they will contain both positive and negative sequence components, i.e.,

$$\boldsymbol{u} = \boldsymbol{u}^{\mathrm{p}} + \boldsymbol{u}^{\mathrm{n}} \tag{93}$$

$$\boldsymbol{i} = \boldsymbol{i}^{\mathrm{p}} + \boldsymbol{i}^{\mathrm{n}} \tag{94}$$

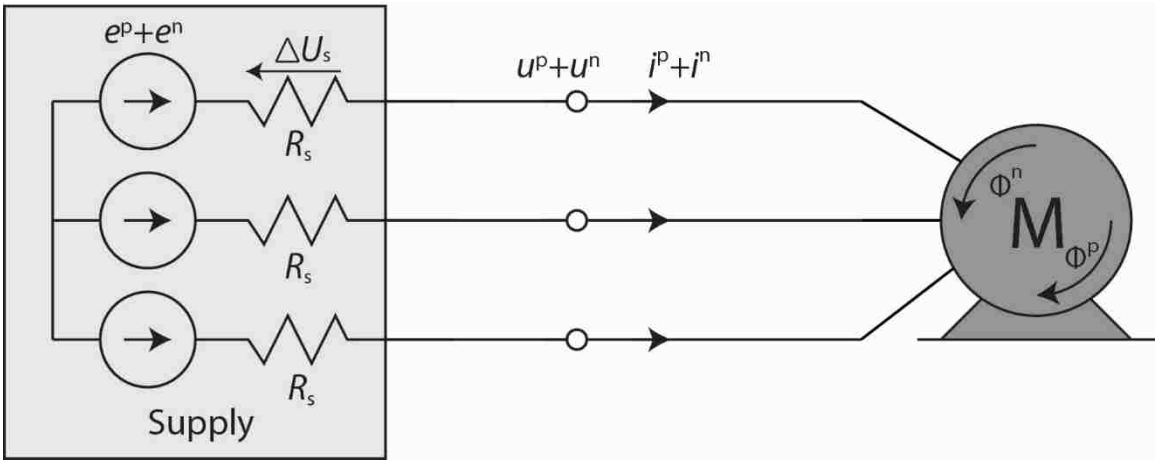

Figure 5.6: Asymmetrical Supply with Induction Motor

Active power is defined as the scalar product of the load voltage and current. Thus, according to (93) and (94), active power is composed of a positive and negative sequence component, i.e.,

$$P = (\boldsymbol{u}, \boldsymbol{i}) = (\boldsymbol{u}^{\mathrm{p}} + \boldsymbol{u}^{\mathrm{n}}, \boldsymbol{i}^{\mathrm{p}} + \boldsymbol{i}^{\mathrm{n}}) = (\boldsymbol{u}^{\mathrm{p}}, \boldsymbol{i}^{\mathrm{p}}) + (\boldsymbol{u}^{\mathrm{n}}, \boldsymbol{i}^{\mathrm{n}}) = P^{\mathrm{p}} + P^{\mathrm{n}} \tag{95}$$

Thus, the voltage and current of the positive and negative sequence convey energy to the motor separately.

It is important to note that both the negative sequence power and the positive sequence power have positive flow, this means that both positive sequence and negative sequence powers originate from the source. This is natural, since the motor is a LTI load and the asymmetry is in the supply. Figure 5.7 shows the direction of energy flow.

The supply current flowing in the stator windings creates a rotating magnetic field in the motor. Since the current is composed of positive and negative sequence currents, there will be a resulting magnetic field rotating in the positive direction and a magnetic field rotating in the negative direction. The positive rotating magnetic field is the dominating one that results in output power on the shaft while the negative rotating magnetic field results in torque in the negative direction.

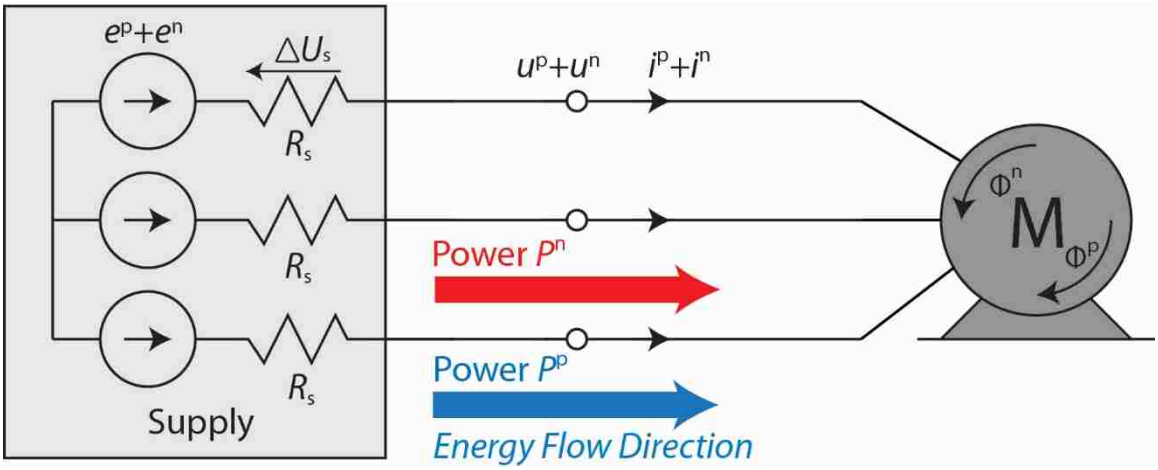

Figure 5.7: Power Flow of Induction Motor with Asymmetrical Supply

Therefore, the positive sequence power, P^p is regarded as useful power as in equation (74), and the negative sequence power, P^n is considered detrimental active power, i.e.,

$$P_d = P^n \tag{96}$$

Thus, active power is composed of two components, one that is useful, and one that is detrimental, i.e.,

$$P = P_w + P_d \tag{97}$$

From equation (93), the working active power, P_w is lower than the active power P and the difference being the detrimental active power, P_d. Customers are normally charged with respects to active power P. But, from equations (96) and (97), it is clear that a portion of the active power

charged is not useful to the customer. Instead, this energy is released as heat in the motor and negative torque. It is not fair that the customer has to pay for energy delivered to him that is not useful, but in fact detrimental.

The second case to analyze is when the supply now contains distortion in the form of higher ordered harmonics. This distorted supply sends energy to the motor that contains voltages and currents harmonics i.e.,

$$\boldsymbol{u} = \sum_{n \in N} \boldsymbol{u}_n = \boldsymbol{u}_1 + \boldsymbol{u}_h \tag{98}$$

$$\boldsymbol{i} = \sum_{n \in N} \boldsymbol{i}_n = \boldsymbol{i}_1 + \boldsymbol{i}_h \tag{99}$$

Again, active power is defined as the scalar product of the load voltage and current. Thus, according to (94) and (95), active power is composed of a fundamental power component, and a higher order harmonic component, i.e.,

$$P = (\boldsymbol{u}, \boldsymbol{i}) = (\boldsymbol{u}_1 + \boldsymbol{u}_h, \boldsymbol{i}_1 + \boldsymbol{i}_h) = (\boldsymbol{u}_1 + \boldsymbol{i}_1) + (\boldsymbol{u}_h + \boldsymbol{i}_h) = P_1 + P_h \tag{100}$$

The fundamental active power and the harmonic active power can be defined in terms of working active power and detrimental active power. The fundamental positive sequence power, P_1 is considered working power as in equation (61). Now, notice that since the distortion is from the supply side. The harmonic power, P_h is positive, i.e.,

$$P_h = (P_2 + P_3 + \ldots + P_n) \geq 0 \tag{101}$$

The supply current flowing in the stator windings is now composed of fundamental and higher order harmonic currents, there will be a resulting magnetic field rotating at approximately ω_1 angular velocity and other magnetic fields rotating at higher speeds of $n\omega_1$ angular velocity. The magnetic field with angular velocity of ω_1 is the dominating magnetic field resulting in output power on the shaft.

The current harmonics of order $n = 3k\text{-}1$ are negative sequenced with respects to the fundamental current. Therefore, the negative sequence currents create a magnetic field rotating faster and in the opposite direction of the fundamental magnetic field that results in torque reduction. Since the voltage induced in the rotor is proportional to the relative rotational speed of the magnetic field, depending on the harmonic order, the voltage could be every high even though the magnetic field itself is relatively weak. This results in energy dissipation in the rotor and increased temperatures.

The current harmonics of order $n = 3k+1$ are positive sequenced with respects to the fundamental current. This will result in a magnetic field that rotates at a higher angular velocity than the primary magnetic field. Again, the voltage induced in the rotor can become significant even though the magnetic field is relatively weak depending on harmonic order. The positive rotating magnetic field at higher angular velocity than the fundamental magnetic field acts in a similar fashion as a locked rotor in the induction motor. Naturally, this is a waste of energy that is in turn dissipated as heat in the motor.

Therefore, the harmonic active power cannot be regarded as useful power, but instead is interpreted as detrimental active power, i.e.,

$$P_{\mathrm{d}} = P_{\mathrm{h}} \tag{102}$$

Also, it is clear that the fundamental active power component is considered useful active power and thus working active power as in equation (61). Again, similar to the previous part, active power is composed of two components, one that is useful, and one that is detrimental as in equation (97).

With these two cases of supply quality issues examined individually, a supply that is both distorted and asymmetrical should be analyzed. The load voltages and currents can be decomposed into,

$$\boldsymbol{u} = \boldsymbol{u}_1^{\mathrm{p}} + \boldsymbol{u}_1^{\mathrm{n}} + \boldsymbol{u}_{\mathrm{h}} \tag{103}$$

$$\boldsymbol{i} = \boldsymbol{i}_1^{\mathrm{p}} + \boldsymbol{i}_1^{\mathrm{n}} + \boldsymbol{i}_{\mathrm{h}} \tag{104}$$

Active power is the scalar product of the load voltages and currents. Thus, with equations (98) and (99), the active power can be expressed as,

$$P = (\boldsymbol{u}, \boldsymbol{i}) = (\boldsymbol{u}_1^{\mathrm{p}} + \boldsymbol{u}_1^{\mathrm{n}} + \boldsymbol{u}_{\mathrm{h}}, \boldsymbol{i}_1^{\mathrm{p}} + \boldsymbol{i}_1^{\mathrm{n}} + \boldsymbol{i}_{\mathrm{h}}) \tag{105}$$

Voltages and currents of different sequences are orthogonal as well as voltages and currents of different harmonic orders. Therefore, equation (105) can be simplified to,

$$P = (\boldsymbol{u}_1^{\mathrm{p}}, \boldsymbol{i}_1^{\mathrm{p}}) + (\boldsymbol{u}_1^{\mathrm{n}}, \boldsymbol{i}_1^{\mathrm{n}}) + (\boldsymbol{u}_{\mathrm{h}}, \boldsymbol{i}_{\mathrm{h}}) = P_1^{\mathrm{p}} + P_1^{\mathrm{n}} + P_{\mathrm{h}} \tag{106}$$

From equations (97) and (102), active power of the negative sequence and active power of harmonic order are considered detrimental, therefore detrimental active power can be rewritten,

$$P_{\mathrm{d}} = P_1^{\mathrm{n}} + P_{\mathrm{h}} \tag{107}$$

Detrimental active power can also be considered for other loads, such as a three phase rectifier shown in figure 5.8. Assume that the supply voltage is distorted, but symmetrical. In the circuit, the supply voltages and currents can be decomposed as so,

$$\boldsymbol{u} = \boldsymbol{u}_1^{\mathrm{p}} + \boldsymbol{u}_{\mathrm{h}} \tag{108}$$

$$\boldsymbol{i} = \boldsymbol{i}_1^{\mathrm{p}} + \boldsymbol{i}_{\mathrm{h}} \tag{109}$$

This current decomposition has a special instance, as harmonic generation originates from the supply and the load side. Mentioned before, this leads to some short fallings of the working

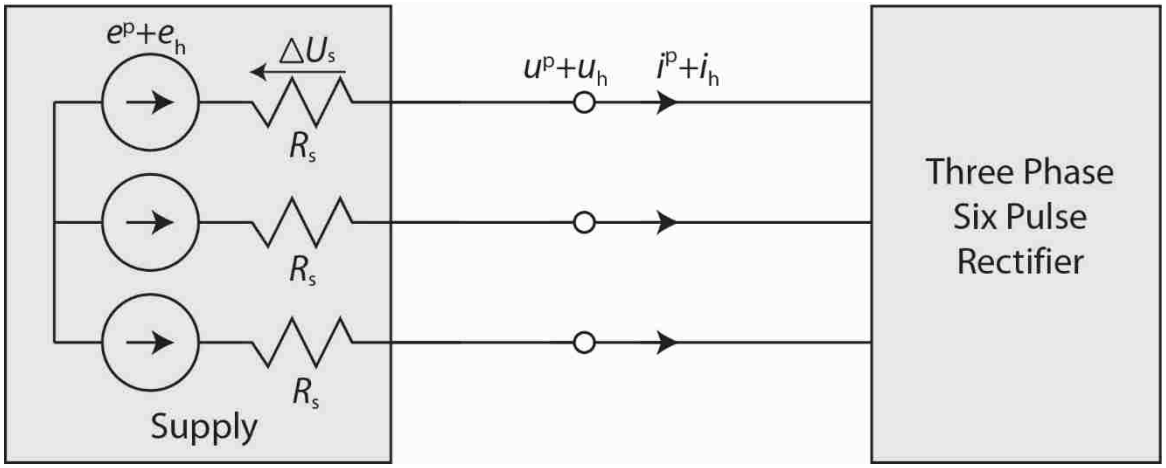

Figure 5.8: Three Phase Rectifier with Distorted Supply

active power concept. Sources of harmonics of different orders are orthogonal to each other, but when two sources exist on the same harmonic order, they are not orthogonal. Therefore, the dominating source for the specific harmonic should be taken into account and the lesser ignored. This will lead to a slight error in the calculations. Realistically, the effects of this this exception does not affect the economic model drastically if at all noticeable.

The active power at the load terminals consist of,

$$P = (\boldsymbol{u}, \boldsymbol{i}) = (\boldsymbol{u}_1^{\mathrm{p}}, \boldsymbol{i}_1^{\mathrm{p}}) + (\boldsymbol{u}_{\mathrm{h}}, \boldsymbol{i}_{\mathrm{h}}) + P_1^{\mathrm{p}} + P_{\mathrm{h}} \tag{110}$$

And working active power is denoted as the positive sequence active power of the fundamental harmonic, i.e.,

$$P_{\mathrm{w}} = P_{\mathrm{l}}^{\mathrm{p}} \tag{111}$$

The harmonic active power is separated into negative and positive energy flow. According to equation (30), active power originating from the source belongs to the set N_{C} and active power originating from the load belongs to the set N_{L}. i.e.,

$$P_{\mathrm{h}} = \sum_{n \in N_{\mathrm{C}}} P_n - \sum_{n \in N_{\mathrm{L}}} P_n \tag{112}$$

Higher order harmonics disturb the operation and performance of the rectifier. Non-sinusoidal voltages contribute to commutation problems and increasing the output ripple of the DC voltage. Increased current rms will also lead to higher temperatures in the equipment. Therefore, the harmonic powers of set N_{C} is considered detrimental, i.e.,

$$P_{\mathrm{d}} = \sum_{n \in N_{\mathrm{L}}} P_n \tag{113}$$

Harmonic active powers of the set N_{L} is considered reflected active power as per equation (40), thus reflected active power can be defined as,

$$P_{\mathrm{r}} = \sum_{n \in N_{\mathrm{C}}} P_n \tag{114}$$

Thus, in such a system, the active power P contains both reflected active power P_{r} and detrimental active power P_{d}. i.e.,

$$P = P_{\mathrm{w}} + P_{\mathrm{d}} - P_{\mathrm{r}} \tag{115}$$

CHAPTER 6. MEASUREMENT OF ACTIVE POWER

6.1 Measuring CRMS for the Fundamental Component

The traditional active power P and the fundamental active power P_1 needs to be measured for the working active power concept. Thus, the voltage and current quantities needs to be measured. The DSP hardware must be configured to simultaneously acquire the load voltage and current samples, $u(k)$ and $i(k)$ respectively. Then, the DSP software can be configured to mathematically calculate the active power and working active power.

For single phase measurements only two simultaneous sampling channels for the load voltage and current are required. Simultaneous sampling is very important, as any delay in one of the samples will alter the phase shift and rms magnitudes. With the sampled voltages and currents, the active power can be calculated over N samples, i.e.,

$$P = \frac{1}{N}\sum_{k=0}^{N-1} u(k) \times i(k) \tag{116}$$

Measuring the working active power requires using Fourier analysis to extract the fundamental voltage and currents component from voltage and current samples. A minimum sampling rate must be used in the Discrete Fourier Transform (DFT) to ensure there is no aliasing components in the results. In this case, the highest order harmonic needed is the fundamental, n = 1. Thus, to meet the Nyquist's criterion of having twice the sampling of the highest harmonic order, N is chosen to be 3, N = 3. Thus, the DFT for the crms of the fundamental load voltage, $\boldsymbol{U}_1$ is,

$$\boldsymbol{U}_1 = \frac{\sqrt{2}}{N}\sum_{k=0}^{N-1} u(k) e^{-j2\frac{\pi}{N}k}, N = 3 \tag{117}$$

Similarly, the DFT for the crms of the fundamental load current, $\boldsymbol{I}_1$ is,

$$\boldsymbol{I}_1 = \frac{\sqrt{2}}{N}\sum_{k=0}^{N-1} i(k)e^{-j2\frac{\pi}{N}k}, N = 3 \tag{118}$$

Finally, the working active power can be calculated as,

$$P_{\mathrm{w}} = \mathrm{Re}\{\boldsymbol{U}_1 \times \boldsymbol{I}_1^*\} \tag{119}$$

To measure the active power for a three wire, three phase system, two voltages and currents waveforms need to be measured with the DSP equipment. Then, the third voltage and current can be calculated since their sum must always equal zero at any point in time assuming no DC voltage component, i.e.,

$$i_{\mathrm{R}}(t) + i_{\mathrm{S}}(t) + i_{\mathrm{T}}(t) \equiv 0 \tag{120}$$

$$u_{\mathrm{R}}(t) + u_{\mathrm{S}}(t) + u_{\mathrm{T}}(t) \equiv 0 \tag{121}$$

Again, simultaneous sampling is necessary not only to have accurate phase shift, but for equations (120) and (121) to hold true. Similar to measurements of single phase systems, the active power can be measured, i.e.,

$$P = \frac{1}{N}\sum_{k=0}^{N-1} u_R(k) \times i_{\mathrm{R}}(k) + u_S(k) \times i_{\mathrm{S}}(k) + u_T(k) \times i_{\mathrm{T}}(k) \tag{122}$$

Calculating the working active power for three phase is more complex than the single phase systems, as the positive sequenced fundamental crms load voltages and currents are needed. The fundamental load voltages and current crms values can be obtained per phase using the DFT techniques from equations (117), (118), (120), and (121) giving us the three fundamental load voltages, $\boldsymbol{U}_{\mathrm{R1}}$, $\boldsymbol{U}_{\mathrm{S1}}$, $\boldsymbol{U}_{\mathrm{T1}}$ and three fundamental load currents, $\boldsymbol{I}_{\mathrm{R1}}$, $\boldsymbol{I}_{\mathrm{S1}}$, $\boldsymbol{I}_{\mathrm{T1}}$. Then, the positive sequenced components of the load voltages can be calculated using the formula,

$$\boldsymbol{U}_1^{\mathrm{p}} = \frac{1}{3}[\boldsymbol{U}_{\mathrm{R1}} + \alpha\boldsymbol{U}_{\mathrm{S1}} + \alpha^*\boldsymbol{U}_{\mathrm{T1}}] \tag{123}$$

Similarly, the positive sequenced component of the load current can be calculated as,

$$\boldsymbol{I}_1^{\mathrm{p}} = \frac{1}{3}[\boldsymbol{I}_{\mathrm{R1}} + \alpha \boldsymbol{I}_{\mathrm{S1}} + \alpha^* \boldsymbol{I}_{\mathrm{T1}}] \tag{124}$$

Finally, the with the positive sequenced fundamental crms of the load voltages and currents, the working active power can be calculated as,

$$P_{\mathrm{w}} = \mathrm{Re}\{\boldsymbol{U}_1^{\mathrm{p}} \times \boldsymbol{I}_1^{\mathrm{p}*}\} \tag{125}$$

6.2 National Instruments DSP Hardware Programming

To measure the active power and working active power, the National Instrument's (NI) DSP hardware system, DAQmx, will be used to acquire the load voltage and current from the system. For measurements of three phase, three wire systems, four simultaneously sampled channels will be needed. Sufficient resolution and sampling speed must be acquired for accurate measurement of load voltages and currents as well.

The NI's DAQmx system composes of a USB based plug and play module. A USB chassis is used to relay information from the DSP module to the computer for integration into the NI software, Labview. The main feature of this chassis is the portability, and the ability to interface with several DSP devices. The chassis is shown in figure 6.1 along with the DSP module. The DSP module used is a NI 9215 module. This module has 4 analog channels for simultaneous sampling in a range of 10 to -10 Volts. The sampling rate is 100kS/sec with a 16 bit resolution [16]. This far exceeds the requirements to sample at the 60 Hz power system frequency. Table 6.1 shows the specifications of the NI 9215 module.

Figure 6.1: National Instrument's DAQmx System

Table 6.1: National Instrument's NI 9215 Module Specifications

Product Name	NI 9215
Simultaneous Channels	4
Resolution	16 bits
Sampling Rate	100 kS/s
Range	10 to -10 V ± 0.6%
Temperature Range	-40° to 70° C

To interface and protect the NI DAQmx system, current and voltage isolators are used to convert the power system voltage and current levels of 120 volts, and 10 ampere to the NI DAQmx system's ±10 V voltage inputs [17]. The experiment's equipment used in the laboratory are a Canadian brand, LabVolt. The LabVolt experiment equipment includes voltage and current isolators, model 9056-1 along with power supply module, model 8840 shown in figure 6.2.

The isolator provides electrical isolation from the experimental setup and the NI DAQmx system with addition of lowering the voltage and current levels much like a current transformer (CT) and potential transformer (PT) in the power system. The specifications of the current isolator can be found on table 6.2.

Figure 6.2: Lab Volt's Current and Voltage Isolators.

Table 6.2: Lab Volt's Model 9056-1 Specifications

Product Name	Lab Volt Model 9056-1
Current Isolation Range	1/10 A
Current Isolation Impedance	0.2/0.02 Ω
Voltage Isolation Range	30/300 V
Voltage Isolation Impedance	27/280 kΩ
Current/Voltage Output	0 to ±10 V ±1% (Full Scale)

Figure 6.3 shows the flow diagram for reading voltages and currents to calculate the working and traditional active powers.

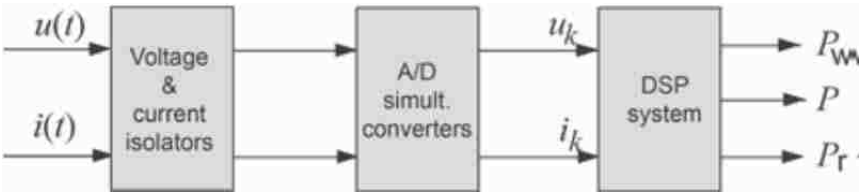

Figure 6.3: Data Acquisition for Measurement of Working Active Power

6.3 National Instruments DSP Software Programming

The software, LabView, will be used to calculate the working active power P_1 and active power P from the sampled voltages $u(k)$ and $i(k)$ from the load terminals. First, the single phase program is built in LabView as block diagrams. This includes reading the samples from the hardware, calculating active power P, extracting fundamental voltages and currents, calculating working active power P_1, and calculating reflected P_r or detrimental active power P_d. Then, the program is modified to sample three phase quantities, mainly positive and negative sequence calculations.

For single phase system, the LabView program will connect with the NI DAQmx hardware via a USB cable interface to a laptop. This program will then read the sampled data from the hardware and perform any type of data manipulation or computation programmed. The algorithm is shown in table 6.3 with inputs of voltage and current samples, $u(k)$ and $i(k)$ and displays the voltage and current waveforms as well as active power P, working active power P_w, and reflected active power P_w. See Appendix C for the full Labview block diagram.

Table 6.3: Lab View Single Phase Measurement Algorithm

Sequence	Single Phase Measurement Algorithm
1	Acquire samples $u(k)$ and $i(k)$ from hardware.
2	Calculate active power P from $u(k)$ and $i(k)$
3	Extract fundamental crms voltage, $\boldsymbol{U}_1$
4	Extract fundamental crms current, $\boldsymbol{I}_1$
5	Calculate fundamental phase angle from $\boldsymbol{U}_1$ and $\boldsymbol{I}_1$
6	Calculate working active power P_w
7	Calculate reflected active power P_r

In step 1, the voltage and current samples are acquired from the DAQmx hardware. This hardware samples at the highest rate possible and stores everything in the local hardware memory. The software will then take samples according to the user's specifications. In this case, the number of samples per period chosen are $N = 128$ and the sampling frequency was chosen as f_s = 7,680Hz. This was chosen to have accuracy up to the 63rd order harmonic and while satisfying the Nyquist criterion.

Steps 3 and 4 calculate the fundamental crms of the voltages and current inputs. This is done by using formula (117) and (118) for the fundamental crms voltage and current values respectively. This yields a magnitude and phase angle for both the voltages and currents. Then, step 5 calculates the difference between the phase angles of the fundamental crms voltage and current.

Step 2 and step 6 are a simple process to calculate the active power P and the working active power P_w respectively. The active power can be calculated from equation (116). Then, to calculate the working active power, there is an additional step of calculating the phase angle which was completed in step 5. Thus, the working active power is calculated via the equation (119). Finally, step 7 calculates the difference of the working active power and the active power, meaning the reflected active power P_r or detrimental active power P_d.

For three phase system measurements, the core algorithm of the single phase syste m stays the same but with additional steps to accommodate three phase voltage and current inputs and calculating the active power. The main difference is the additional steps 6 and 7 shown in table 6.4 below. Using symmetrical components, the three phase fundamental crms voltages can be transformed into positive sequence voltages of the fundamental harmonic using equation (123). The same steps are used to transform the three phase fundamental current using equation

(124). Also, using equations (122) the active power can be calculated for three phase voltages and currents. The algorithm block diagram is shown below in figure 6.4.

Table 6.4: Lab View Three Phase Measurement Algorithm

Sequence	Three Phase Measurement Algorithm
1	Acquire samples $u(k)$ and $i(k)$ from hardware.
2	Calculate active power P from $u(k)$ and $i(k)$
3	Extract fundamental crms voltages for each phase, $\boldsymbol{U}_1$
4	Extract fundamental crms currents for each phase, $\boldsymbol{I}_1$
5	Calculate fundamental phase angles for each phase from $\boldsymbol{U}_1$ and $\boldsymbol{I}_1$
6	Calculate the fundamental positive sequence voltages, $\boldsymbol{U}_1^{\mathrm{p}}$
7	Calculate the fundamental positive sequence currents, $\boldsymbol{I}_1^{\mathrm{p}}$
8	Calculate working active power P_{w}
9	Calculate reflected or detrimental active power P_{r} , P_{d}

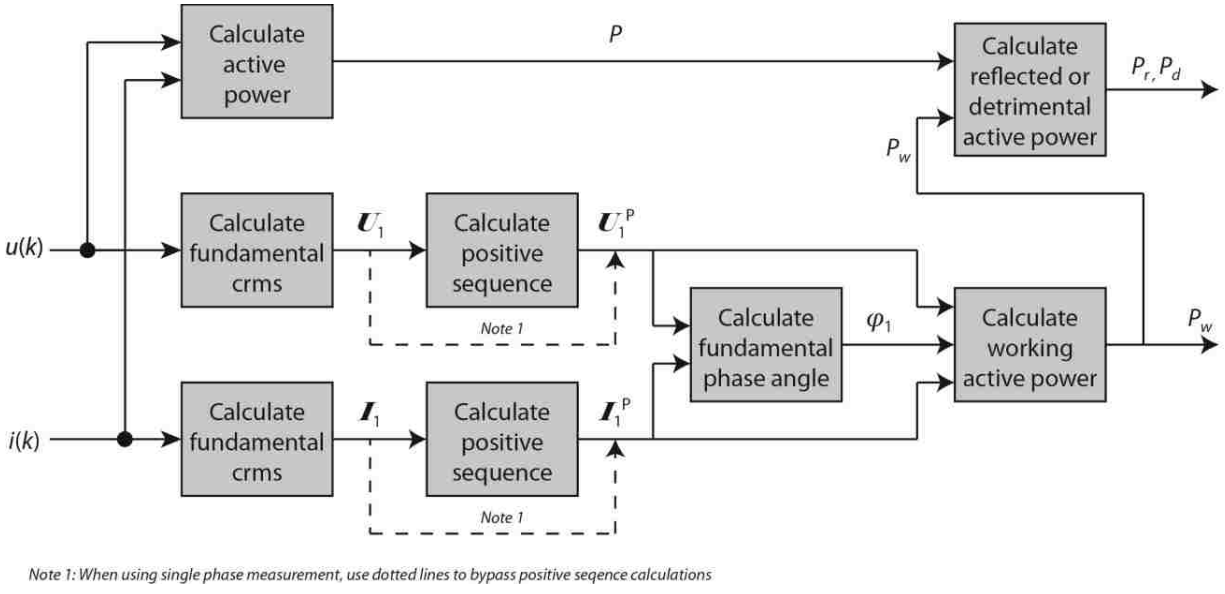

Figure 6.4: Working Active Power Measurement Algorithm Block Diagram

6.4 Measurement Testing and Accuracy

With any experimental measurements, and especially true in billing, measurement accuracy is of vital importance. One should note, the core subject of this dissertation is not measurement accuracy, but measurement accuracy should be noted for credible measurement results. The accuracy of each device in the experiment should be documented and the combined accuracy of the equipment should be determined.

First, the measurement devices should be tested against a known good measurement device. Typically, for commercial units this is a fully calibrated meter according to IEEE standards. Unfortunately, these are not readily available at the local university. Thus, the best standard available is an accurate volt meter. To accurately measure the phase voltage, an old, well made Weston analog voltmeter manufactured in 1920 with an error of 0.25% (full scale deflection) will be used. The measured quantity was near the full scale of the meter, thus 0.25% is the worst case scenario. The old analog meter was chosen as the meter relies on physical phenomenon that is proven to be accurate to measure the voltage rather than digital and electronic devices that could have human or calibration errors.

To measure the combined error of all devices, the sum of squares will give a probable error percentage rather than aggregating as it is very rare that all meters will perform at the worst case scenarios. The ambient temperature of the experiments was well within the typical temperature ranges for all of the equipment. Thus, the error was calculated where ε_a stands for error of the analog meter, ε_o stands for error of the isolator, and ε_d stands for error of the NI DAQmx DSP hardware i.e.,

$$\varepsilon = \sqrt{\varepsilon_a^2 + \varepsilon_o^2 + \varepsilon_d^2} \tag{126}$$

Table 6.5 shows each error percentage along with the combined error of the system.

Table 6.5: Error Percentages for Experimental Equipment

Analog Meter Error ε_a	Voltage Isolator Error ε_o	DSP Hardware Error ε_o	Total Error ε
0.25%	1.0%	0.6%	1.19%

The voltage isolator hardware is the dominating factor of error. This is due to the low cost of such device in an educational laboratory rather than a commercial research laboratory. Secondly, the DSP hardware error is the typical error for the inexpensive NI DAQmx system designed for educational use. There are calibrated versions with the isolation built in offers much higher accuracy of 0.02% that could be used for commercial and/or industrial applications.

CHAPTER 7. SINGLE PHASE EXPERIMENTATION

7.1 Experimental Setup and Control

The control test observed is purely a resistive load in a single phase system. The resistive load is supplied from a sinusoidal voltage supply E with internal impedance, R_s. and load impedance R_L of 98 Ω. This supply resistance is chosen to have close to a 5% voltage drop of the supply voltage E. Table 7.1 shows the values of the various components of the experiment.

Table 7.1: Single Phase Control Experiment Data

Experimental Component	Symbol	Measured Value
Supply Voltage	E	120 V
Supply Resistance	R_s	6.0 Ω
Load Current rms	$\|i\|$	1.15 A
Active Power	P	139 W
Working Active Power	P_r	139 W
Reflected Active Power	P_w	0.0 W
Percent of P_r to P	*n/a*	0%

The results of the experiments show that the active power P = 139 W and working active power P_w = 139.0 W. Consequently, the reflected active power P_r = 0.0 W. This confers that a purely resistive load with a sinusoidal voltage supply produces no harmful effects to the system.

7.2 Experiment #1: Microwave Oven

The first test that will be conducted uses a General Electric (GE) 1200 W microwave as a common household device. The microwave is supplied from a sinusoidal voltage supply E with internal impedance, R_s. This supply resistance is chosen to have a 5% voltage drop of the supply voltage E. Table 7.2 shows the values of the various components of the experiment.

Table 7.2: Experiment #1 Microwave Data

Experimental Component	Symbol	Measured Value
Supply Voltage	E	126 V
Supply Resistance	R_s	0.5 Ω
Load Current rms	$\|i\|$	12.1 A
Active Power	P	1280 W
Working Active Power	P_r	1310 W
Reflected Active Power	P_w	30.0 W
Percent of P_r to P	*n/a*	2.3%

The results of the experiments show that the active power P = 1280 W and the working active power P_w = 1310 W. Consequently, the reflected active power is P_r = 30 W. Thus the percentage of reflected active power versus active power is 2.3%. This means that the HGL draws additional current from the source and an extra 30 W in addition to the 5% ΔP is wasted on the supply impedance. Figure 7.1 shows the voltage waveform in red and the current waveform in white.

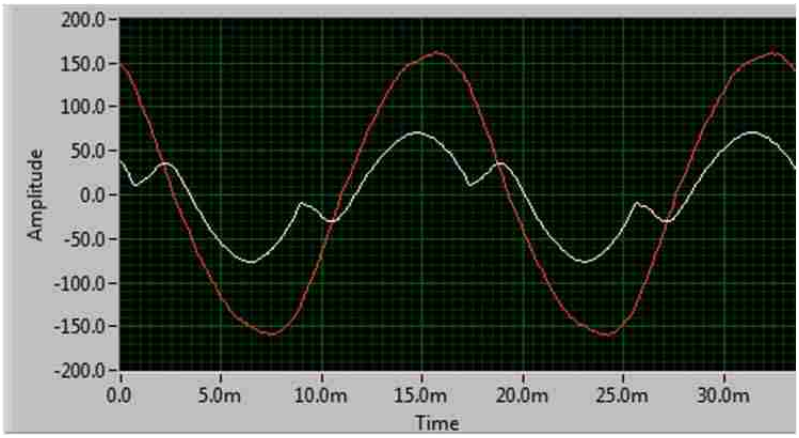

Figure 7.1: Experiment #1 Microwave Waveform

7.3 Experiment #2: Compact Fluorescent Light Bulbs

The second experiment consists of ten CFL bulbs in parallel. The CFL bulbs are supplied from a sinusoidal voltage supply E with internal impedance, R_s. This supply resistance approximately has a 5% voltage drop of the supply voltage E. Table 7.3 shows the values of the components of the experiment.

Table 7.3: Experiment #2 Compact Fluorescent Light Bulbs Data

Experimental Component	Symbol	Measured Value
Supply Voltage	E	120 V
Supply Resistance	R_s	4.0 Ω
Load Current rms	$\|i\|$	1.62 A
Active Power	P	132 W
Working Active Power	P_r	139 W
Reflected Active Power	P_w	7.0 W
Percent of P_r to P	*n/a*	5.3%

The results of the experiments show that the active power P = 132 W and working active power P_w = 139 W. Consequently, the reflected active power P_r = 7.0 W. Thus the percentage of reflected active power versus active power is 5.3%. This means that the HGL draws additional current from the source and an extra 7 W in addition to the 5% ΔP is wasted on the supply impedance. Figure 7.2 shows the voltage waveform in red and the current waveform in white.

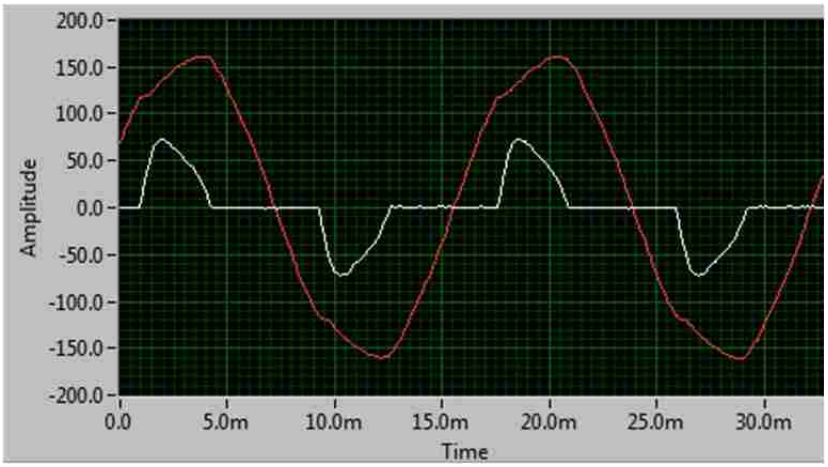

Figure 7.2: Experiment #2 Compact Fluorescent Light Bulbs Waveform

7.4 Experiment #3: Xbox360 Gaming Console

The third experiment is a Microsoft Xbox360 gaming system and its power converter. The gaming system is supplied from a sinusoidal voltage supply E with internal impedance, R_s. This supply resistance approximately has a 5% voltage drop of the supply voltage E. Table 7.4 shows the values of the components of the experiment.

Table 7.4: Experiment #3 Microsoft Xbox360 Data

Experimental Component	Symbol	Measured Value
Supply Voltage	E	120 V
Supply Resistance	R_s	7.0 Ω
Load Current rms	$\|i\|$	0.9 A
Active Power	P	74 W
Working Active Power	P_r	78 W
Reflected Active Power	P_w	4.0 W
Percent of P_r to P	*n/a*	5.4 %

The results of the experiments show that the active power P = 74 W and working active power P_w = 78 W. Consequently, the reflected active power P_r = 4.0 W. Thus the percentage of reflected active power versus active power is 5.4%. This means that the HGL draws additional current from the source and an extra 4 W in addition to the 5% ΔP is wasted on the supply impedance. Figure 7.3 shows the voltage waveform in red and the current in white.

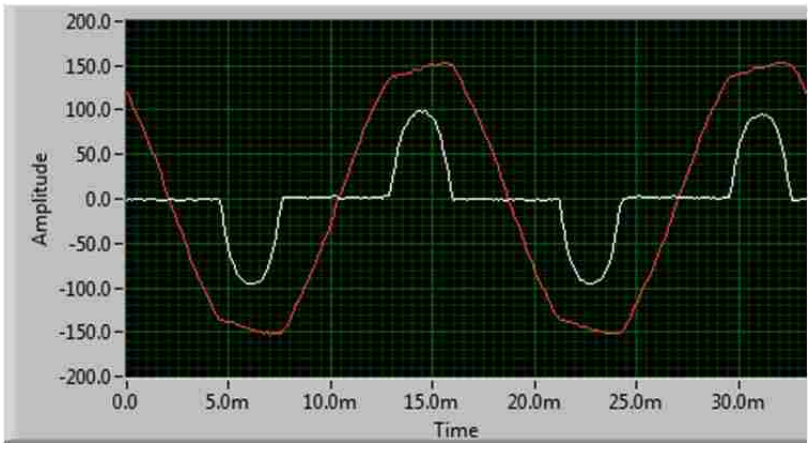

Figure 7.3: Experiment #3 Microsoft Xbox360 Waveform

7.5 Experiment #4: Single-Phase Rectifier

The fourth experiment is a single phase rectifier with a capacitive filter and a resistive load. The rectifier is supplied from a sinusoidal voltage supply E with internal impedance, R_s. This supply resistance approximately has a 5% voltage drop of the supply voltage E. Table 7.5 shows the values of the components of the experiment.

Table 7.5: Experiment #4 Single Phase Rectifier with Capacitive Filter Data

Experimental Component	Symbol	Measured Value
Supply Voltage	E	120 V
Supply Resistance	R_s	3.0 Ω
Load Current rms	$\|i\|$	2.10 A
Active Power	P	178 W
Working Active Power	P_r	185 W
Reflected Active Power	P_w	7.0 W
Percent of P_r to P	*n/a*	3.9 %

The results of the experiments show that the active power P = 178 W and working active power P_w = 185 W. Consequently, the reflected active power P_r = 7.0 W. Thus the percentage of reflected active power versus active power is 3.9%. This means that the HGL draws additional current from the source and an extra 7 W in addition to the 5% ΔP is wasted on the supply impedance. Figure 7.4 shows the voltage waveform in red and the current waveform in white. Note, that there is a phase shift of the current due to the capacitive filter.

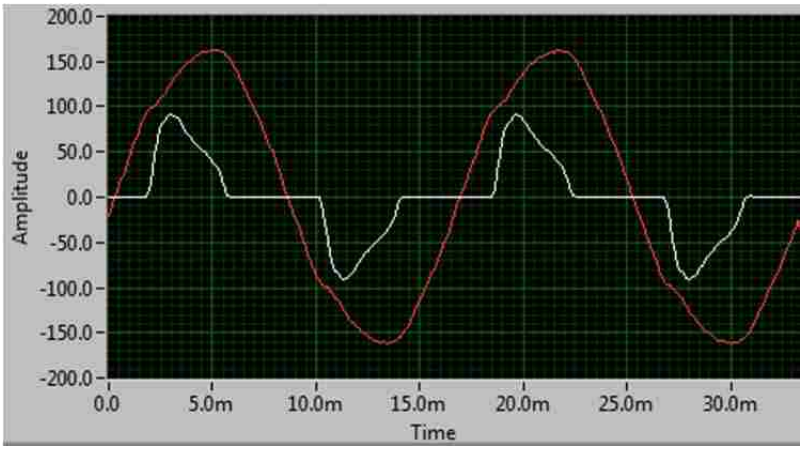

Figure 7.4: Experiment #4 Rectifier with Capacitive Filter Waveform

7.6 Experimental Results for Single Phase Loads

The single phase experiments consisted of one control experiment and four experiments of common household HGLs that was the cause of the reflected active power P_r. The results show that all four HGLs current waveforms were distorted and required a working active power P_w that was higher than the traditional active power P for load operation. The percentage shown displays the amount of reflected active power P_r needed in addition to the active power, P. Table 7.6 shows the combined experimental results.

Table 7.6: Experimental Results for Single Phase Loads

Exp.	Active Power	Working Active Power	Reflected Active Power	Percentage $(P_w\text{-}P)/P$
Ref.	131 W	131 W	0.0 W	0.0%
No. 1	1280 W	1310 W	30.0 W	2.3%
No. 2	132 W	139 W	7.0 W	5.3%
No. 3	74.0 W	78 W	4.0 W	5.4%
No. 4	178 W	185 W	7.0 W	3.9%

Common household items do not consume much energy, so the reflected active power loss looks miniscule. But, one should look at the percentage of reflected active power versus active power. Relative to load size, this shows the rate of energy wasted on the supply impedance, and more importantly, not billed from meters using traditional active power P method. Thus, a few percentages here and there do not equate to much on its own, but when an entire customer base shows this trend, the reflected active power could drastically add up to several kW worth of losses.

Another point of view is to consider the percentage of reflected active power P_r versus with typical system impedance active power losses ΔP. Roughly, 5% losses are about the limits of acceptability in a power system. With the highest percentage at 5.4% and the lowest at 2.3%, ignoring the control experiment, the power loss due to HGLs can be from 5% to over 10% of the system in addition to the 5% system impedance losses ΔP.

These results show that the reflected active power loss of household items can be on the same level as system losses on the utility grid, or even worse. Meaning, the utility must provide a working active power component to the load that is higher than the currently billed active power component. Thus, the utility will suffer nearly double the economic loss for sending energy to these household HGL as compared to an equivalent LTI load were reflected active power P_r is nearly non-existent.

CHAPTER 8. THREE PHASE EXPERIMENTATION

8.1 Experimental Setup and Control

The next test observed is a purely resistive load in a three phase system. A three phase balanced resistive load is supplied from a sinusoidal symmetrical voltage supply E with internal impedance, R_s. and load impedance R_L of 240 Ω per phase. The supply resistance is chosen to approximate a 5% voltage drop of the supply voltage E. Table 8.1 shows the values of the various components of the experiment.

Table 8.1: Three Phase Control Experiment Data

Experimental Component	Symbol	Measured Value
Supply Voltage	E	100 V
Supply Resistance	R_s	10.5 Ω
Load Current rms	$\|i_a\|, \|i_b\|, \|i_c\|$	0.4/0.4/0.4 A
Active Power	P	115 W
Working Active Power	P_r	115 W
Reflected Active Power	P_w	0.0 W
Percent of P_r to P	*n/a*	0%

The results of the experiments show that the active power P = 115.0 W and a working active power P_w = 115 W. Consequently, the reflected active power P_r = 0.0 W. This confers that a purely resistive balanced load with a sinusoidal symmetrical voltage supply produces no harmful effects to the system.

8.2 Experiment #5: Unbalanced Three Phase Load

The fifth test conducted is an unbalanced wye connected resistive load where phases A and B have resistive loads of 115 Ω each and the load on C phase is left open. The unbalanced resistive load is supplied from a symmetrical sinusoidal voltage supply E with internal impedance, R_s. This supply resistance is chosen to approximate a 5% voltage drop of the supply voltage E. Table 8.2 shows the values of the various components of the experiment.

Table 8.2: Experiment #5 Three Phase Unbalanced Load Data

Experimental Component	Symbol	Measured Value
Supply Voltage	E	100 V
Supply Resistance	R_s	7.0 Ω
Load Current rms	$\|i_a\|, \|i_b\|, \|i_c\|$	0.7/0.7/0.0A
Active Power	P	115 W
Working Active Power	P_r	118 W
Reflected Active Power	P_w	3.0 W
Percent of P_r to P	*n/a*	2.6%

The results of the experiment shows that the active power P = 115 W and working active power P_w = 118 W. Consequently, the reflected active power P_r = 3.0 W. Thus the percentage of reflected active power versus active power is 2.6%. This means that the unbalanced resistive load has a higher supply impedance power loss, ΔP, than an equivalent three phase balanced load. Figure 8.1 shows the voltage waveform on the left and the current waveform on the right.

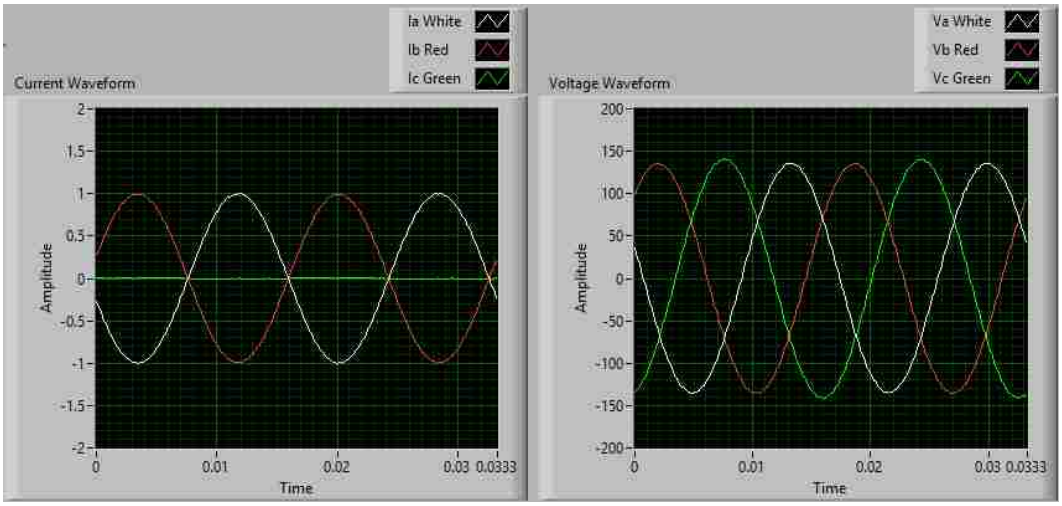

Figure 8.1: Experiment #5 Three Phase Unbalanced Load Waveform

8.3 Experiment #6: Three Phase Rectifier

The sixth test is a three phase rectifier with a capacitive filter and a resistive load of 473 Ω. The rectifier is supplied from a sinusoidal symmetrical voltage supply E with internal impedance, R_s. This supply resistance is chosen to approximate a 5% voltage drop of the supply voltage E. Table 8.3 shows the values of the components of the experiment.

Table 8.3: Experiment #6 Three Phase Rectifier with Capacitive Filter Data

Experimental Component	Symbol	Measured Value
Supply Voltage	E	100 V
Supply Resistance	R_s	10.5 Ω
Load Current rms	$\|i_a\|, \|i_b\|, \|i_c\|$	0.42/0.41/0.41 A
Active Power	P	115 W
Working Active Power	P_r	118 W
Reflected Active Power	P_w	2.8 W
Percent of P_r to P	*n/a*	2.4%

The results of the experiments show that the active power P = 115 W and working active power P_w = 118 W. Consequently, the reflected active power P_r =2.8 W. Thus the percentage of reflected active power versus active power is 2.4%. This means that the HGL draws additional current from the source and an extra 2.8 W in addition to the 5% ΔP is wasted on the supply impedance. Figure 8.2 shows the voltage waveform on the left and the current waveform on the right.

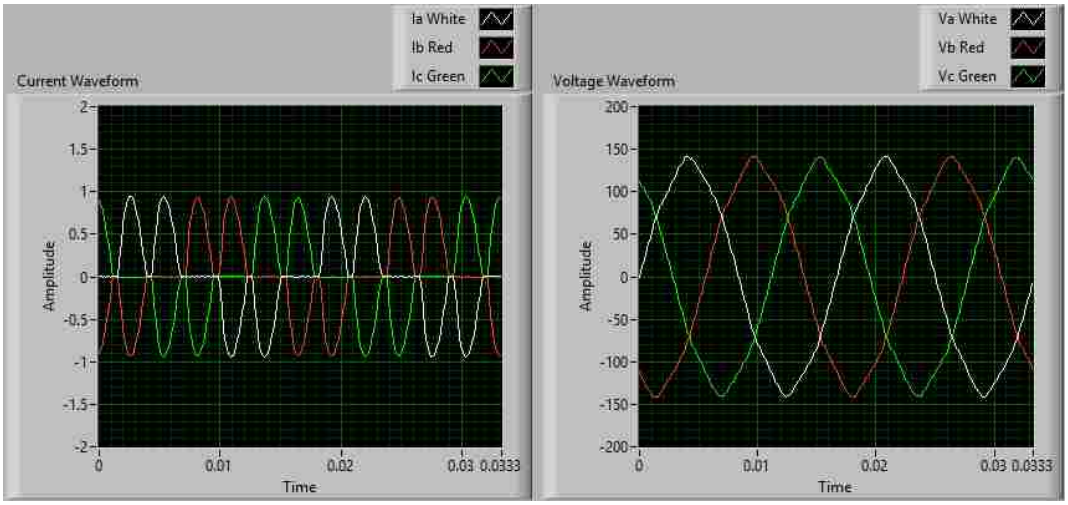

Figure 8.2: Experiment #6 Three Phase Rectifier with Capacitive Filter Waveform

8.4 Experiment #7: Three Phase Induction Motor I

The seventh test is using a 175W three phase, two pole induction motor to test asymmetrical voltage supplies. The induction motor is supplied from a sinusoidal but asymmetrical voltage supply E with phase A voltage at 110 V and phase B and C at 120 V. The supply resistance R_s is chosen to approximate a 5% voltage drop of the supply voltage E. Table 8.4 shows the values of the components of the experiment.

Table 8.4: Experiment #7 Induction Motor with Asymmetrical Supply Data

Experimental Component	Symbol	Measured Value
Supply Voltage	E_a, E_b, E_c	110/120/120 V
Supply Resistance	R_s	10.0 Ω
Load Current rms	$\|i_a\|, \|i_b\|, \|i_c\|$	0.73/0.85/0.89 A
Active Power	P	173 W
Working Active Power	P_r	169 W
Detrimental Active Power	P_d	4.1 W
Percent of P_d to P	*n/a*	2.4 %

The results of the experiments show that the active power P = 173 W and working active power P_w = 169 W. Unlike the previous experiments, this experiment shows that there exists a detrimental active power P_d = 4.1 W. Thus, the percentage of detrimental active power versus active power is 2.4%. This means that the asymmetrical voltage supply is supplying extra power to the motor that is wasted in the motor windings instead of being converted to torque. Figure 8.3 shows the voltage waveforms.

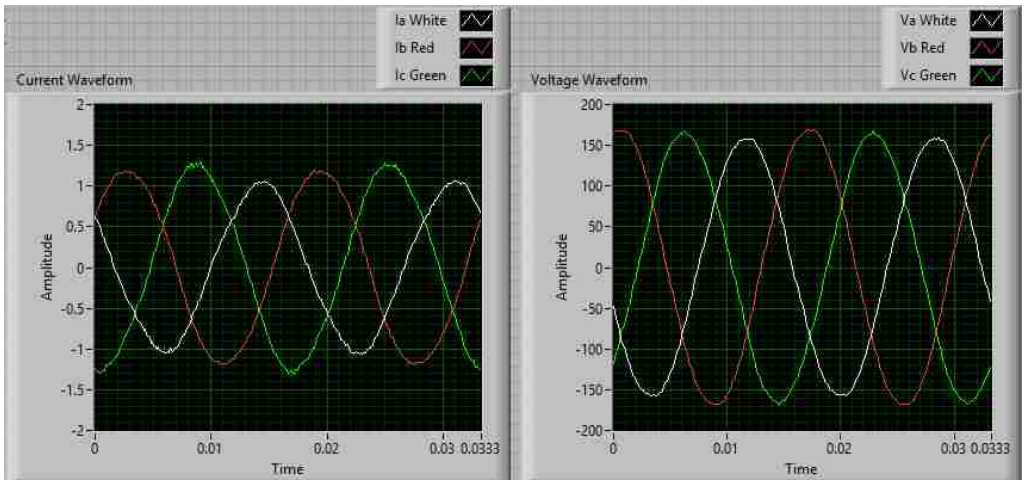

Figure 8.3: Experiment #7 Induction Motor with Asymmetrical Supply Waveform

8.5 Experiment #8: Three Phase Induction Motor II

The eighth and final test consists of the same 175 W three phase two pole induction motor to test distorted voltage supply. The induction motor is supplied from a symmetrical but distorted voltage supply E with 120 V and 5.3% total harmonic distortion (THD) mainly consisting of 5^{th} and 7^{th} order harmonics. The supply resistance R_s is chosen to have a 5% voltage drop of the supply voltage E. Table 8.5 shows the values of the components of the experiment.

Table 8.5: Experiment #8 Induction Motor with Distorted Supply Data

Experimental Component	Symbol	Measured Value
Supply Voltage	E	120 V
Supply Resistance	R_s	10.0 Ω
Load Current rms	$\|i_a\|, \|i_b\|, \|i_c\|$	0.83/0.81/0.86 A
Active Power	P	173 W
Working Active Power	P_r	169 W
Detrimental Active Power	P_d	3.7 W
Percent of P_d to P	*n/a*	2.1 %

The results of the experiments show that the active power P = 173 W and working active power P_w = 169 W. Similar to the previous experiment, this experiment shows that detrimental active power P_d = 3.7 W is present in the circuit. Thus the percentage of detrimental active power versus active power is 2.1%. This means that the distorted voltage supply is supplying extra power to the motor that is wasted as heat in the motor windings instead of being converted to torque. Figure 8.4 shows the voltage waveforms.

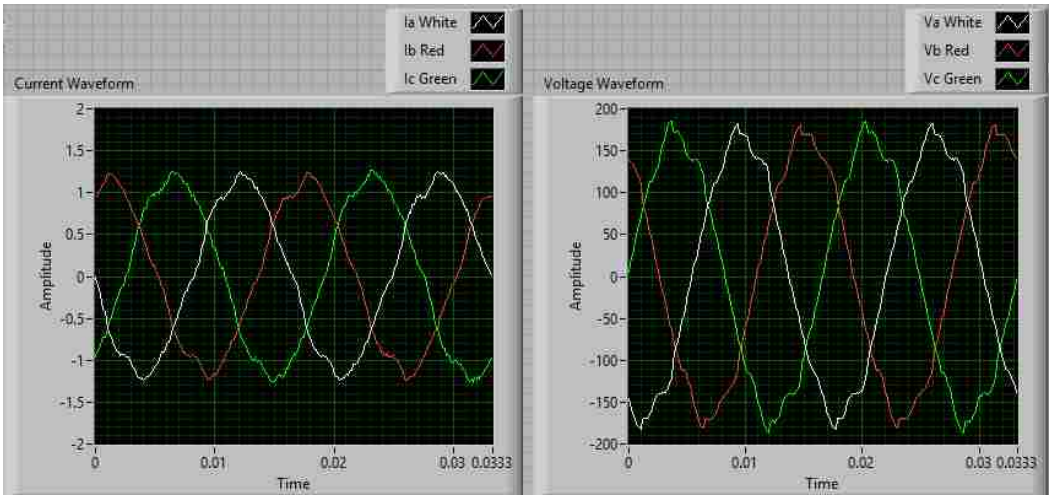

Figure 8.4: Experiment #8 Induction Motor with Distorted Supply Waveform

8.6 Experimental Results for Three Phase Loads

The three phase experiments consisted of one control experiment and four experiments of common three phase loads that would be the sources of reflected active power P_r and susceptible to detrimental active power P_d. The results show that the first two experiment's load current waveforms were asymmetrical and distorted respectively. This required a working active power P_w that is higher than the traditional active power P by the difference of the reflected active power P_r for normal load operations. The results of the last two experiments showed energy conveyed by the asymmetrical and distorted component of the active energy does not convert to the output shaft of the motor. Table 8.6 shows the combined results of all single phase experiments.

The fifth and sixth experiments shows that the working active power P_r is higher than active power P. One should look at the percentage of reflected active power versus active power. Relative to load size, this rate of energy wasted on the supply impedance is not billed by traditional revenue meters. A few percentages of power loss are when servicing large loads can

have a large effect on billing. Thus, the reflected active power could drastically add up to several thousand dollars' worth of losses unaccounted for.

Table 8.6: Experimental Results for Three Phase Loads

Exp	Active Power	Working Active Power	Reflected/Detrimental Active Power	Percentage $(P_w\text{-}P)/P$
Ref.	115 W	115 W	0.0 W	0.0%
No. 1	115 W	118 W	3.0 W	2.6%
No. 2	115 W	118 W	2.8 W	2.4%
No. 3	173 W	169 W	4.1 W (P_d)	2.4%
No. 4	173 W	169 W	3.7 W (P_d)	2.1%

The last two experiments shows the effects of detrimental active power on the induction motors. Both the asymmetrical supply and the distorted supply have a detrimental active power component of 4.1 W and 3.7 W respectively. In the motor, this detrimental active power P_d is wasted as additional heat on the windings of 2.4% and 2.1% of the motor's ratings. A typical induction motor can have normal internal energy loss of 2% to 3% which determines the life span of the motor. With the addition of detrimental active power, the energy loss in the windings doubles to 4% to 5%. Remember that heat loss directly affects the motors life span. This means that the motors life span could be reduced drastically. Now it is not as simple as overpaying the monthly energy bill, but also replacing motors faster than they should be which is financially devastating for any company.

CHAPTER 9. MICROGRID APPLICATIONS

9.1 Issue of Distortion in Microgrids

Renewable energies, microgrids, and new age power electronic devices are fast approaching widespread adoption. While new technologies are certainly beneficial to the overall quality of a microgrid; one must not forget the most important concept of power engineering, economics. Rising fuel costs, strict regulations on nuclear entities, and high capital cost of renewable sources leads to a high cost for utilities. This leads us to take a look at the power quality of the grid and customer billing in terms of economics.

In today's microgrids, there are a large number of harmonic generating loads such as compact fluorescent light bulbs, variable speed drives, and other power electronic devices [18]. These devices contribute to high levels of distortion on the grid, especially in low MVA systems such as microgrids. This harmonic distortion and asymmetry in the power system causes additional system losses and load efficiency issues. Several methods have been proposed to pinpoint the sources of distortion [14] with additional regards to economics [19-22]. Thus, economic incentives, similar to power factor penalties, are needed to lower distortion and asymmetry.

In the power system, the majority of revenue meters are the older mechanical type. Unfortunately, these mechanical meters are incapable of distinguishing harmonic and negative sequenced components of the active power. To create the economic incentives mentioned above, newer digital signal processing (DSP) based meters are needed. Fortunately, the power industry is slowly accepting newer microprocessor based revenue meters in the form of a new advanced metering infrastructure (AMI). This will enable the calculation of a new concept of working,

detrimental and reflected active power based on the idea of categorizing active power into useful and useless components based on the point of origin.

9.2 Advanced Metering Infrastructure

In the power system, relays and meters are installed as an essential part in maintaining reliability. New electronic meters are capable of sampling voltages and currents that will be processed via their digital signal processor (DSP) and shared to the rest of the AMI via network. AMI enhances the microgrid by having a network of meters installed in the distribution system to relay critical information to the rest of the network in real time. With the AMI's network, microgrids and the present power system can benefit with improved grid efficiencies and moderating energy usage [15].

The AMI has many capabilities that will enhance the power system and microgrids for distribution operations. With the automotive industry showing signs of interest in hybrid plug-in vehicles, AMI serves as the access point for charging electric vehicles from the power grid [23,24]. With an ever growing infrastructure in size and technology, load forecasting becomes more complicated, in which detailed hourly load forecasting available by the AMI system will be utilized [25-27]. Furthermore, transformer load modeling and management on the distribution system can be possible with AMI [28,29].

Additionally, AMI is capable for enhancing billing and power quality. Two way communication with revenue meters and central control stations can relay information billing and distributed generation units [30,31]. Even the ability to control individual household loads is possible; scaling power usage for the distribution system [32,33]. Lastly, with AMI's digital processing power, power quality can be addressed in terms of harmonic content and asymmetry identification [15,34,35].

9.3 Working Active Power Single Bus Simulation

To quantify the concept of working active power, a Matlab model using Simulink's power module will be used. There will be three loads that will be observed; rectifier with capacitive filter, a three phase resistive heater, and an auxiliary induction motor. Calculating the working active power will show how distortion and unbalance affect the induction motor.

The source consists of a three phase symmetrical and sinusoidal voltage source of 480 V rms. The supply impedance is modeled as resistors with an approximate 5% voltage drop of the supply voltage. The three phase rectifier's diodes are considered lossless and the capacitive filter keeps the DC voltage ripple at 5%. Next, the induction motor is rated at 10 HP at 1760 rpm at 460V. Lastly, a total of four metering points are at the loads and before the bus.

There are a total of four scenarios to test. The first is the control test in which all devices are running at near sinusoidal and balanced conditions. The second test has the rectifier and the induction motor running to test the effects of distortion. The third test has the resistive load only connected to two phases creating an unbalanced load to test the effects of asymmetry. Finally, the last test has all three devices on with the rectifier's distortion and the unbalanced load's asymmetry.

A. Simulation #1: Control Test

The control experiment tests that all loads are running at a near sinusoidal and symmetrical mode. Meaning, the rectifier has the capacitive filter turned off to reduce distortion, the resistive load is perfectly balanced, and the induction motor is fully loaded. The active power for each device is chosen to reflect a scaled scenario of industrial loads such as a DC drive and/or

unbalanced load with a small auxiliary induction motor. The auxiliary motor in this case is 1/10th of main load's power. The magnitudes of the active powers are much less than a real life scenario which was chosen so that the experiment can be tested in a laboratory environment on a later date.

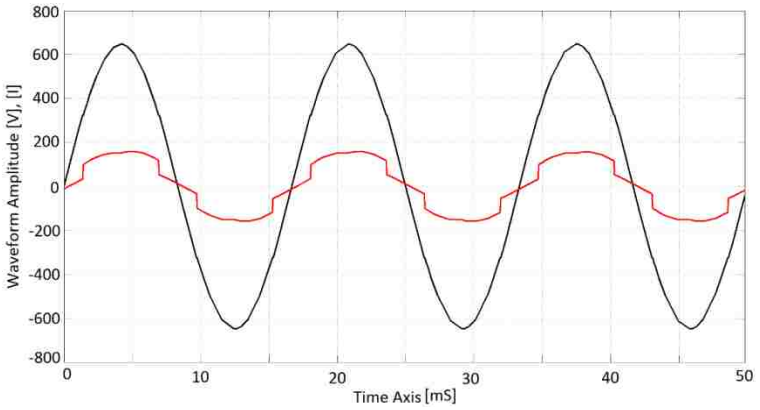

Figure 9.1: Simulation #1: Voltage and Current Waveforms for A Phase

Results for the control test are shown as the source's voltage and current waveforms for A phase. The voltages for all three phases are V_a = 456.6 V, V_b = 455.7 V, V_c = 457.6 V, and the currents for all three phases are I_a = I_b = I_c = 62.2 A. The active, working active, and reflected/detrimental active powers are shown in Table 9.1.

Table 9.1: Single Bus Simulation #1 Results

Simulation 1	Active Power	Working Active Power	Reflected/Detrimental Active Power	Percentage (P_w-P)/P
Bus	83,514 W	83,594 W	80 W	0.1%
Rectifier	37,750 W	37,830 W	80 W	0.2%
Resistors	37,690 W	37,960 W	0 W	0.0%
Ind. Motor	7,804 W	7,804 W	0 W	0.0%

B. Simulation #2: Rectifier and Induction Motor Test

The second experiment tests the effects of the rectifier's harmonic distorted current on the voltage supplying the induction motor. Meaning, how badly is the motor's operations degraded due to distortion. The total harmonic distortion (THD) of the load current of the rectifier is 70%.

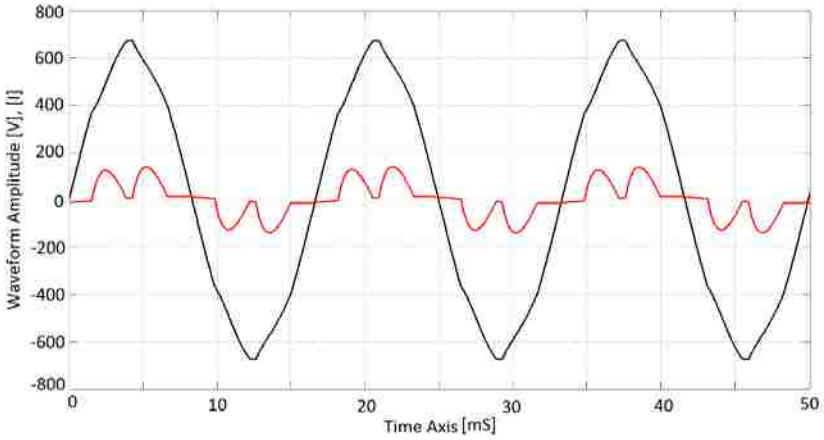

Figure 9.2: Simulation #2: Voltage and Current Waveforms for A Phase

Results of the experiments show that the voltages for all three phases are the same from the control experiment. Phase A voltage of the bus has a THD of 3.56%. In Fig. 9.2, the phase A current distortion is quite apparent, while the voltage distortion is barely noticeable. The low voltage THD stems from the fact that the voltage drop across the resistor is only 5% of the supply. This 5% voltage drop is due to the current flowing to the bus which has a 70% THD. Therefore, 5% of the 70% current THD produces the 3.5% voltage THD. As a result, the induction motor did not suffer much degradation. Line currents are I_a = 73.87 A, I_b = 74.01 A, I_c = 74.01 A.

Table 9.2: Single Bus Simulation #2 Results

Simulation 2	Active Power	Working Active Power	Reflected/Detrimental Active Power	Percentage $(P_w\text{-}P)/P$
Bus	83,704 W	85,571 W	1,867 W	2.2%
Rectifier	75,380 W	77,250 W	1,870 W	2.5%
Ind. Motor	8,324 W	8,321 W	-3 W (P_d)	0.04%

C. Simulation #3: Unbalanced Resistive Load and Induction Motor Test

The third experiment tests the effects of unbalanced current on the voltage supplying the induction motor. Meaning, how badly is the motor's operations degraded due to asymmetry. The resistive load has R_a = 3.4 Ω, R_b = 3.4 Ω, and R_c is open.

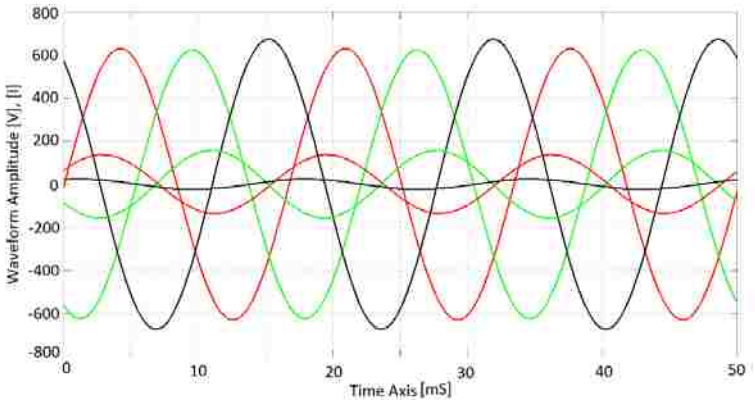

Figure 9.3: Simulation #3: Voltage and Current Waveforms for Three Phases

Results of the experiments show that the currents for all the phases are I_a = 96.37 A, I_b = 110.8 A, I_c = 16.9 A and voltages are V_a = 445.8 V, V_b = 450.7 V, V_c = 477.6 V. Since R_c is open, only the current from the induction motor causes a voltage drop on A phase supply impedance. At the motor terminals, the currents are I_a = 7.28 A, I_b = 10.28 A, I_c = 16.9 A. This shows that a small amount of voltage asymmetry can cause significant current imbalance in the motor windings.

Table 9.3: Single Bus Simulation #3 Results

Simulation 3	Active Power	Working Active Power	Reflected/Detrimental Active Power	Percentage $(P_w\text{-}P)/P$
Bus	83,628 W	87,380 W	3,752 W	4.5%
Rectifier	75,650 W	79,541 W	3,891 W	5.1%
Ind. Motor	7,978 W	7,839 W	-139 W (P_d)	1.74%

D. Simulation #4: Rectifier, Unbalanced Resistive Load, and Induction Motor Test

The fourth experiment tests the effects of both the harmonic distorted current and current asymmetry on the voltage supplying the induction motor. This will show the aggregated effects of both loads on the induction motor.

Results of the experiments show that the currents for all the phases are Ia = 80.65 A, Ib = 81.02 A, Ic = 49.66 A and voltages are Va = 450.3 V, Vb = 450.8 V, Vc = 464.5 V. Additionally, THD for the current equals 35.6% and 2.3% for the voltage. Because the individual loads are smaller than the previous experiments, the distortion and asymmetry have less effect on the voltage supply individually. Fig. 9.4 shows the current waveforms are more sinusoidal and symmetrical than on the previous two experiments respectively.

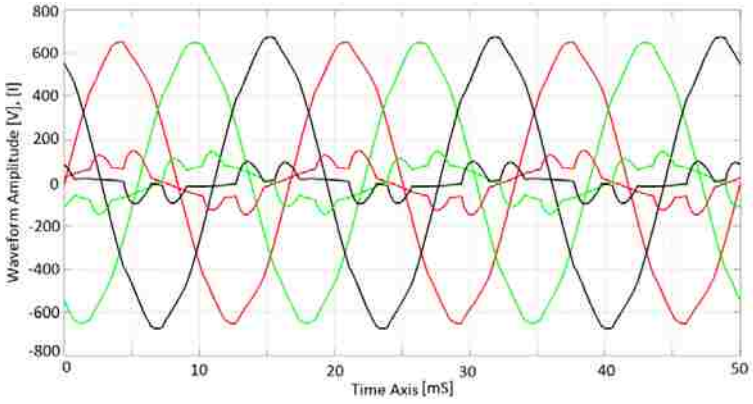

Figure 9.4: Simulation #4: Voltage and Current Waveforms for Three Phases

Table 9.4: Single Bus Simulation #4 Results

Simulation 4	Active Power	Working Active Power	Reflected/Detrimental Active Power	Percentage $(P_w\text{-}P)/P$
Bus	83,730 W	85,225 W	1,495 W	1.8%
Rectifier	38,590 W	39,360 W	770 W	2.0%
Resistors	37,290 W	38,040 W	750 W	2.0%
Ind. Motor	7,850 W	7,825 W	-25 W (P_d)	0.3%

E. Simulation Results

Results of the experiments show that adding a HGL or unbalanced load on a bus affects other loads except for purely resistive loads. That is because the distorted and/or unbalanced current results in a voltage drop across the system impedance. This appears as a small component of distortion and/or asymmetry on the bus voltage.

In simulation #2, the rectifier's current load contained distortion that did not degrade the induction motor's performance noticeably. The rectifier's current distortion resulted in the working active power, P_w to be greater than the active power, P. The difference of 2.5% is the reflected active power, P_r which means that the rectifier is injecting a harmful component back into the system and is not being billed for it. This resulted in the bus voltage being affected with a 3.6% THD. Since the THD level on the voltage is so low, the harmonic current flow is minimal. Therefore, the motor's performance did not suffer noticeable degradation.

In simulation #3, the unbalanced load's current caused a more noticeable degradation on the induction motor's performance. The unbalanced C phase load being left open resulted in the working active power, P_w to be greater than the active power, P. The difference of 5.1% is the

reflected active power, P_r. This means that the unbalanced load is injecting a harmful component back into the system and not being billed for it.

The load current on the incoming source for the bus resulted in a voltage drop across the system impedance that resulted in the phase C bus voltage, V_c having a 31.8 V higher rms than A phase and 26.9 V higher rms than B phase. Thus, the motor's current magnitude suffered drastic imbalance. Meaning, the working active power, P_w was less than the active power, P. Thus, the difference of 1.8% is detrimental active power, P_d that degrades their motor's operation, yet is still billed for.

In simulation #4 both the rectifier and unbalanced load current's resulted in degrading the motor's performance, but at a much less combined rate. As in the previous experiments, both the rectifier and unbalanced load produced reflected power, P_r. This in turn affected the bus voltage in the form of distortion and asymmetry, but at a lower magnitude than the previous experiments. The main difference now is that phase C is loaded with current from the rectifier, albeit with some distortion giving the difference of the phase voltages as 14.2 V. This drastically reduced the amount of unbalanced current in the motor compared to simulation #3 reducing the detrimental active power, P_d to 0.3% of the active power, P.

9.4 Working Active Power Microgrid Simulation

The next step to take is to build upon the simulation model from the single bus system. A small microgrid system will be simulated with Matlab to further quantify the concept of working active power. There will be three loads that will be observed; rectifier with capacitive filter, a three phase RL load, and a two phase resistive load. This will show the effects of distortion and asymmetry in a microgrid system.

The microgrid system consists of two independent sources of energy and three different loads connected in a small microgrid configuration. The two generator's terminal voltage are rated at 19kV phase to phase and have a short circuit power of 600 MVA. Load 1 is an unbalanced load with A phase open circuited and the other two phases loaded at 16.5MW. Load 2 is a three phase rectifier that has a distortion coefficient δ_i = 36% and an output power of 16.5MW. Load 3 is a balanced RL load is loaded at 16.5 MW. Lastly, the line impedances are rated at 0.02536Ω per km and 0.9337mH per km. The microgrid topology is shown in figure 9.5 while detailed tables of system parameters are shown on the next page.

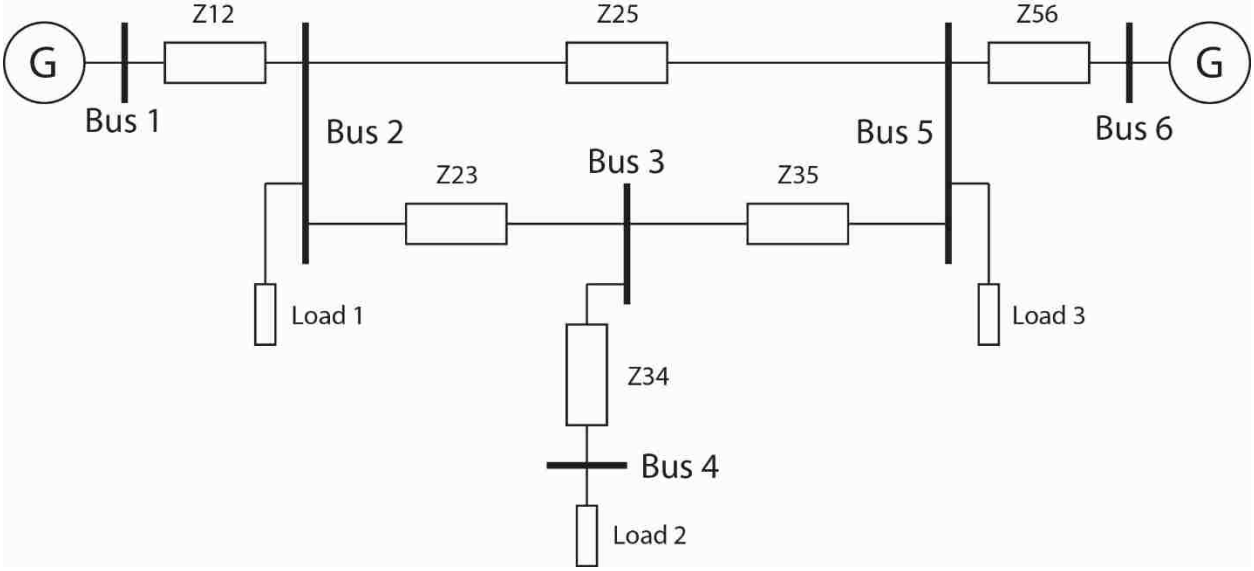

Figure 9.5: Microgrid System One Line Diagram

Table 9.5: Microgrid Generator Data

Generator Name	Rated Voltage	Short Circuit MVA	X/R Ratio	Output Power
West Gen	19 kV (L-L)	600 MVA	5:1	17.2 MW
East Gen	19 kV (L-L)	600 MVA	5:1	32.9 MW

Table 9.6: Microgrid Line Impedance Data

Line Name	Line Length	Ω /km	Henry/km	Total Impedance
Z12	8 km	0.02536Ω	0.9337mH	2.823 $e^{j85.88°}$
Z23	3 km	0.02536Ω	0.9337mH	1.059 $e^{j85.88°}$
Z25	10 km	0.02536Ω	0.9337mH	3.529 $e^{j85.88°}$
Z34	3 km	0.02536Ω	0.9337mH	1.059 $e^{j85.88°}$
Z45	5 km	0.02536Ω	0.9337mH	1.765 $e^{j85.88°}$
Z56	2 km	0.02536Ω	0.9337mH	0.706 $e^{j85.88°}$

Table 9.7: Microgrid Load Data

Load Name	Load Type	Loading Power	Connected Bus
Load 1	Unbalanced Load	16.5 MW	Bus 2
Load 2	Rectifier	16.5 MW	Bus 4
Load 3	RL Load	16.5 MW	Bus 5

Working active power meters were placed on each of the loads to measure the working, reflected, and detrimental active powers. Load 1's (unbalanced load) meter measured a reflected active power, P_w = 17.2 MW with the active power P = 16.5 MW. Load 2's (rectifier) meter measured a reflected active power, P_w = 17.3 MW with the active power P = 16.5 MW. Lastly, load 3's (RL load) meter measured a detrimental active power, P_w = 16.5 MW with the active power P = 16.5 MW. The metered data is shown below in table 9.8.

Table 9.8: Microgrid Metered Results

Load Name	Active Power	Working Active Power	Reflected/Detrimental Active Power	Percentage $(P_w\text{-}P)/P$
Unbalanced Load	16.5 MW	17.1 MW	0.6 MW	3.6%
Rectifier	16.5 MW	17.4 MW	0.9 MW	5.5%
RL Load	16.5 MW	16.5 MW	0.0 MW	0.0%

The results show that there is an additional 3.6% power loss upon delivery to the unbalanced load and an additional 5.5% power loss upon delivery for the rectifier load. This is compared to the RL load that has no additional power loss upon delivery. It is worthy to note that the entire power system losses for the line impedances are 0.6 MW. Thus, it costs more than double the amount of energy to deliver to the unbalanced and rectifier load as compared to the RL load.

When a utility uses active power, P, for billing purposes, all three loads are billed the same for energy usage. But, the utility suffers more than double the loss to deliver energy to the unbalanced load and rectifier load. Normally, the utility will see the extra losses on their accounting sheets and spread the cost out upon the entire customer base. Thus, the customer with the resistive load will get a higher surcharge to cover the extra monetary loss from the reflected active power, P_r, losses caused by the unbalanced load and rectifier load. When using working active power, P_w, as the billing component, the extra energy losses are accounted for each customer, thus providing a fair and accurate billing method for everyone.

CHAPTER 10. CASE STUDY: HGL IN A THREE PHASE SYSTEM

10.1 Background for Case Study: HGL

HGL are becoming more common than ever in the power grid due to advancements and cost reduction in power electronic devices. Some examples of everyday household HGL are light dimmers that use TRIACs (triode for alternating current), CFL, computer and monitor power supplies, and microwaves. Moreover, three phase industrial loads such as HGLs such as VFDs (variable speed drives), thyristor based converters, and arc furnaces are common.

10.2 Experimental Setup for Case Study: HGL

An experiment is setup to study the effects of distortion and asymmetry on the utility grid by measure the working and reflected active power at the load terminals. The National Instruments DAQmx system will be used along with the LabVolt power station to experiment on various loading and system specifications. A balanced delta HGL will represent the three phase load under varying distortion levels. In addition, the short circuit power to load power ratio will vary to observe the effects of working and reflected active power to supply impedance.

The first experiment will measure the working and reflected active power for a linear, three phase load as a reference point. The load will be connected in delta topology with a distortion, $\delta_i = 0\%$. First, data will be collected with all three loads on while changing the short circuit to load power ratio. Second, an unbalanced condition will be introduced by disconnecting one of the loads and collecting data while again changing the short circuit to load power ratio. Third, to introduce an unbalanced condition, two loads will be disconnected and recorded.

The next experiments will be conducted in similar fashion to measure the working and reflected active power. The loads will change to a HGL with distortion levels of δ_i = 100%. The load topology will be the same delta connection. The data will be collected in three sections, balanced load to represent normal operations, one load, and two loads disconnected. Finally, each section will have data collected while varying the short circuit to load power ratio.

The final experiment will be conducted with the load changing to a HGL with δ_i = 171%. HGL with distortion levels of δ_i = 171% represents the most severe case of distortion. The load topology will be the same delta connection in which data will be collected in three sections, balanced load, one load disconnected, and finally two loads disconnected similar as the paragraph before. In addition, each section will have data collected while varying the short circuit to load power ratio.

10.3 Experimental Results for Case Study: HGL

The experimental results are shown in three sections representing different levels of distortion with subsets representing different load topologies and different short circuit versus load powers. The first section consists of loads with distortion level, δ_i = 0% and the next two sections having loads with distortion levels of δ_i =100%, and δ_i =171% obtained via thyristors. Each section contains three data sets representing a balanced delta load, a delta load with one branch open, and a delta load with two branches open. For all experiments, the load power and system impedance will be changed to obtain a short circuit versus load power ratio of 2, 3, 4, 5, 10, 15, and 20. The circuit topology is shown in figure 10.1.

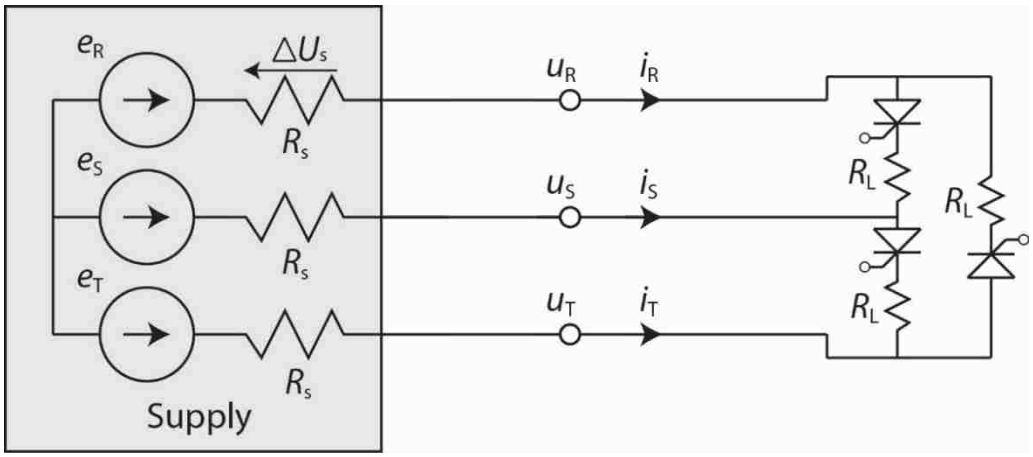

Figure 10.1: Experimental Circuit for HGL Simulation

A. Experiment Section #1: Test with $\delta_i = 0\%$

The first experimental section tests the active power, working active power, and detrimental active power on a LTI load, meaning distortion level, $\delta_i = 0\%$. The load is connected in delta formation with the short circuit power versus load power varying in the experiment. Results are shown below in table 10.1.

Table 10.1: HGL Simulation Results for $\delta_i = 0\%$

P_{SC} vs P_L	Balanced Load P_w/P	Two Loads ON P_w/P	One Load ON P_w/P
2	1.000	1.054	1.182
3	1.000	1.048	1.143
4	1.000	1.042	1.115
5	1.000	1.036	1.082
10	1.000	1.022	1.052
15	1.000	1.010	1.023
20	1.000	1.004	1.009

The results show that the balanced load showed no change while the unbalanced loads showed varying degree of reflected active power that increased when the short circuit power versus load power increased. The balanced load's results for this section are as expected; in which purely balanced LTI load has no ill effects on the power system. When one of the branches of the delta loads is disconnected, reflected active power is present and the ratio of working active power to active power is greater than 1. When two branches are disconnected, the P_w/P ratio increases even further. This is due to the fact that when there is only one branch operating, one of phase current is zero causing a drastic current imbalance.

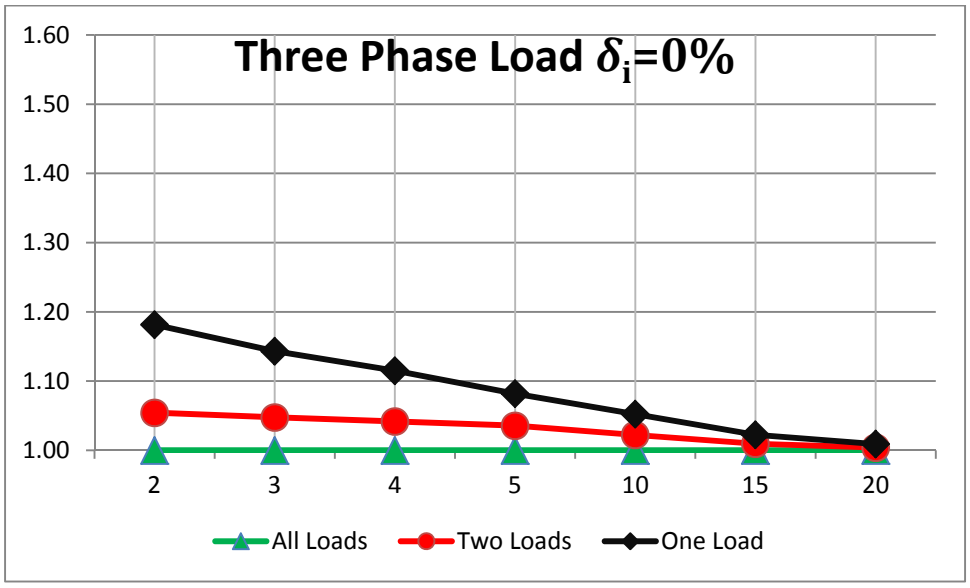

Figure 10.2: HGL Simulation Graph for $\delta_i = 0\%$

Additionally, it is observed that as the short circuit power vs load power increases, the P_w/P ratio increases, meaning more power loss is suffered because of the unbalanced loading as shown in figure 10.2. This is due to the higher supply impedance that the reflected active power dissipates from. Ultimately, the utility has to pay extra for energy delivery to this load by the percentage shown.

B. Experiment Section #2: Test with $\delta_i = 100\%$

The next experimental section tests the active power, working active power, and detrimental active power on a HGL of distortion level, $\delta_i = 100\%$. The load is connected in delta formation with the short circuit power versus load power varying in the experiment. Results are shown below in table 10.2 and figure 10.3.

Table 10.2: HGL Simulation Results for $\delta_i = 100\%$

P_{SC} vs P_L	Balanced Load P_w/P	Two Loads ON P_w/P	One Load ON P_w/P
2	1.262	1.382	1.508
3	1.209	1.304	1.364
4	1.143	1.208	1.274
5	1.095	1.148	1.184
10	1.054	1.094	1.111
15	1.043	1.066	1.086
20	1.019	1.033	1.050

The results show that the balanced load showed an increased ratio of P_w/P to a max of 1.262 while the unbalanced loads P_w/P increased even more when the short circuit power versus load power increased to a maximum of 1.382 and 1.508. These results are expected as an increase in the supply impedance causes a greater reflected active power component. Similar to the previous experiment, additional reflected active power is a consequence of load unbalancing. It is worthy to note that the most extreme case causes a 50.8% additional power loss due to reflected active power which is a drastic amount of energy unaccounted for.

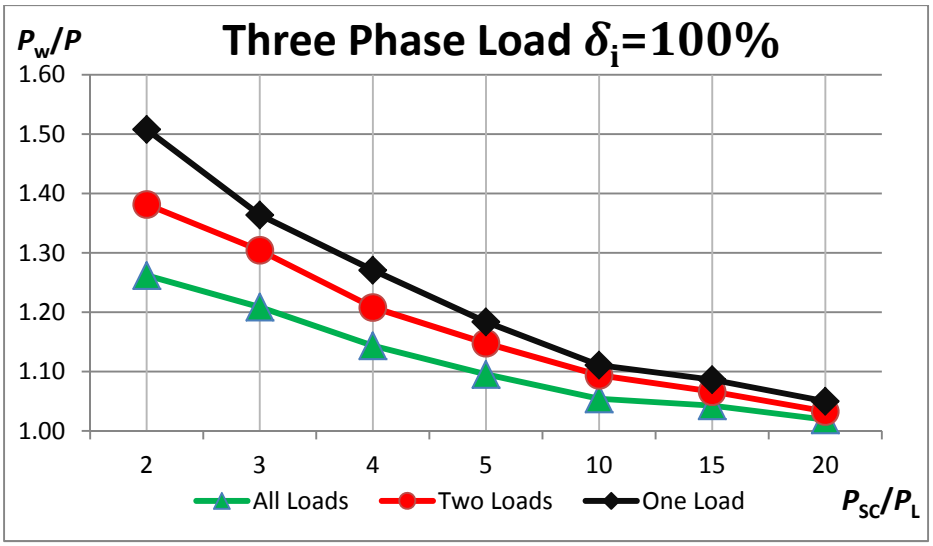

Figure 10.3: HGL Simulation Graph for δ_i = 100%

C. Experiment Section #3: Test with δ_i = 171%

The next experimental section tests the active power, working active power, and detrimental active power on a HGL of distortion level, δ_i = 171%. The load is connected in delta formation with the short circuit power versus load power varying in the experiment. Results are shown below in table 10.3 and figure 10.4.

Table 10.3: HGL Simulation Results for δ_i = 171%

P_{SC} vs P_L	Balanced Load P_w/P	Two Loads ON P_w/P	One Load ON P_w/P
2	1.405	1.480	1.582
3	1.311	1.370	1.420
4	1.201	1.250	1.297
5	1.158	1.188	1.214
10	1.104	1.129	1.147
15	1.093	1.107	1.115
20	1.092	1.104	1.112

The final results show that the balanced load showed an increased ratio of P_w/P to a max of 1.405 while the unbalanced loads P_w/P increased even more when the short circuit power versus load power increased to a maximum of 1.480 and 1.582. These results are expected the HGL has a higher distortion level than the previous experiments, thus the P_w/P ratio is higher on at all points. In this final experiment, the worst case scenario was a P_w/P ratio of 1.582.

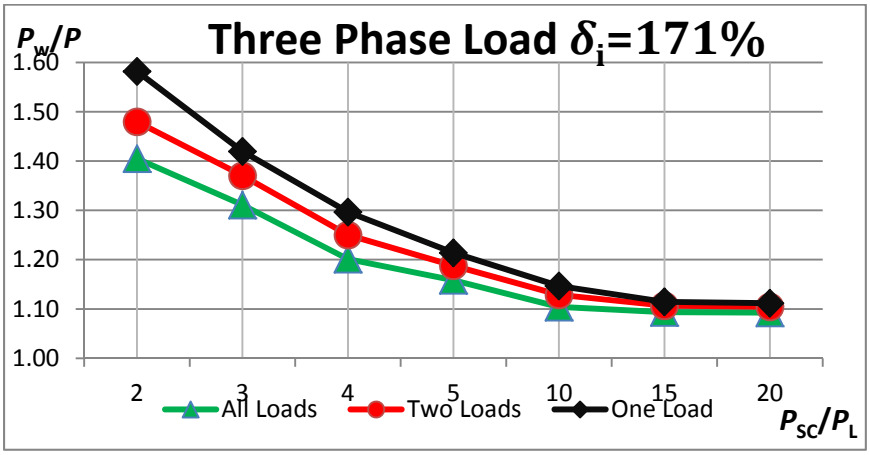

Figure 10.4: HGL Simulation Graph for δ_i = 171%

D. Experimental Results Summary

The results from the experiment show a trend as the short circuit to load power increases, meaning a higher system impedance, unbalanced and distortion of the current causes a higher amount of reflected active power, P_w. Looking at figures 10.2, 10.3, and 10.4, the trend shows that as the delta load becomes more unbalanced, there is a distinct trend of a higher reflected active power for all three levels of distortion. This difference gets amplified as the short circuit to load power increases.

Comparing the different distortion levels per load shows an increased trend of reflected active power show in figures 10.5, 10.6, and 10.7. As the short circuit to load power increases, the difference between the LTI load and the HGL with δ_i = 100% jumps increases at a higher pace. Additionally, the delta load with one branch loaded has the largest reflected active power as compared to the other two loads. Lastly, the difference between the HGL with δ_i = 100% and the HGL with δ_i = 171% is apparent, but not as much as the LTI vs HGL with δ_i = 100%.

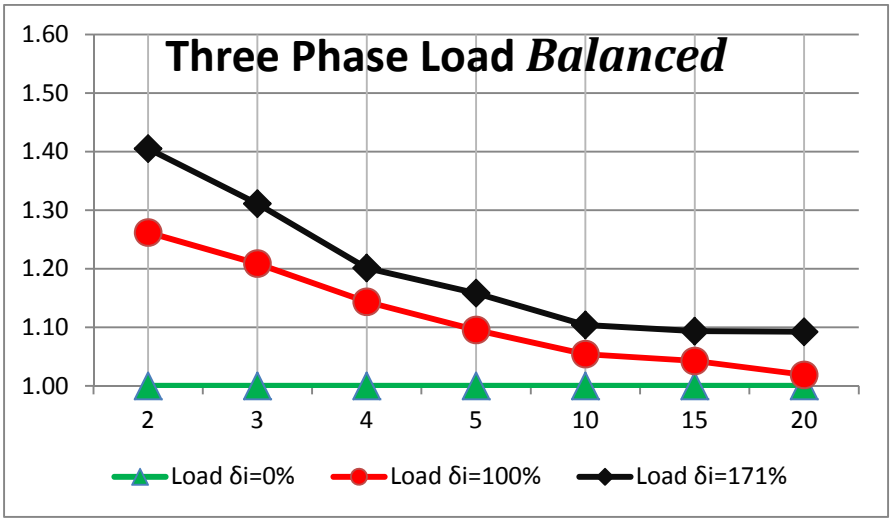

Figure 10.5: HGL Simulation Graph for Balanced Three Phase Delta Load

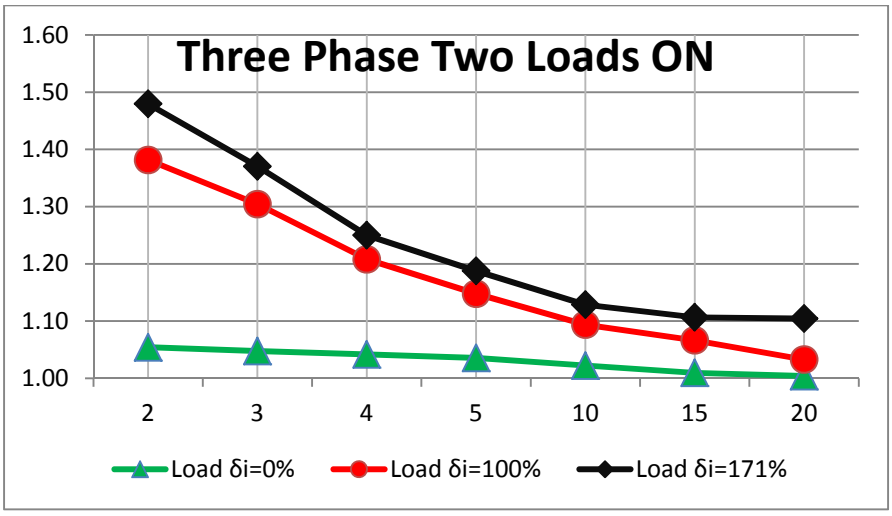

Figure 10.6: HGL Simulation Graph for Delta Load with One Branch Open

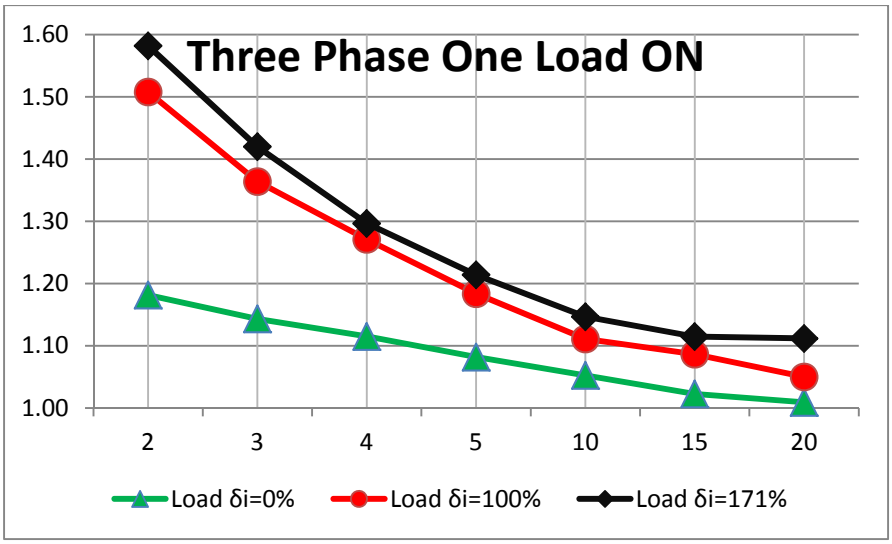

Figure 10.7: HGL Simulation Graph for Delta Load with Two Branches Open

For all phase of the experiment, there was a reoccurring trend that the more distorted the load, the higher the reflected active power. Additionally, the more unbalanced a load becomes, the higher the reflected active power. This reflected active power is then amplified as the short circuit to load power increases, meaning supply impedance becomes larger. This means that when a distorted and/or unbalanced load is supplied from a low quality system with a higher impedance losses in the system, the reflected active power loss can become quite costly for the generation owner.

CHAPTER 11. CONCLUSION

11.1 Conclusion

Presently, almost everyone relies on the national power grids to send energy to households and businesses in the United States. Naturally, the demand for energy has risen drastically within the last few decades. In the power industry, two major parties are present; paying consumers and energy providers. With respects to these two parties, supply quality and loading quality levels of voltage and current waveforms are regulated.

Using CPC as a foundation, sources of distortion in the power system can be classified as originating from the supply or originating from the load. Distortion in the supply system causes many problems including the need for higher rated equipment, degrading lifespan, reduced torque on motor shafts, and interference to the operation of sensitive electronic equipment. In addition, asymmetry in the power system can lead to many of the same problems associated with distortion. Thus, energy sent to the load should be classified as either useful or useless. Useful energy can be categorized as energy delivered and converted to useful work and useless energy can be categorized as energy delivered that is wasted as heat or interferes in load operations. Therefore, working active power is defined as the component of active power that sends useful energy to the customer.

The active power is decomposed into several components, working active power, reflected active power, and detrimental active power. Working active power is calculated as the fundamental power, and in the case of three phase systems, positive sequenced active power component of the active power that sends energy from the source to the load. Then, the reflected active power can be calculated as the higher order harmonic powers, and in the case of three phase systems, negative sequenced active powers that send energy from the load back to the

supply, ultimately dissipating on the supply resistance. Lastly, detrimental active power can be calculated as higher order harmonic power, and in the case of three phase systems, negative sequenced active power that sends energy from the supply to the load.

To measure the working active power concept, the traditional active power and the fundamental active power needs to be measured. This is accomplished with a DSP device capable of simultaneously sampling three phase quantities. NI DAQmx hardware and Labvolt's optical isolators are setup to measure three phase quantities in real time. The raw sampled data is then processed via the NI LabView software to acquire the working active power, reflected active power and detrimental active power. Measurement accuracy for voltage and current samples was tested against traditional analog metering devices and quantified at 1.19% combined error.

Four experiments were performed for single phase measurements to verify the working active power concept. These results show that the reflected active power loss of household items can on the same level as system losses on the utility grid. Meaning, the utility must provide a working active power component to the load that is higher than the currently billed active power component used by traditional meters. Thus, the utility will higher economic losses for sending energy to these household HGL as compared to an equivalent LTI load of the same active power.

Four more experiments were performed for three phase measurements to verify the working active power concept. These results show that the reflected active power from the single phase experiments also hold true for three phase HGLs and unbalanced loads. More interestingly, the induction motors supplied with asymmetrical and distorted supplies was supplied with less working active power than the metered active power with the difference being the detrimental active power. Meaning, the customer is being billed for additional energy that is

detrimental to his machinery by not producing any torque on the output shaft and ultimately being dissipated inside the motor causing problems in the induction motor.

Microgrids and AMI infrastructure showed an application for the working active power concept. The combination of powerful converters producing distortion, low MVA system, and unbalanced loads show that the working active power concept could help differentiate different power components. The modeling of a single bus showed results that unbalanced loads and HGL are causes of reflected active power, P_r, while the induction motor suffers from detrimental active power losses, P_r. Additionally, a model of microgrid system consisting of an unbalanced load, rectifier load, and balanced load showed an even stronger effect of reflected active power in the microgrid system. This resulted in additional power losses greater than the line impedance losses for energy delivery.

Lastly, a case study for HGLs in a three phase system showed that increasing levels of distortion and asymmetry causes an increase in reflected active power that is amplified as the system impedance becomes larger. In total, nine scenarios were tested with different load configurations and distortion levels of δ_i = 0%, 100%, and 171%. Within these nine scenarios, the supply impedance parameter was increased to represent a system power loss between 5% and 33%. These experiments showed the significance of reflected active power with the worst case scenario of over 51% extra power loss.

The main point to be addressed is the traditional standards for billing energy in the power system are old and outdated. The use of traditional active power standards and older mechanical revenue meters hides the fact that HGLs and unbalanced loads are causing additional power losses that are not taken into account thus causing a revenue loss on the utility side. Additionally, when the utility has a distorted or asymmetrical voltage profile, certain customers with sensitive

loads, such as induction motors, are also affected. The traditional active power standards does not distinguish useful energy from useless energy, thus the customer ends up paying for energy that is delivered to him that is not useful, but in fact detrimental to his own equipment.

With the new concept of working active power, energy billing can be fairer and accurately pinpoint the parties that are responsible for distortion and asymmetry in the power system. This will enable economic penalties for faulty parties and fairly bill other parties based on useful energy transferred. With economic penalties in place, this will give an incentive for faulty parties to clean up their act which will have an overall effect of lower levels of distortion and asymmetry in the system. This ultimately results in an efficient and economic power system.

11.2 Future Progress

The next step to verify the working active power concept is to build a more robust, accurate, and portable metering device that can directly interface with the power system. This would need a DSP hardware device that is capable of sampling 120V ac signals and up to 5A current signals from high quality potential transformers and current transformers found in substations and industrial complexes. This would let the new working active power meter read data in a realistic environment and see if this issue is serious enough to be considered relevant.

If the issues are relevant enough, this working active power concept can be brought to light in the power industry. The first step would be to show people the problem at hand, as most are not even aware that the problem exists in the first place. Then, if there is enough interest, the issue should be brought to the regulatory committee for the power industry and reviewed. If deemed successful, new standards and practices should be written to use the new working active power concept as a new metering standard.

REFERENCES

[1] Mohamed A. El-Sharkawi, *Electric Energy An Introduction 2nd Ed.* (Florida, Boca Raton, 2009)

[2] U.S. Energy Information Administration International Energy Statistics Janurary 29th 2014< http://www.eia.gov/cfapps/ipdbproject/IEDIndex3.cfm?tid=2&pid=2&aid=12>

[3] U.S. Energy Information Administration Frequency Asked Questions January 29th, 2014 <http://www.eia.gov/tools/faqs/faq.cfm?id=207&t=3>

[4] Entergy Operations Information February 3rd, 2014 <http://entergy.com/operations_ information/>

[5] DEMCO Profile February 3rd, 2014 <http://www.demco.org/about-us/profile>

[6] U.S. Energy Information Administration Electricity Net Generation February 3rd, 2014 <http://www.eia.gov/totalenergy/data/monthly/pdf/sec7_5.pdf >

[7] U.S. EIA Average Monthly Residential Energy Consumption Prices and Bills by State February 6th, 2014 < http://www.eia.gov/electricity/sales_revenue_price/xls/table5_a.xls>

[8] AOE2014 Early Release Overview February 6th, 2014 <http://www.eia.gov/forecasts /aeo/er/early_consumption.cfm>

[9] Average Residential Retail Electricity Prices for Feb. 2011. February 10th 2014 < http://www.targetmap.com/viewer.aspx?reportId=9037>

[10] Understanding Demand & Demand Charges Feb 15th, 2014 <http://www.cec-co.com/Understanding%20Demand%20.pdf>

[11] John J. Grainger, William D. Stevenson, Jr., *Power System Analysis* (New York, New York, 1994)

[12] L.S. Czarnecki (2005) "Current's Physical Components (CPC) In Circuits with Nonsinusodial Voltages and Currents Part 1" Electrical Power Quality and Utilization Journal, Vol. X, No.1 pp. 1-14.

[13] L.S. Czarnecki (2006) "Current's Physical Components (CPC) In Circuits with Nonsinusodial Voltages and Currents Part 1" Electrical Power Quality and Utilization Journal, Vol. XI, No.2.

[14] A Ferraro, M. Prioli, and S. Salicone. "A Metrological Comparison Between Different Methods for Harmonic Pollution Metering" *IEEE Transaction on Instrumentation and Measurement*, Vol. 61, No. 11 Nov. 2012

[15] C. Selvam, K Srinivas, G.S. Ayyappan, “Advanced Metering Infrastructure for Smart Grid Applications” *Recent Trends in Information Technology Conference (ICRTIT)*, Apr. 2012.

[16] Operating Instructions and Specifications NI9215 February 23rd, 2014 <http://www.ni.com/pdf/manuals/373779f.pdf >

[17] Lab-Volt Power Electronics Control Devices Models 8840, 9029, 9030, 9033, 9034, 9056 February 23rd, 2014 <https://www.labvolt.com/downloads/dsa8840.pdf>

[18] L. Sainz and J. Balcells, "Harmonic Interaction Influence Due to Current Source Shunt Filters in Networks Supplying Nonlinear Loads" *IEEE Trans. Power Delivery*, Vol. 27, No. 3, Jul. 2012

[19] T. Toups, "Working Active Power, Reflected Active Power, and Detrimental Active Power in the Power System" Master’s Thesis, Dept. Elec. Eng., Louisiana State University, Baton Rouge, 2011.

[20] L. Czarnecki and T. Toups, “Working Energy-based Economic Incentives for the Supply and Loading Qualities Improvement in Islanded Micro-grids” *International Conference on Harmonics and Quality of Power (ICHQP)* June 2012.

[21] L. Czarnecki and T. Toups, “Working and Reflected Active Powers of Harmonics Generating Single-Phase Loads” *International School on Nonsinusoidal Currents and Compensation (ISNCC)*, June 2013.

[22] T. Toups and L. Czarnecki, “Development of Economic Incentives for harmonic and Asymmetry Reduction Based on the Concept of Working Power” *IEEE International Instrumentation and Measurement Technology Conference (I2MTC)*, May 2013.

[23] W. Shireen and S. Patel, “Plug-in Hybrid Electric Vehciles in the Smart Grid Environment” *Transmission and Distribution Conference and Exposition (PES)*, 2010

[24] D. Rua, D. Issicaba, F. Soares, P. Almeida, R. Rei, and A Lopes “Advanced Metering Infrastructure Functionalities for Electric Mobility” *Innovative Smart Grid Technologies Conference Europe (ISGT Europe)*, 2010

[25] H. Sui, H. Wang, M. Lu, and W. Lee, “An AMI System for the Deregulated Electricity Markets” *IEEE Transactions on Industry Applications*, Vol. 45, No. 6, Nov. 2009

[26] T. Hong, J. Wilson, and J. Xie, “Long Term Probabilistic Load Forecasting and Normalization With Hourly Information” *IEEE Transactions on Smart Grid*, Vol. 5, No.1, Jan. 2014

[27] J. Kwac, J. Flora, and R. Rajagopal, “Household Energy Consumption Segmentation Using Hourly Data” *IEEE Transactions on Smart Grid*, Vol. 5, No. 1, Jan. 2014

[28] Tom. Short, “Advanced Metering for Phase Identification, Transformer Identification, and Secondary Modeling” *IEEE Transactions on Smart Grid*, Vol. 4, No. 2, Jun. 2014

[29] Y. Lo, S. Huang, and C. Lu, "Transformational Benefits of AMI Data in Transformer Load Modeling and Management" *IEEE Transactions on Power Delivery*, Vol. 29, No. 2, Apr. 2014.

[30] R. Brown "Impact of Smart Grid on Distribution System Design" *Power and Energy Society General Meeting – Conversion and Delivery of Electrical Energy in the 21st Century*, July 2008

[31] Z. Luhua, Y. Zhonglin, W. Sitong, Y. Ruiming, Z. Hui, and Y. Qingduo, "Effects of Advanced Metering Infrastructure (AMI) on Relations of Power Supply and Application in Smart Grid" *China International Conference on Electricity Distribution (CICED)*, 2010.

[32] I. Choi, J. Lee, and S. Hong, "Implementation and Evaluation of the Apparatus for Intelligent Energy Management to Apply to the Smart Grid at Home" *Instrumentation and Measurement Technology Conference (I2MTC),* May 2011.

[33] T. Choi, K, Ko, S. Park, Y. Jang, Y. Yoon, and S. Im "Analysis of Energy Savings using Smart Metering System and IHD (In-Home-Display)" *Transmission & Distribution Conference & Exposition: Asia and Pacific*", Oct. 2009.

[34] S. Depuru, L. Wang, V. Devabhaktuni, and N. Gudi, "Smart Meters for Power Grid – Challenges, Issues, Advantages and Status" *Power Systems Conference and Exposition (PSCE),* Mar. 2011.

[35] H. Sui, and W. Lee, "An AMI Based Measurement and Control System in Smart Distribution Grid" *Industrial and Commercial Power Systems Technical Conference (I&CPS)*, May. 2011.

APPENDIX A: CRMS CALCULATIONS FOR ILLUSTRATION

Fundamental current crms calculations:

$$i(t) = \frac{120\sqrt{2}\cos(\omega_1 t) - 120}{0.8 + 0.2}$$

$$\boldsymbol{I}_1 = \boldsymbol{X}_1 e^{-j\frac{\pi}{2}} - \boldsymbol{X}_1 e^{-j\frac{3\pi}{2}}$$

$$\boldsymbol{X}_1 = \frac{1}{\sqrt{2}\pi}\int_{-\pi/4}^{\pi/4}(I_{\max}\cos\theta - 120)e^{-j\theta}d\theta = \frac{I_{\max}}{\sqrt{2}\pi}\int_{-\pi/4}^{\pi/4}\cos\theta\, e^{-j\theta}d\theta - \frac{1}{\sqrt{2}\pi}\int_{-\pi/4}^{\pi/4}120e^{-j\theta}d\theta$$

$$= \frac{I_{\max}}{\sqrt{2}\pi}\int_{-\pi/4}^{\pi/4}\frac{e^{j\theta}+e^{-j\theta}}{2}e^{-j\theta}d\theta - \frac{120}{\sqrt{2}\pi}\int_{-\pi/4}^{\pi/4}e^{-j\theta}d\theta = \frac{I_{\max}}{2\sqrt{2}\pi}\int_{-\pi/4}^{\pi/4}1 + e^{-2j\theta}d\theta - \frac{120}{\sqrt{2}\pi}\int_{-\pi/4}^{\pi/4}e^{-j\theta}d\theta$$

$$= \frac{I_{\max}}{2\sqrt{2}\pi}\theta\Big|_{-\pi/4}^{\pi/4} + \frac{I_{\max}}{2\sqrt{2}\pi}\frac{e^{-2j\theta}}{-2j}\Big|_{-\pi/4}^{\pi/4} - \frac{120}{\sqrt{2}\pi}\frac{e^{-j\theta}}{-j}\Big|_{-\pi/4}^{\pi/4}$$

$$= \frac{I_{\max}}{2\sqrt{2}\pi}\left[\frac{e^{-j\frac{\pi}{2}} - e^{j\frac{\pi}{2}}}{-2j}\right] - \frac{120}{\sqrt{2}\pi}\left[\frac{e^{-j\frac{\pi}{4}} - e^{j\frac{\pi}{4}}}{-j}\right] + \frac{I_{\max}}{2\sqrt{2}\pi}\left[\frac{\pi}{4} - \frac{-\pi}{4}\right]$$

$$= \frac{I_{\max}}{2\sqrt{2}\pi}\left[\frac{-j-j}{-2j}\right] - \frac{120}{\sqrt{2}\pi}\left[\frac{\left(\frac{1}{\sqrt{2}} - j\frac{1}{\sqrt{2}}\right) - \left(\frac{1}{\sqrt{2}} + j\frac{1}{\sqrt{2}}\right)}{-j}\right] + \frac{I_{\max}}{2\sqrt{2}\pi}\frac{\pi}{2}$$

$$= \frac{I_{\max}}{2\sqrt{2}\pi}\left[\frac{2j}{2j}\right] - \frac{120}{\sqrt{2}\pi}\left[\frac{\sqrt{2}j}{j}\right] + \frac{I_{\max}}{4\sqrt{2}} = \frac{I_{\max}}{2\sqrt{2}\pi} - \frac{120}{\pi} + \frac{I_{\max}}{4\sqrt{2}}$$

$$= \frac{120\sqrt{2}}{2\sqrt{2}\pi} - \frac{120}{\pi} + \frac{120\sqrt{2}}{4\sqrt{2}} = \frac{60}{\pi} - \frac{120}{\pi} + 30 = 10.9e^{j0^\circ}$$

$$\boldsymbol{I}_1 = \boldsymbol{X}_1 e^{-j\frac{\pi}{2}} - \boldsymbol{X}_1 e^{-j\frac{3\pi}{2}} = 10.9e^{-j\frac{\pi}{2}} + 10.9e^{-j\frac{\pi}{2}} = 21.8e^{-j\frac{\pi}{2}}$$

Fundamental voltage crms calculations:

$$u(t) = 120\sqrt{2}\cos(w_1 t) - 0.8i(t)$$

$$\boldsymbol{U}_1 = \boldsymbol{A}_1 + \boldsymbol{B}_1 e^{-j\frac{\pi}{2}} - \boldsymbol{A}_1 e^{-j\pi} - \boldsymbol{B}_1 e^{j\frac{\pi}{2}}$$

$$\boldsymbol{X}_1 = \frac{1}{\sqrt{2}\pi}\int_{-\pi/4}^{\pi/4} E_{\max}\cos\theta\, e^{-j\theta}d\theta = \frac{E_{\max}}{\sqrt{2}\pi}\int_{-\pi/4}^{\pi/4}\cos\theta\, e^{-j\theta}d\theta = \frac{E_{\max}}{\sqrt{2}\pi}\int_{-\pi/4}^{\pi/4}\frac{e^{j\theta}+e^{-j\theta}}{2}e^{-j\theta}d\theta$$

$$= \frac{E_{\max}}{2\sqrt{2}\pi}\int_{-\pi/4}^{\pi/4} 1 + e^{-2j\theta}\theta = \frac{E_{\max}}{2\sqrt{2}\pi}\left[\theta\Big|_{-\pi/4}^{\pi/4} + \frac{e^{-2j\theta}}{-2j}\Big|_{-\pi/4}^{\pi/4}\right] = \frac{E_{\max}}{2\sqrt{2}\pi}\left\{\left[\frac{\pi}{4} - \frac{-\pi}{4}\right] + \left[\frac{e^{-j\frac{\pi}{2}} - e^{j\frac{\pi}{2}}}{-2j}\right]\right\}$$

$$= \frac{E_{\max}}{2\sqrt{2}\pi}\left[\frac{\pi}{2} + \frac{-j-j}{-2j}\right] = \frac{E_{\max}}{2\sqrt{2}\pi}\left[\frac{\pi}{2}+1\right] = \frac{120\sqrt{2}\left[\frac{\pi}{2}+1\right]}{2\sqrt{2}\pi} = 49.1e^{j0^\circ}$$

$$\boldsymbol{B}_1 = \boldsymbol{X}_1 - 0.8\boldsymbol{I}_1 = 49.1e^{j0^\circ} - 0.8\left(10.9e^{j0^\circ}\right) = 49.1e^{j0^\circ} - 8.72e^{j0^\circ} = 40.38e^{j0^\circ}$$

$$\boldsymbol{A}_1 = \frac{1}{\sqrt{2}\pi}\int_{-\pi/4}^{\pi/4} E_{\max}\sin\theta\, e^{-j\theta}d\theta = \frac{E_{\max}}{\sqrt{2}\pi}\int_{-\pi/4}^{\pi/4}\sin\theta\, e^{-j\theta}d\theta = \frac{E_{\max}}{\sqrt{2}\pi}\int_{-\pi/4}^{\pi/4}\frac{e^{j\theta}-e^{-j\theta}}{2j}e^{-j\theta}d\theta$$

$$= \frac{E_{\max}}{\sqrt{2}\pi}\int_{-\pi/4}^{\pi/4}\frac{1-e^{-2j\theta}}{2j}d\theta = \frac{E_{\max}}{\sqrt{2}\pi}\left[\frac{\theta}{2j}\Big|_{-\pi/4}^{\pi/4} + \frac{e^{-2j\theta}}{-2j(2j)}\Big|_{-\pi/4}^{\pi/4}\right] = \frac{E_{\max}}{\sqrt{2}\pi}\left\{\left[\frac{\frac{\pi}{4}-\frac{-\pi}{4}}{2j}\right] + \left[\frac{-e^{-j\frac{\pi}{2}} + e^{j\frac{\pi}{2}}}{4}\right]\right\}$$

$$= \frac{E_{\max}}{\sqrt{2}\pi}\left[\frac{-(-j)+j}{4} + \frac{\pi}{4j}\right] = \frac{E_{\max}}{\sqrt{2}\pi}\left[\frac{j}{2} + \frac{\pi}{j4}\right] = \frac{120\sqrt{2}\left[\frac{j}{2} - j\frac{\pi}{4}\right]}{\sqrt{2}\pi} = -10.9e^{j\frac{\pi}{2}}$$

$$\boldsymbol{U}_1 = \boldsymbol{A}_1 + \boldsymbol{B}_1 e^{-j\frac{\pi}{2}} - \boldsymbol{A}_1 e^{-j\pi} - \boldsymbol{B}_1 e^{j\frac{\pi}{2}} = -10.9e^{j\frac{\pi}{2}} + 40.38e^{-j\frac{\pi}{2}} + 10.9e^{-j\frac{\pi}{2}} - 40.38e^{j\frac{\pi}{2}}$$

$$\boldsymbol{U}_1 = 102.56e^{-j\frac{\pi}{2}}$$

Current rms calculations:

$$i(t) = \frac{120\sqrt{2}\sin(\omega_1 t) - 120}{0.8 + 0.2}$$

$$\|i\| = \sqrt{\|x\|^2 + (-\|x\|)^2}$$

$$\|x\|^2 = \frac{1}{2\pi}\int_{\pi/4}^{3\pi/4} i^2(t)\,dt = \frac{1}{2\pi}\int_{\pi/4}^{3\pi/4} [120\sqrt{2}\sin(\omega_1 t) - 120]^2\,dt$$

$$= \frac{120^2}{2\pi}\int_{\pi/4}^{3\pi/4} [2\sin^2(\omega_1 t) - 2\sqrt{2}\sin(\omega_1 t) + 1]\,dt$$

$$= \frac{120^2}{2\pi}\left[\left(t - \frac{\sin(2\omega_1 t)}{2}\right)\Big|_{\pi/4}^{3\pi/4} + 2\sqrt{2}\cos(\omega_1 t)\Big|_{\pi/4}^{3\pi/4} + t\Big|_{\pi/4}^{3\pi/4}\right]$$

$$= \frac{120^2}{2\pi}\left[2\left(\frac{3\pi}{4} - \frac{\pi}{4} - \left(\frac{1}{2} - \frac{1}{2}\right)\right) + 2\sqrt{2}\left(-\frac{1}{\sqrt{2}} - \frac{1}{\sqrt{2}}\right) + \frac{\pi}{2}\right] = \frac{120^2}{2\pi}\left(\frac{\pi}{2} + 1 - 4 + \frac{\pi}{2}\right)$$

$$\|x\| = 18.0$$

$$\|i\| = \sqrt{\|x\|^2 + (-\|x\|)^2} = \sqrt{18.0^2 + (-18.0)^2} = 25.48$$

DC current calculations:

$$i(t) = \frac{120\sqrt{2}\cos(\omega_1 t) - 120}{0.8 + 0.2}$$

$$\overline{|i|} = \frac{1}{\pi/2}\int_0^{\pi/4} 120\sqrt{2}\cos(\omega_1 t) - 120\;dt = \frac{240}{\pi}\left[\sqrt{2}\sin(\omega_1 t)\Big|_0^{\pi/4} - t\Big|_0^{\pi/4}\right]$$

$$= \frac{240}{\pi}\left[\sqrt{2}\left(\frac{1}{\sqrt{2}} - 0\right) - \frac{\pi}{4}\right] = \frac{240}{\pi}\left(1 - \frac{\pi}{4}\right)$$

$$\overline{|i|} = 16.39$$

APPENDIX B: ORTHOGONALITY PROOFS

Proof of orthogonality of harmonics of different order

$$x(t) = X_r \sin(r\omega_1 t) \quad , \quad y(t) = Y_s \sin(s\omega_1 t) \qquad s \neq r$$

$$(x_r, y_s) = \frac{1}{T}\int_o^T X_r \sin(r\omega_1 t)\, Y_s \sin(s\omega_1 t)\, dt = \frac{X_r Y_s}{T}\int_o^T \sin(r\omega_1 t)\sin(s\omega_1 t)\, dt$$

$$= \frac{X_r Y_s}{T}\int_o^T \frac{1}{2}\cos[(r-s)\omega_1 t]\cos[(r+s)\omega_1 t]\, dt$$

Integration of $\cos\theta = 0$ over the period, but $\cos(0) = 1$ As long as $s \neq r$ then

$\cos[(r-s)\omega_1 t] = 0$.

Therefore, $(x_r, y_s) = 0$ such that harmonics of different order are orthogonal to each other.

$$(x_r, y_s) = 0$$

Proof of orthogonality of positive sequence components and negative sequence components

$$\alpha = 1e^{j120°}$$

$$\begin{bmatrix} \boldsymbol{x}^{\mathrm{p}} \\ \boldsymbol{x}^{\mathrm{n}} \end{bmatrix} = \frac{1}{3}\begin{bmatrix} 1 & \alpha & \alpha^* \\ 1 & \alpha^* & \alpha \end{bmatrix}\begin{bmatrix} X_r \\ X_s \\ X_t \end{bmatrix}$$

$$(\boldsymbol{x}^{\mathrm{p}}, \boldsymbol{y}^{\mathrm{n}}) = \frac{1}{T}\int_o^T \boldsymbol{x}^{\mathrm{p}^{\mathrm{T}}}\boldsymbol{y}^{\mathrm{n}} dt = \frac{1}{T}\int_o^T [X_{\mathrm{r}} \quad \alpha X_{\mathrm{s}} \quad \alpha^* X_{\mathrm{t}}]\begin{bmatrix} Y_{\mathrm{r}} \\ \alpha^* Y_{\mathrm{s}} \\ \alpha Y_{\mathrm{t}} \end{bmatrix} dt$$

$$= \frac{1}{T}\int_o^T X_{\mathrm{r}}Y_{\mathrm{r}} + \alpha X_{\mathrm{s}}\alpha^* Y_{\mathrm{s}} + \alpha^* X_{\mathrm{t}}\alpha Y_{\mathrm{t}} dt = \frac{1}{T}\int_o^T X_{\mathrm{r}}Y_{\mathrm{r}} + X_{\mathrm{s}}Y_{\mathrm{s}} + X_{\mathrm{t}}Y_{\mathrm{t}} dt$$

$$= \frac{1}{T}\int_o^T X_{\mathrm{r}}Y_{\mathrm{r}} + \alpha X_{\mathrm{r}}\alpha Y_{\mathrm{r}} + \alpha^* X_{\mathrm{r}}\alpha^* Y_{\mathrm{r}} dt = \frac{X_{\mathrm{r}}Y_{\mathrm{r}}}{T}\int_o^T (1 + \alpha^* + \alpha) dt = 0$$

APPENDIX C: LABVIEW AND SIMULINK BLOCK DIAGRAMS

Block diagram for single phase measurements:

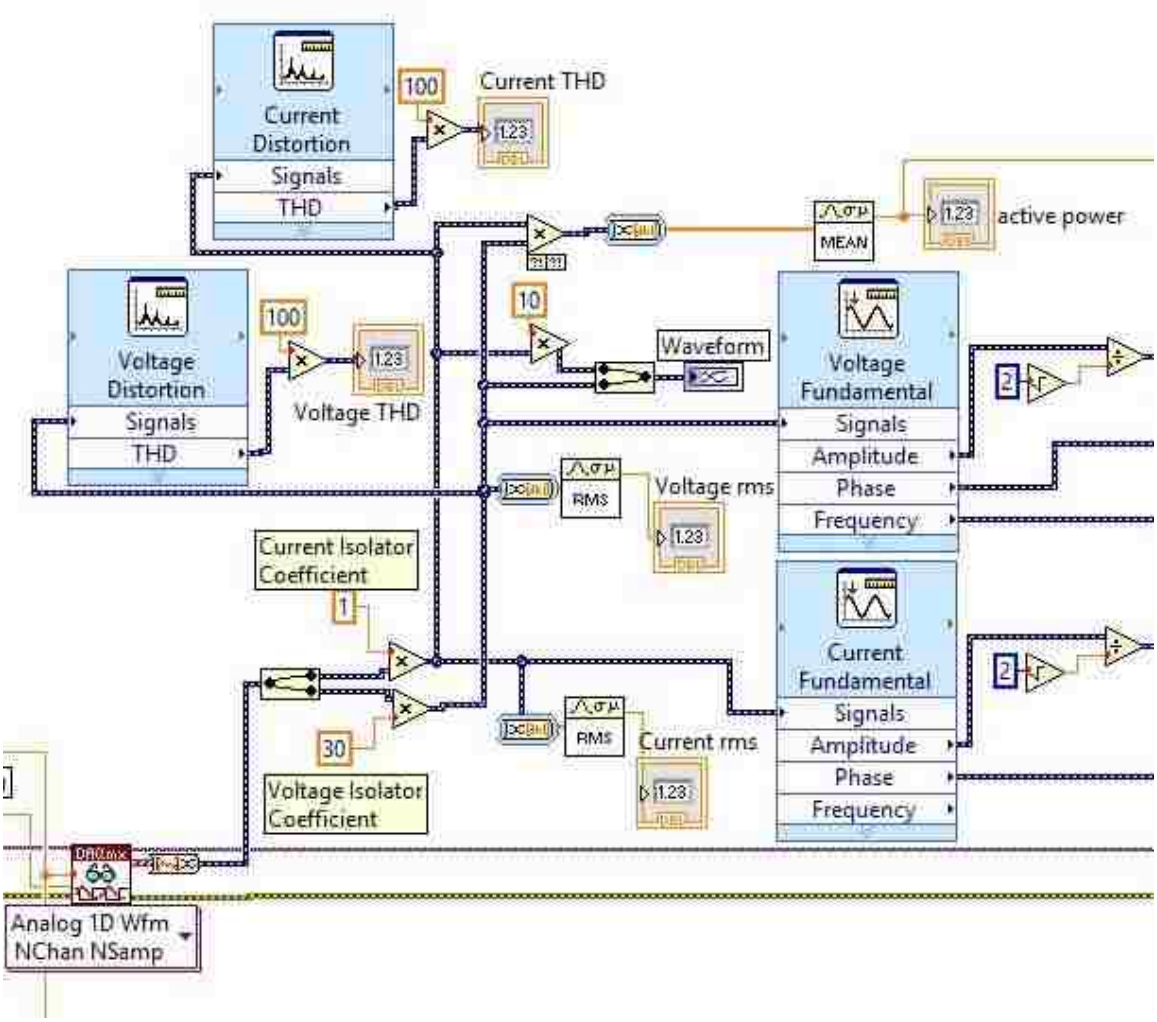

Block diagram for single phase measurements:

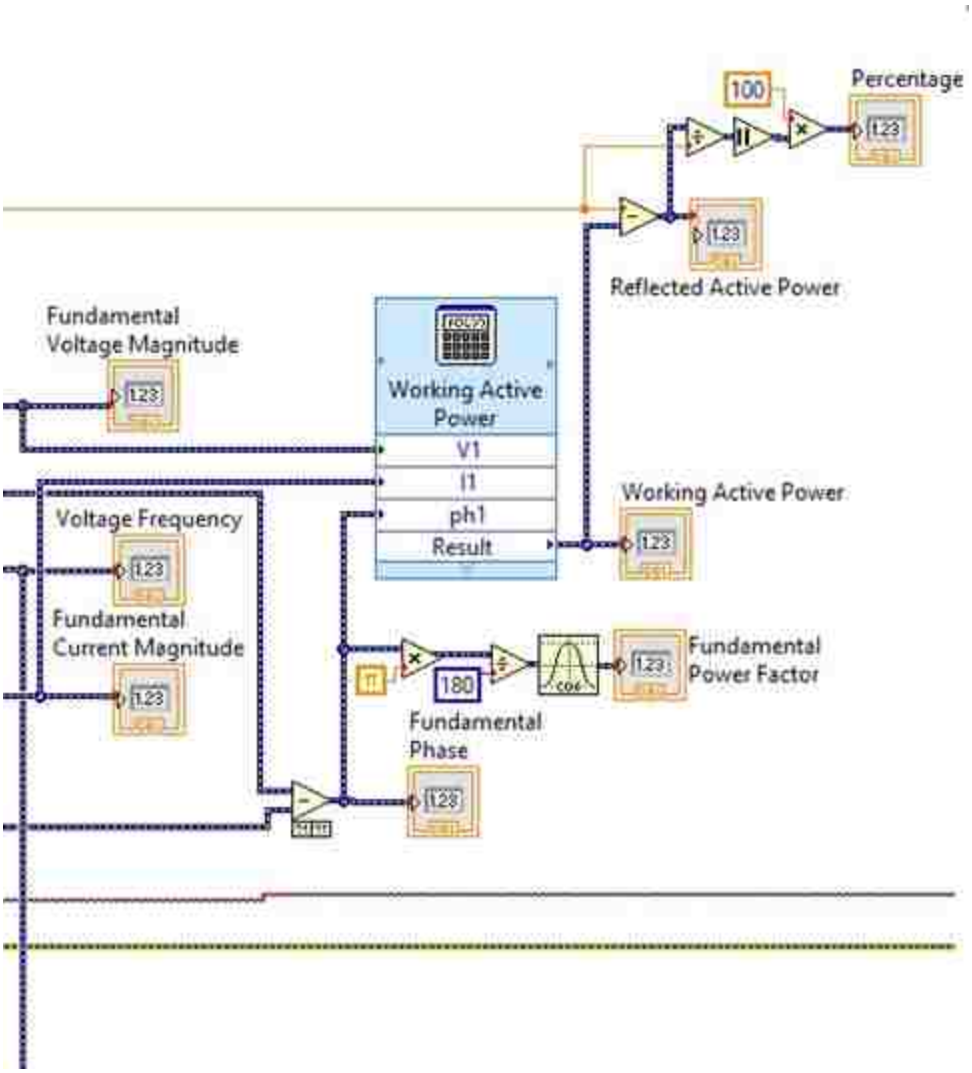

Block diagram for three phase measurements:

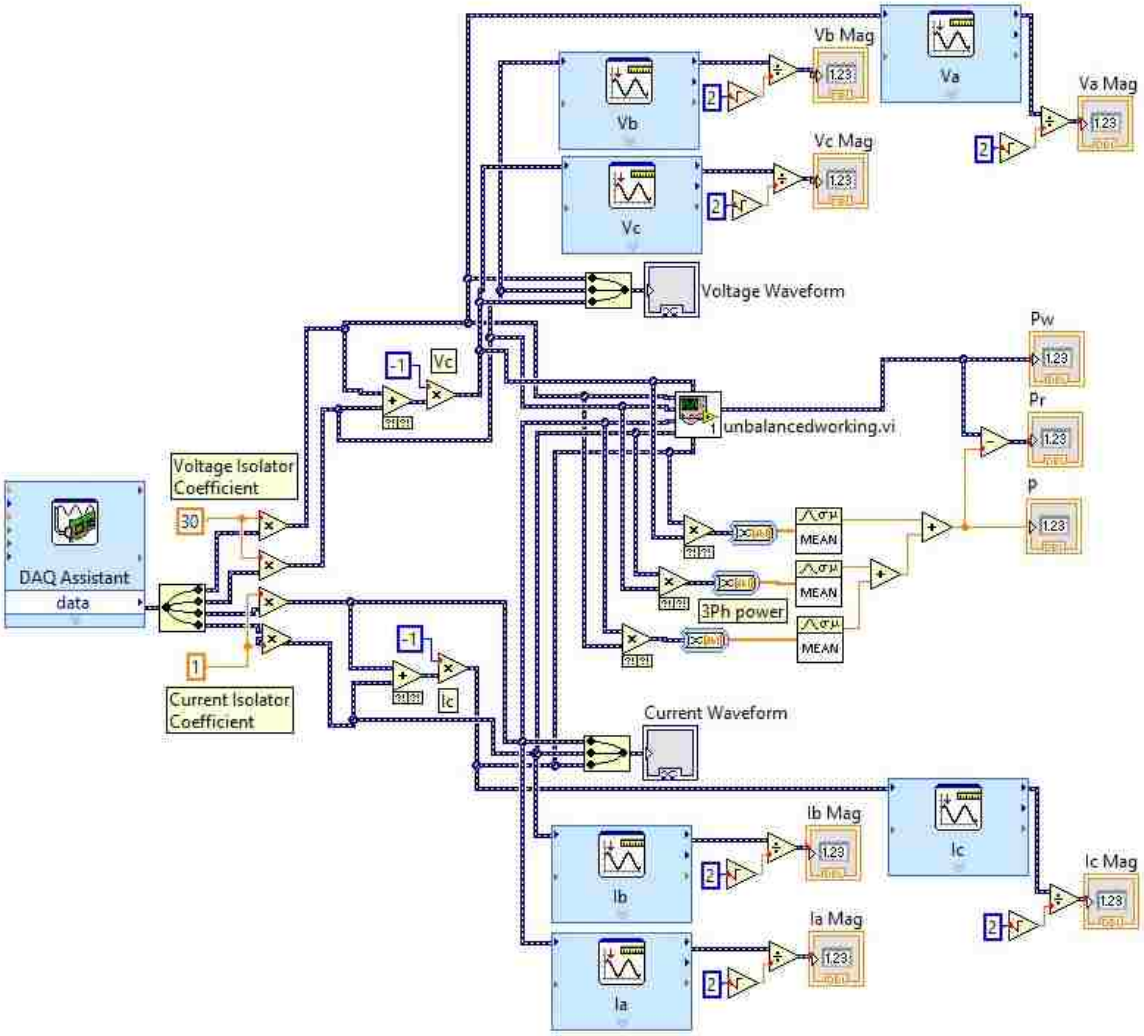

Block diagram for subsystem unbalancedworking.vi:

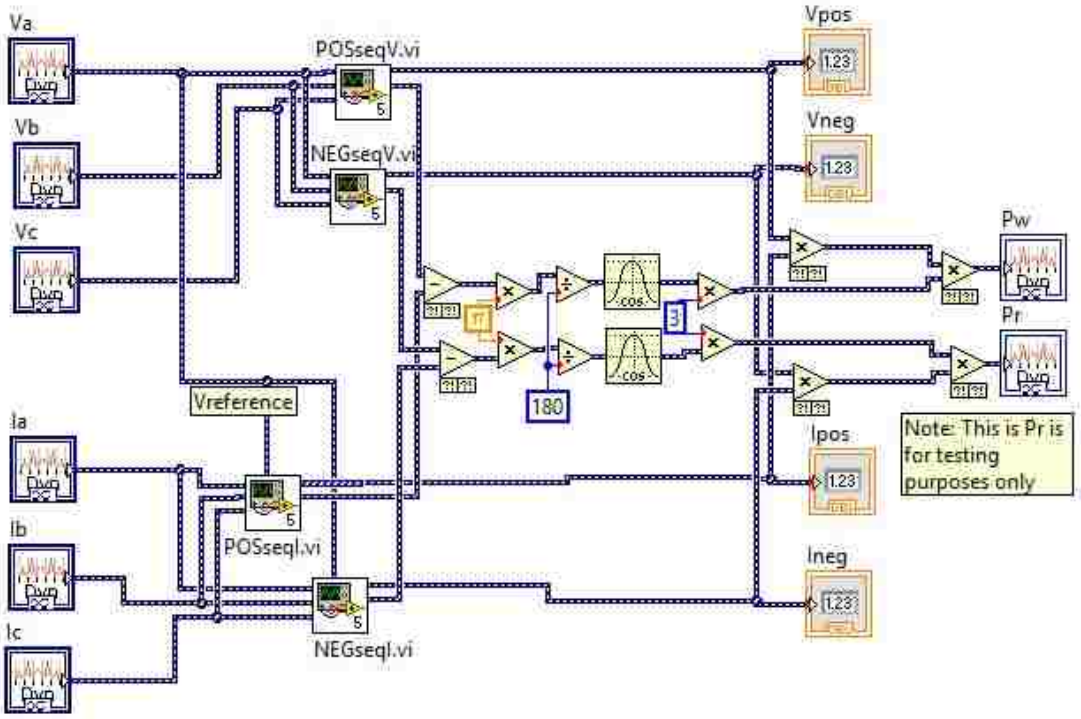

Block Diagram for subsystem POSseqV.vi and POSseI.vi:

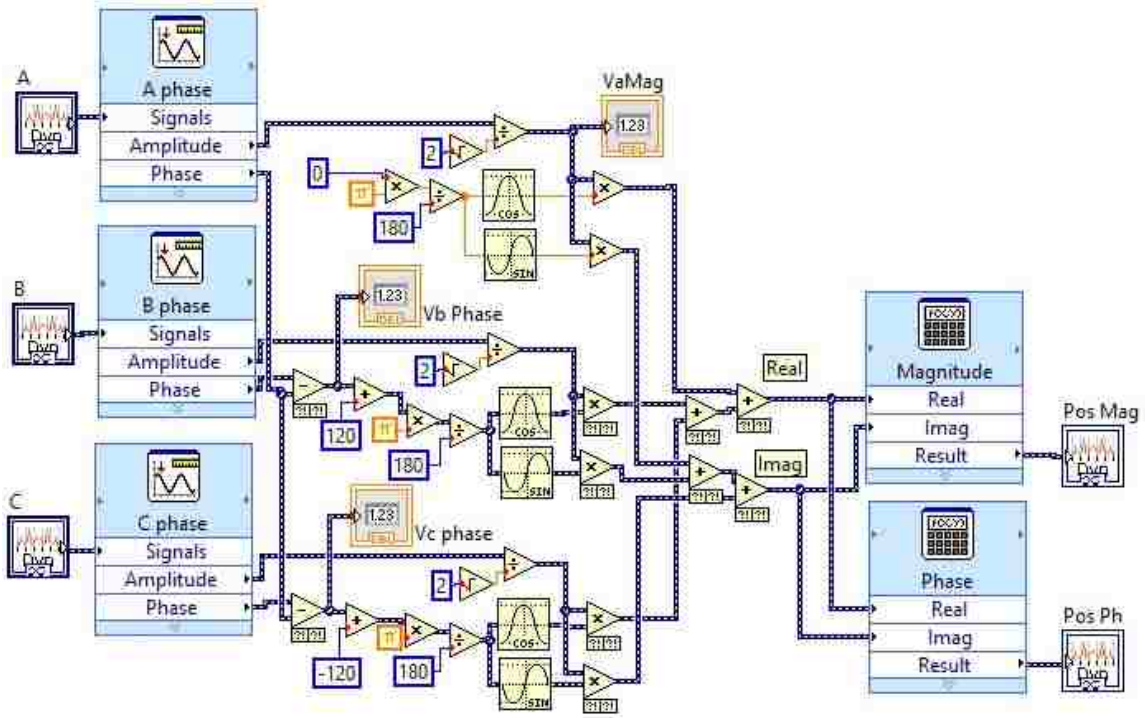

Block Diagram for subsystem NEGseqV.vi and NEGseI.vi:

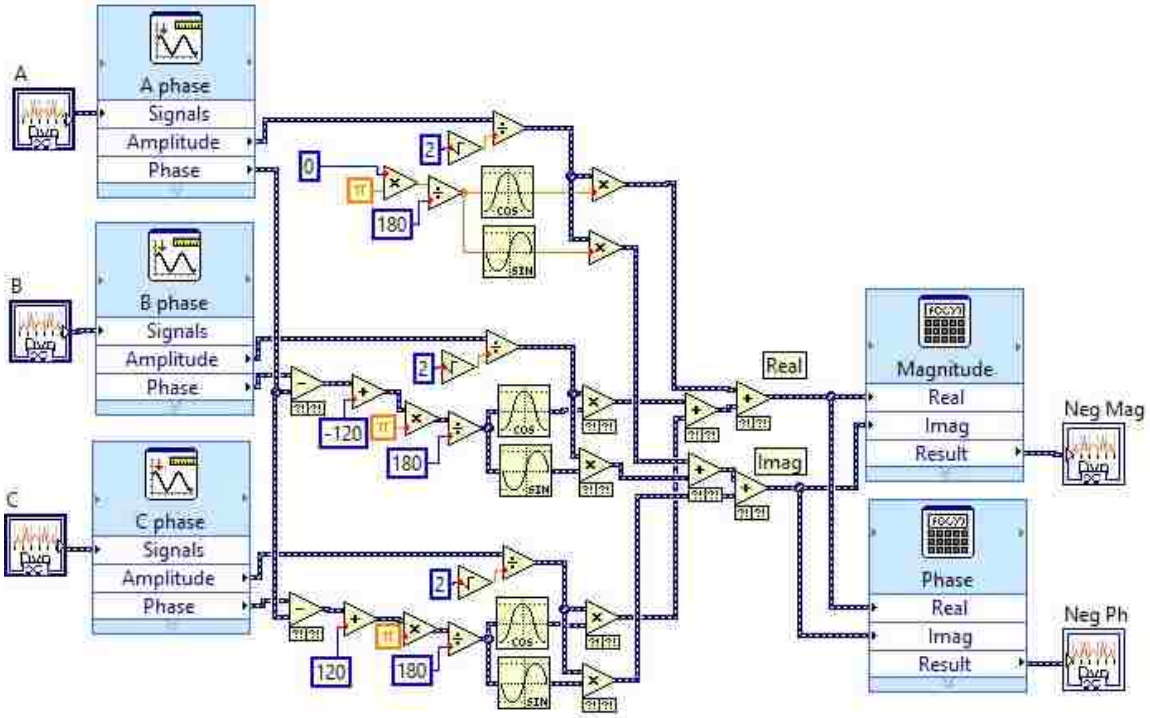

Block diagram for single bus simulation:

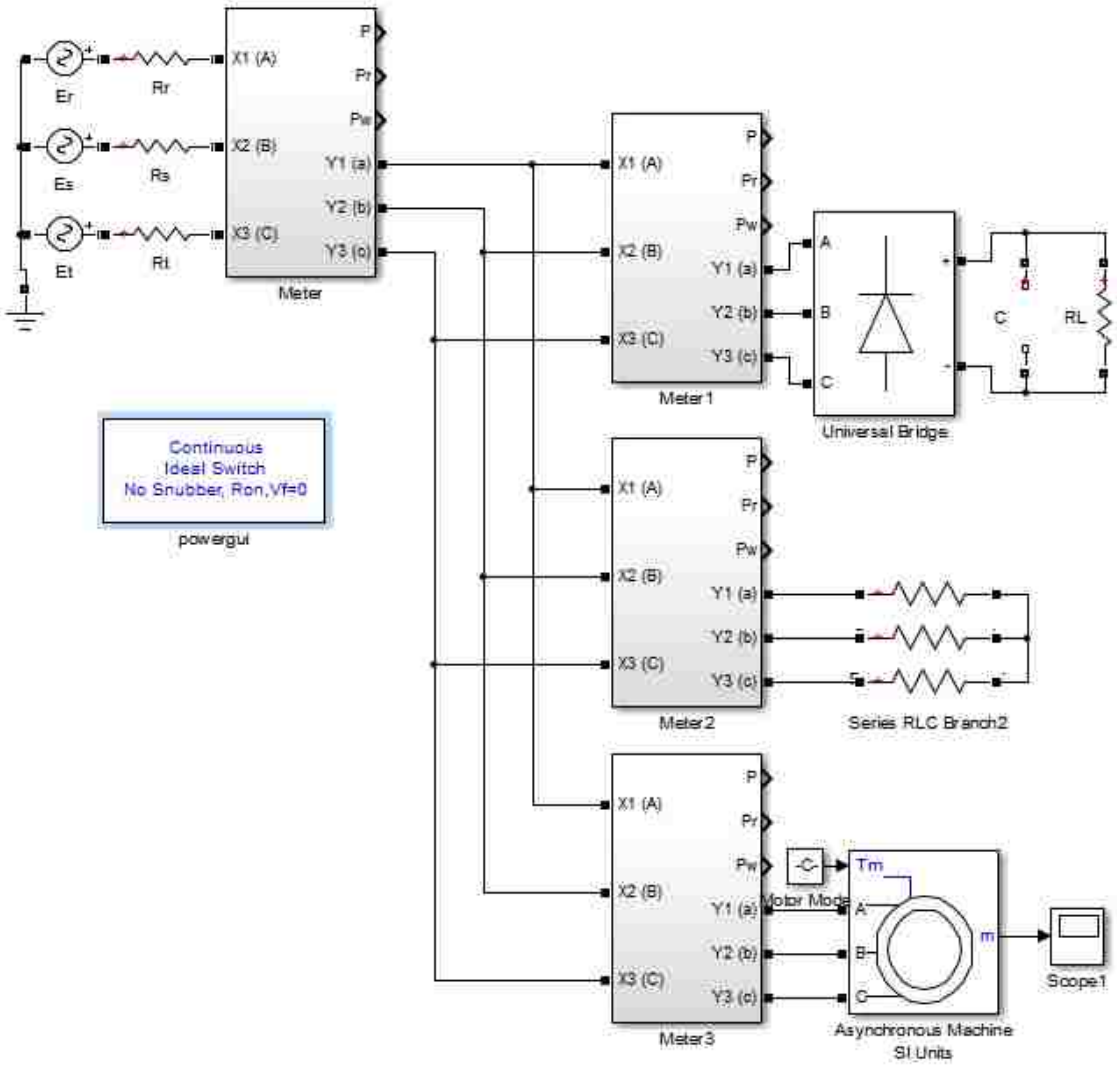

Block diagram for microgrid simulation:

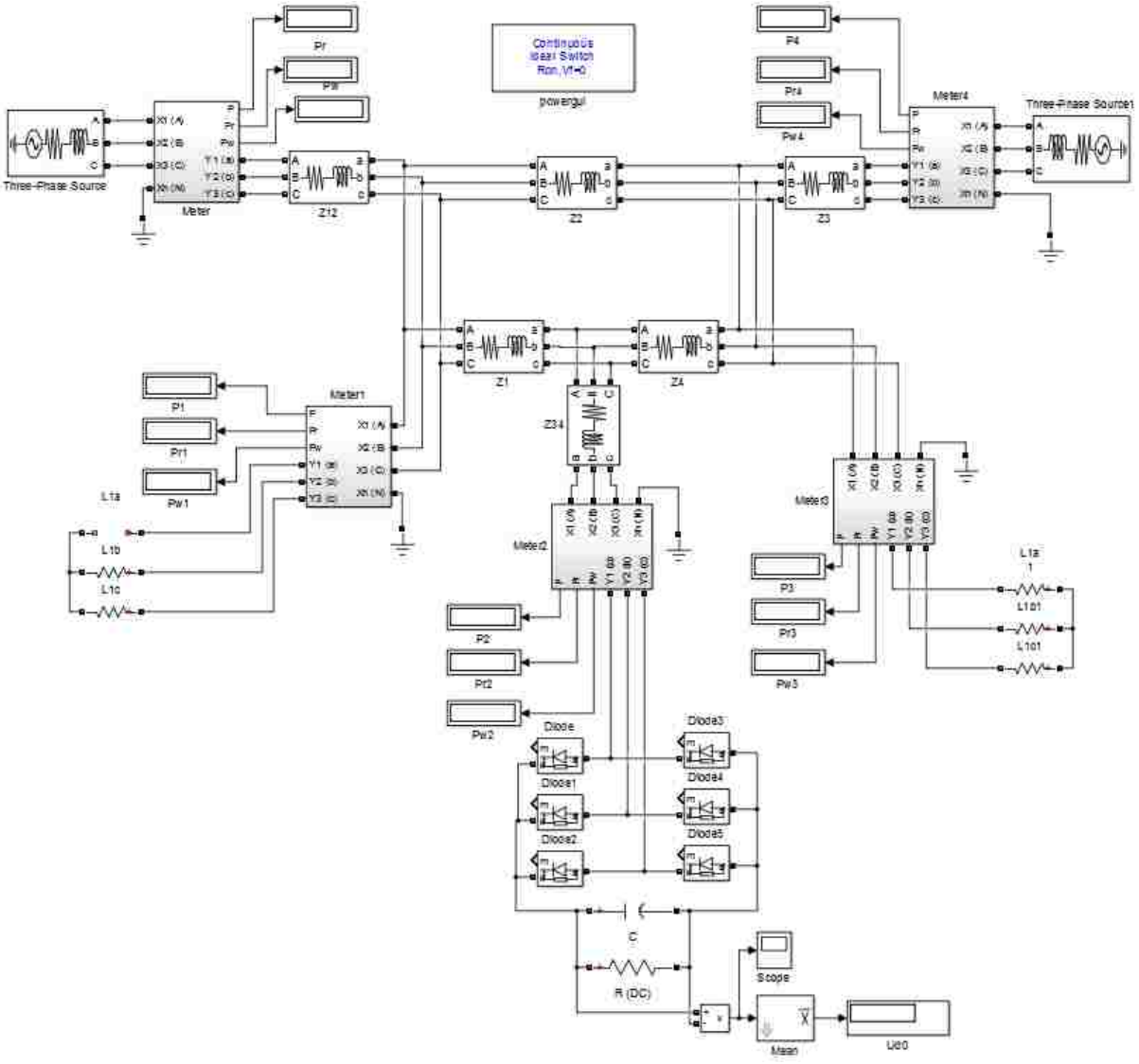

APPENDIX D: EXPERIMENTAL SETUP PHOTOS

Photos of the working active power meter,

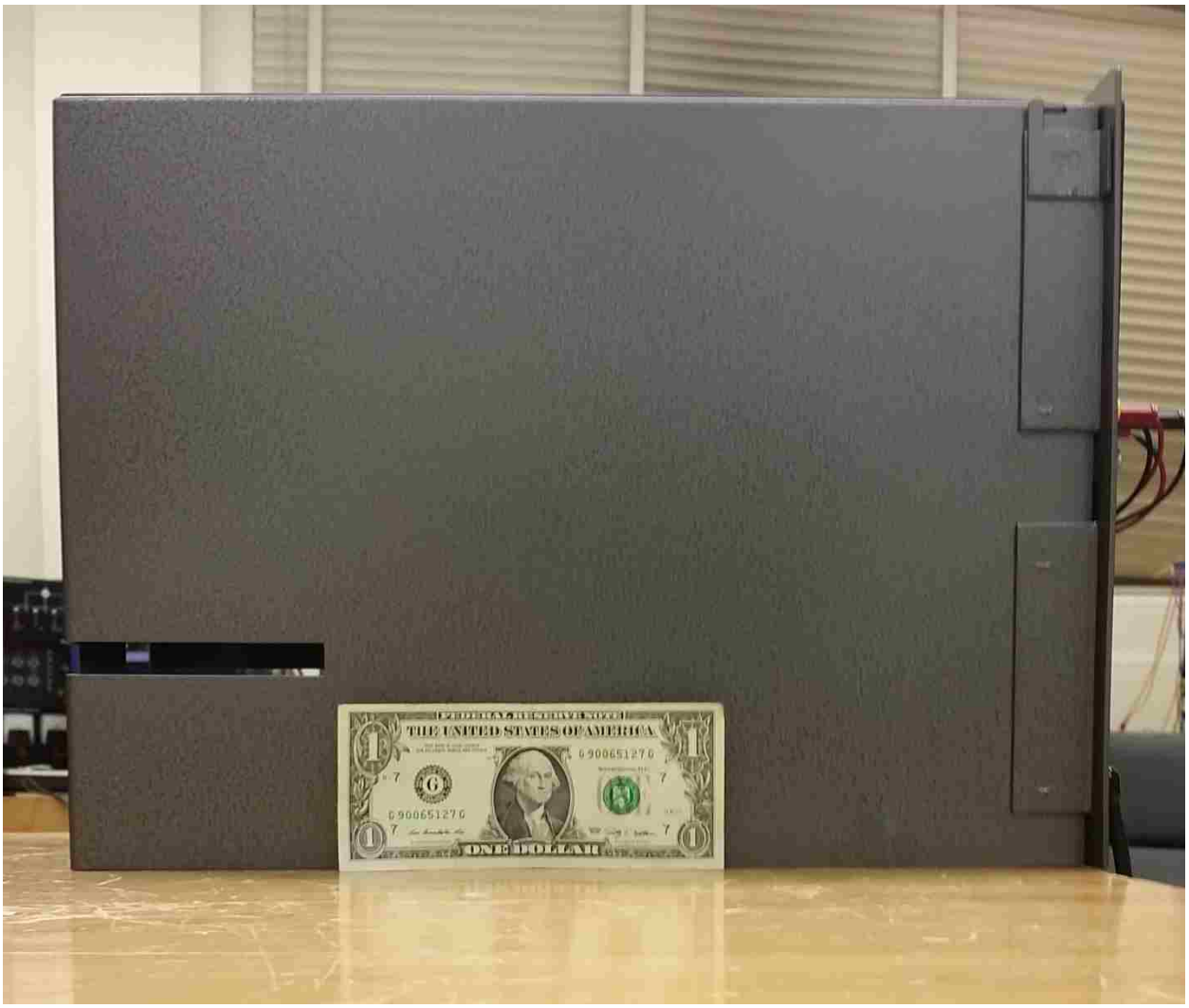


CURRENT / VOLTAGE ISOLATOR
I
E
INPUT [A]
INPUT [V]
COM
COM
ISOLATION: 600 V
OUTPUTS
CURRENT / VOLTAGE ISOLATOR
I
E
INPUT [A]
INPUT [V]
COM
COM
ISOLATION: 600 V
OUTPUTS
POWER SUPPLY
+15 V 0.5 A
-15 V 0.5 A
+5 V 1 A
0 V
120 V ~ 0.8 A 60 Hz
Lab-Volt

VITA

Tracy Toups was born in 1984 in Thibodaux, Louisiana. He graduated high school from Baton Rouge Magnet High in Baton Rouge, LA. After attending Louisiana State University, he acquired a Bachelor of Science in Electrical Engineering in 2007. Shortly after, he enrolled at Louisiana State University as a graduate student to pursue a doctoral degree in electrical engineering. During the summers, Tracy works as a relay engineer at Power Control Systems Inc. in Baton Rouge, LA.